THE UNIVERSITY OF QUEENSLAND

AUSTRALIA

Molecular mechanisms of perineural spread of cutaneous carcinoma: a potential role for receptor tyrosine kinases and other biomarkers

Campbell Schmidt

MBBS(Hons), BSc

A thesis submitted for the degree of Master of Philosophy at

The University of Queensland in 2017

The University of Queensland Faculty of Medicine

Abstract

Perineural invasion and spread of cutaneous squamous cell carcinoma of the head and neck (cSCCHN) is associated with worse prognosis and high rates of locoregional recurrence. It occurs in less than 5% of cases, but given the high incidence of cSCC in Australia, portends significant morbidity and mortality. Primary tumour biology remains poorly understood and precise molecular mechanisms by which malignant squamous cells invade and progress axially within the perineural space remain unclear. Thus, there is no targeted therapy for perineural spread of cSCCHN or other neurotropic malignancies. Dysregulation of cell membrane receptor trafficking is a hallmark of cancer and such receptors are potential therapeutic targets. Over-expression of the epidermal growth factor receptor (EGFR) is well described in squamous cell carcinoma and the monoclonal antibody cetuximab is approved for advanced mucosal head and neck SCC. Other members of the ErbB family (HER2, ErbB3 and ErbB4) are less well understood in SCC. The erythropoietin-producing hepatocellular carcinoma (Eph) family of RTKs is similarly dysregulated in a wide range of cancers. Given their physiological roles in neural development and skin homeostasis, these receptors represent other potential therapeutic targets in perineural spread. The aim of this thesis was to investigate the expression and cellular distribution of molecular receptors involved in perineural spread, particularly those with targeted therapies in development or clinical use for other indications. Four SCC cell lines and one human keratinocyte line were examined by immunoblotting and immunofluorescence. Human tissue specimens of perineural spread from cSCCHN were collected over an 18-month period and immunostained for EGFR, HER2 and other cancer biomarkers. Ki-67 proliferation index was examined for the first time as a potential prognostic factor and marker of aggressiveness in perineural spread. Cell cycle regulators p16 and p53 were examined as novel biomarkers and to shed light on possible non-RTK dependent mechanisms implicated in the disease process. The work with p53 builds on recent data published by our collaborators suggesting dysregulation of the p53 pathway in clinical perineural invasion. P16 is an established prognostic factor and surrogate marker for carcinogenic viral infection in oropharyngeal SCC not previously investigated in perineural spread cSCCHN. To our knowledge, this is the first study to demonstrate over-expression of the EGFR in perineural spread cSCCHN, in 90% (n=18/20) cases evaluated. This suggests a potential mechanistic role and reveals a valuable therapeutic target. Moreover, half of these cases had strong plasma membrane expression in the absence of cytoplasmic labelling, consistent with dysregulation of receptor trafficking and RTK escape, a new hallmark of cancer. Conversely, perineural spread

specimens were uniformly HER2 negative effectively ruling this out as a therapeutic target. These findings will have implications for treatment of advanced cSCCHN with perineural spread of carcinoma. Patients with recalcitrant and/or resistant disease could be offered existing anti-EGFR therapies or enrolled in clinical trials testing novel or combination therapeutics. Ultimately, we aim to improve survival and quality of life for sufferers of this morbid form of tumour spread. Our findings may also have implications for other neurotropic malignancy, including pancreatic, gastric, colorectal and prostate cancers.

Declaration by author

This thesis is composed of my original work, and contains no material previously published or written by another person except where due reference has been made in the text. I have clearly stated the contribution by others to jointly-authored works that I have included in my thesis.

I have clearly stated the contribution of others to my thesis as a whole, including statistical assistance, survey design, data analysis, significant technical procedures, professional editorial advice, and any other original research work used or reported in my thesis. The content of my thesis is the result of work I have carried out since the commencement of my research higher degree candidature and does not include a substantial part of work that has been submitted to qualify for the award of any other degree or diploma in any university or other tertiary institution. I have clearly stated which parts of my thesis, if any, have been submitted to qualify for another award.

I acknowledge that an electronic copy of my thesis must be lodged with the University Library and, subject to the policy and procedures of The University of Queensland, the thesis be made available for research and study in accordance with the Copyright Act 1968 unless a period of embargo has been approved by the Dean of the Graduate School.

I acknowledge that copyright of all material contained in my thesis resides with the copyright holder(s) of that material. Where appropriate I have obtained copyright permission from the copyright holder to reproduce material in this thesis.

Publications during candidature

No publications.

Publications included in this thesis

No publications included.

Contributions by others to the thesis

Significant contribution to the conception and design of this project by my supervisors Prof Ben Panizza and Dr Fiona Simpson.

Statement of parts of the thesis submitted to qualify for the award of another degree

None

Acknowledgements

I am extremely grateful for the support granted by my supervisors, Fiona and Ben, throughout this journey. Your leadership and passion for your work never ceases to inspire. I am indebted to the entire team comprising the Simpson laboratory for their patience and generosity: Laurette, Leanne, Nicola, Satomi, Godwins and Shannon. I am equally indebted to pathologists Dr Ian Brown and Dr Caroline Cooper for your assistance and guidance throughout this study. I am grateful for the support from our collaborators north and south of the river Dr Glen Boyle, Dr Graham Leggatt and Dr Andrew Boyd. Thanks to Paula Ridge and the staff at the Princess Alexandra Hospital pathology department for your assistance with tissue acquisition and immunohistochemistry. Thanks to Crystal Chang at the TRI Histology Core Facility, Ali Ju and Sandrine Roy at the TRI Microscopy Core Facility, Rhiannon Walters at the PA Hospital, Sally Yukiko, Natasa Korica and countless other members of the research team who helped with advice or an extra set of hands. Finally, thanks to the patients who make this work possible and worthwhile.

I must acknowledge and express my gratitude for the financial support provided to me through an APA scholarship and through The University of Queensland Diamantina Institute clinician support scheme. I must also acknowledge the tireless love and support of my wife Lisa while I returned to this period of full-time study.

I also wish to acknowledge the support of the Princess Alexandra Hospital Research Foundation for funding the project grant that enabled this work.

.

Keywords

perineural spread, cutaneous squamous cell carcinoma, monoclonal antibody therapy

Australian and New Zealand Standard Research Classifications (ANZSRC)

ANZSRC code: 111204, Cancer Therapy, 85%

ANZSRC code: 110315, Otorhinolaryngology, 15%

Fields of Research (FoR) Classification

FoR code: 1112, Oncology and Carcinogenesis, 100%

Table of contents

List of figures & tables

Figures

Tables

List of abbreviations

ACC	Adenoid cystic carcinoma
ADCC	Antibody dependent cell cytotoxicity
AK	Actinic keratosis
Akt	AKT8 virus oncogene cellular homolog
ATCC	American Type Culture Collection
BB	Blocking buffer
BCC	Basal cell carcinoma
BDNF	Brain derived neurotrophic factor
BSA	Bovine serum albumin
CAM	Chorioallantoic membrane
CCL2/CCR2	C-C chemokine ligand 2/receptor 2
CDC	Complement dependent cytotoxicity
CDKN2A	Cyclin-dependent kinase inhibitor 2A
CIS	Carcinoma in situ
CLIC	Clathrin-independent carriers
CRGA	Clinically relevant genomic alteration
CX3CL1/CX3CR1	Chemokine (C-X3-C motif) ligand 1/receptor 1
cPNI	Clinical perineural invasion
cSCC	Cutaneous squamous cell carcinoma
cSCCHN	Cutaneous squamous cell carcinoma of the head and neck
DAB	3,3'-diaminobenzidine
DAPI	4’,6-diamidino-2-phenylindole
DFS	Disease free survival
DMEM-F12	Dulbecco’s modified Eagle’s medium: nutrient mixture F-12
DNA	Deoxyribonucleic acid
DRG	Dorsal root ganglion
ECL	Enhanced chemiluminescence
EGF	Epidermal growth factor
EGFR	Epidermal growth factor receptor
Eph	Erythropoietin-producing hepatocellular carcinoma (receptor)
Ephrin	Eph receptor interacting protein
FBS	Foetal bovine serum
FcγR	Fc-gamma receptor

FFPE	Formalin fixed paraffin embedded
FGFR3	Fibroblast growth factor receptor 3
FISH	Fluorescence in situ hybridisation
FoxP3	Forkhead box P3
GAL	Galanin
GDNF	Glial cell-derived neurotrophic factor
GEEC	Glycosylphosphotidylinositol-anchored protein enriched compartments
GFRα1	GDNF receptor-α1
H&E	Haematoxylin and eosin
HER	Human epidermal growth factor receptor
HIER	Heat induced epitope retrieval
5hmC	5-hydroxymethylcytosine
HNSCC	Head and neck squamous cell carcinoma
HPV	Human papilloma virus
HRP	Horseradish peroxidase
IgG	Immunoglobulin G
IHC	Immunohistochemistry
mAb	Monoclonal antibody
MAPK	Mitogen-activated protein kinase
MEK	Mitogen-activated protein kinase
mPNI	Microscopic perineural invasion
MR	Magnetic resonance (imaging)
NFκβ	Nuclear factor kappa-light-chain-enhancer of activated B cells
NGF	Nerve growth factor
NGFR	Nerve growth factor receptor
NK	Natural killer
NMSC	Non-melanoma skin cancer
NRG	Neuregulin
NSCLC	Non-small cell lung cancer
NT	Neurotrophin
PBS	Phosphate buffered saline
PCR	Polymerase chain reaction
PDAC	Pancreatic ductal adenocarcinoma
PFA	Paraformaldehyde

PI3K	Phosphatidylinositol 3-kinase
PIK3CA	Phosphatidylinositol-4,5-bisphosphate 3-kinase catalytic subunit alpha
PNI	Perineural invasion
PNS	Perineural spread
PVDF	Polyvinylidene fluoride
QIMR	Queensland Institute of Medical Research
RET	Rearranged during transfection (RET) receptor tyrosine kinase
RIPA	Radioimmunoprecipitation assay
RNA	Ribonucleic acid
RT	Room temperature
RTK	Receptor tyrosine kinase
SCC	Squamous cell carcinoma
SDS	Sodium dodecyl sulphate
SDS-PAGE	Sodium dodecyl sulphate polyacrylamide gel electrophoresis
SFK	SRC-family kinase
TBS	Tris buffered saline
TBST	Tris buffered saline with tween
TGF-β	Transforming growth factor beta
TKI	Tyrosine kinase inhibitor
TP53	Tumour protein 53
TNBC	Triple-negative breast cancer
TNM	Tumour-node-metastasis (TNM) staging
Tyr	Tyrosine
UQDI	The University of Queensland Diamantina Institute
UVR	Ultraviolet radiation

1.0 Introduction

Cutaneous squamous cell carcinoma (cSCC) is a malignant proliferation of epidermal keratinocytes secondary to the mutagenic effects of ultraviolet radiation.[1] Australia has the highest incidence of cSCC in the world, with the disease occurring predominantly on the sun-exposed head and neck and in males due to occupational exposure.[2,3] Other risk factors include age, fair skin and immunosuppression. With ongoing ozone depletion, an ageing population and increasing survival of immunosuppressed patients, the incidence of cSCC of the head and neck (cSCCHN) continues to rise.[4,5]

In 95% of cases of cSCCHN, complete surgical excision is curative.[6,7] However, there is a well-recognised metastatic potential, with reported rates of regional and distant metastasis 5% and 1%, respectively.[6] The disease-specific death rate is at least 1%, with a recent systematic analysis reporting a range of 1.5-2.1%.[7,8] Although metastatic and disease-specific death rates are low compared to other malignancies, the absolute number of patients with cSCCHN means there is paradoxically significant morbidity and mortality associated with this disease.

Australia has the highest incidence of cSCC in the world with the most recent age-standardised rate reported to be 387 in 100,000 and the rate in males exceeding 1300 in 100,000 in far north Queensland.[3,9] This rate has more than doubled over the preceding 20 year period.[4,5] In 2016, it is estimated that 560 Australians will die from non-melanoma skin cancer (NMSC), the majority from advanced cSCCHN, with an age-standardised mortality rate of 1.9 deaths per 100,000.[5] The estimated incidence of cSCC in the United States is 700,000 cases per year, with associated deaths estimated at up to 9000 annually.[8] The incidence and mortality is significantly higher in the immunosuppressed population, including organ transplant

patients.[8] The annual Australian economic burden of NMSC is estimated at $500 million per year and is expected to more than double by 2020.[10]

Perineural growth is an under-appreciated and distinct form of tumour spread seen across a range of cancers. Perineural spread is associated with both pain and worse outcome, independent of vascular or lymph involvement, in NMSC and cancers of the head and neck, pancreas, stomach, colon and prostate.[11-13] In the head and neck, perineural growth comprises two distinct entities: incidentally detected microscopic perineural invasion (PNI) and clinical perineural spread (PNS) along larger, named nerves with clinical and/or imaging evidence of involvement pre-operatively.[14] Perineural spread is also referred to as clinical PNI (cPNI) as distinct from microscopic PNI (mPNI). Clinical PNI or perineural spread describes tumour that has spread away from the primary site and thus represents a unique form of metastasis.

Despite its prevalence and prognostic significance, the molecular mechanisms underlying perineural invasion and perineural spread remain poorly understood. Moreover, no reliable biomarkers have been identified. Thus, no targeted therapy exists for PNI or PNS in non-cutaneous or cutaneous malignancy and the ability to risk-stratify patients is limited. An improved understanding of the molecular profile of perineural spread and therapeutic strategies targeting the tumour cell and/or the nerve microenvironment would be of immense benefit in treating and prognosticating this aggressive disease.

2.0 Literature review

2.1 Defining perineural growth

Tumour neurotropism in the head and neck was first described as "invasion of tumour in, around and through peripheral nerves."[15] These nerves were theorised to pose a physical path of least resistance to invading malignant cells. Another early proposed mechanism of spread was via endolymphatic spread within the perineurium, as an extension of lymphatic metastasis, but the absence of lymphatics in nerve tissue was later demonstrated, disproving this theory.[16]

The peripheral nerve is composed of many nerve fibres enclosed by a neural sheath comprising three distinct layers (Figure 1).[17] Endoneurium is the innermost layer of loose connective tissue which envelopes individual nerve fibres (axons) including myelin secreting Schwann cells and capillaries, forming nerve bundles within the nerve fascicle. The perineurium, comprised of multilamellar, concentric perineural cells and layers of basement membrane, invests each nerve fascicle. The epineurium is the external fibrous sheath that envelops a group of nerve fascicles to encompass the whole nerve in its entirety.[17] The perineural space is thus a potential space located between the nerve fibre bundles and the surrounding perineurium, which can provide a conduit for tumour spread. Electron microscopy of the perineural sheath reveals that it comprises concentric laminae of perineural cells joined by tight junctions (zonulae occludentes), vested with basement membrane on both sides.[18] Longitudinally disposed elastic and collagen fibres together with fibroblasts occupy the spaces between laminae.[19] It is this sheath that effectively forms the selective "blood-nerve barrier" that separates the peripheral nerve compartment from surrounding tissue.

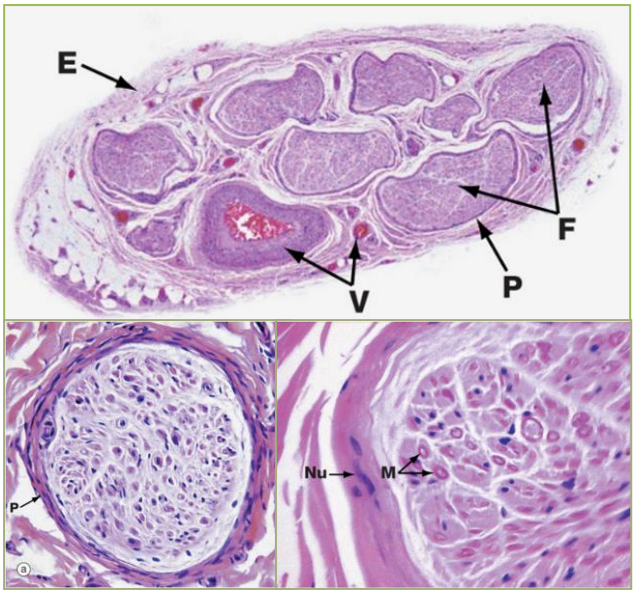

Figure 1 Peripheral nerve shown in transverse section consists of nerve fascicles (F) invested by perineurium (P), which is composed of concentric, multilamellar perineural cells (Nu). Endoneurium is the loose connective tissue encompassing individual nerve fibres, blood vessels (V) and myelin (M) secreting Schwann cells within each fascicle. Epineurium (E) is the loose collagenous tissue sheath encasing the nerve as a whole. Adapted from Wheater's Functional Histology, 5th edition (2006).[17]

Mechanistic understanding of how tumour cells enter the perineural space and traverse along it remains poor. It is thought that in cutaneous malignancy undergoing clinical perineural spread, tumour cells likely enter the perineural space in the subcutis where the perineurium is thin or absent.[14] Once within the perineural space, the perineurium acts as an effective barrier in limiting tumour cells to within this space as they track along the nerve. On the other hand, incidental perineural invasion is a more commonly seen entity detected by microscopy. One postulated mechanism in pancreatic cancer is of neurotropic tumour cells breaching the perineurium to access the perineural space (Figure 2).[12] Pathologists at our centre have not observed this perineural breach in the head and neck with cutaneous malignancy, except in the context of indiscriminate invasion by a large tumour bulk. This third and final group to be

distinguished in the head and neck is such patients with advanced local disease that extends to the skull base and by virtue of the aggressive tumour biology indiscriminately invades nerve tissue.[14] We consider this indiscriminate invasion to be an inherently different process from clinical perineural spread, where tumour tracks along a nerve away from a remote, previously treated or unidentifiable cutaneous primary index lesion. These separate clinical entities in the spectrum of perineural disease are discussed further below. It may be that different physical and molecular mechanisms are involved in these related but distinct processes or alternatively that a common underlying mechanism exists and large-nerve clinical perineural spread is an end-stage result of microscopic perineural invasion that first occurs in the subcutis.

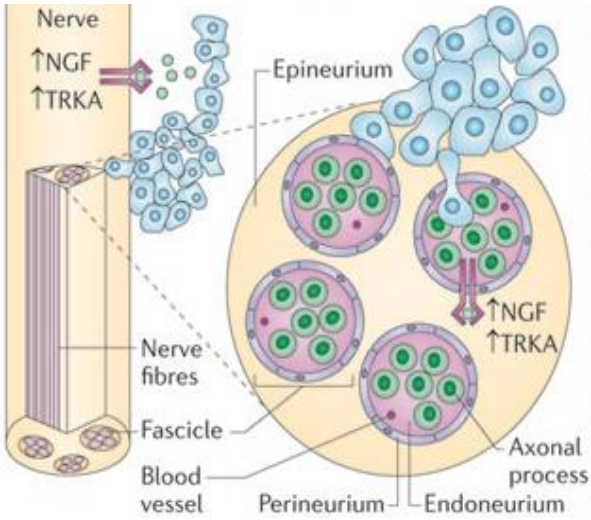

Figure 2 Exploded diagram of three-layered structure of a peripheral nerve showing tumour cells breaching the perineurium. In pancreatic cancer it is thought that neurotropic tumour cells breach the perineurium to access the perineural space.[12] Neurotropic factors in the nerve microenvironment, such as nerve growth factor (NGF) and TRKA (tyrosine receptor kinase A), are thought to play a significant role. Figure adapted from Bapat et al (2011).[12]

In histopathological terms perineural invasion is defined as presence of tumour cells within the perineural space (Figure 3).[20] However, encasement of more than 33% of the nerve circumference or tumour cells within any layer of the neural sheath is considered highly suggestive, if not diagnostic, of PNI.[21] This form of perineural involvement is not evident on clinical or radiological examination and is established by microscopy. Small, unnamed nerves are involved and this process is referred to as microscopic or incidental PNI.

Perineural spread (PNS) is defined as contiguous extension of tumour cells along the perineural space away from the primary site.[21] This is seen predominantly in the large named nerves of the head and neck, most commonly in branches of the facial and trigeminal nerves, consistent with the high incidence of cSCC that occur in these sun-exposed dermatomes.[22] In a recent analysis of 120 patients at our institution, no known or assessable primary was found in almost half the cases.[22] In this cohort 22.5% of the patients presented with PNS from an unknown primary tumour (T0) while a further 21.7% were unable to be assessed (TX) due to a history of multiple potential index lesions and/or non-surgical treatment of these lesions. Furthermore, in cases with an identified likely index lesion, more than a third had no microscopic perineural invasion reported on pathology, indicating that clinical PNS is not necessarily preceded by microscopic PNI and/or there is significant under-detection or under-reporting of microscopic PNI in primary cutaneous tumours.[22]

Perineural spread of carcinoma is associated with symptoms including loss of function, pain, numbness and formication (a sensation of ants crawling), however these are commonly missed or misattributed by clinicians resulting in diagnostic delay.[14] At our institution the median time from an identifiable primary tumour to the onset of PNS symptoms is 16 months, reflecting the typically slowly progressive natural history of the disease.[22] The average time

from symptom onset to diagnosis is 6 months, indicative of the not insignificant diagnostic delay associated with the condition.[22] Tumour spread can occur distally (centrifugal) or more commonly in a retrograde fashion towards the brainstem (centripetal), culminating in central failure. The visualisation of skip lesions consistent with non-contiguous spread along the nerve has previously been described and the concept propagated in the literature.[23,24] However, we consider this likely to represent tissue-sectioning artefact, with a recent histopathological review of 49 patients treated with surgery at our institution demonstrating no evidence of non-contiguous spread in 50 separate cases.[20] Magnetic resonance (MR) neurography detects 95% of PNS and is used in pre-operative planning for resection margins (Figure 4).[22,25]

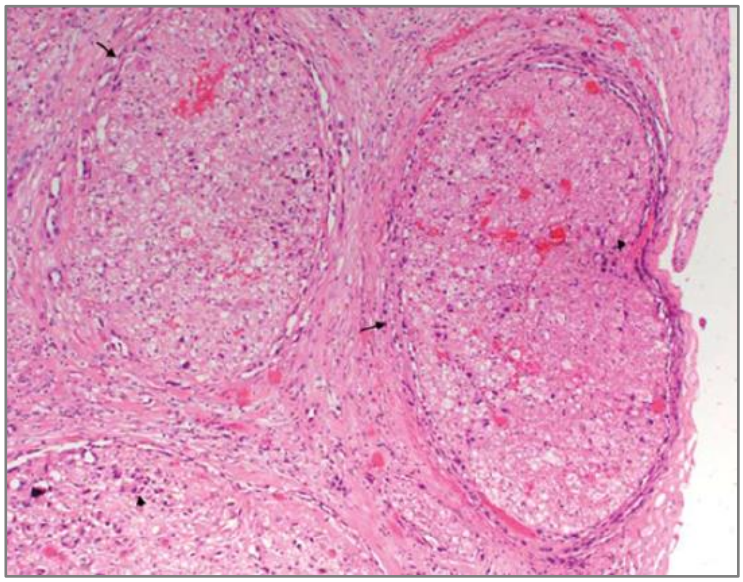

Figure 3 Haematoxylin and eosin stained tissue section showing perineural spread along a cranial nerve. Tumour cells are seen within the perineural space (arrows) consistent with perineural invasion. Areas of intraneural invasion (arrowheads) by tumour cells are also seen. Image from Warren & Panizza (2015).[26]

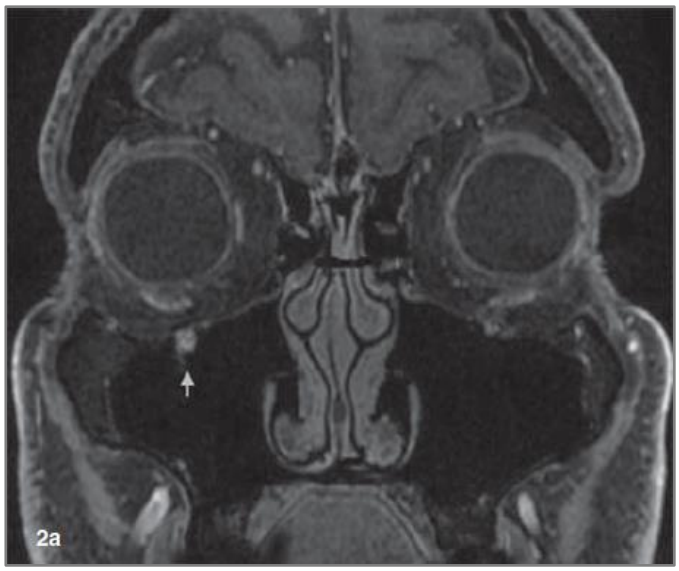

Figure 4 Coronal magnetic resonance neurography showing thickening and enhancement of the right infraorbital nerve characteristic of perineural spread from cutaneous squamous cell carcinoma of the head and neck. Pathological right infraorbital nerve is indicated by the arrowhead. Image from Warren & Panizza (2015).[26]

2.2 Histopathological features of perineural growth

Standard haematoxylin and eosin (H&E) staining is sufficient to identify perineural invasion and spread in most cases (Figure 3). However, in borderline cases where there is clinical suspicion yet no obvious PNI, staining for broad-spectrum keratin (AE1/AE3) or cytokeratin to label epithelial tumour cells or for S-100 to label myelin secreting Schwann cells, can assist in defining the pathology.[27]

Several studies have used a single immunostain to enhance nerve detection and thus identification of tumour cells in the perineural space. Several more recent studies have used double immunohistochemistry staining techniques and demonstrated a significant increase in detection rates.[28] Recently, $p75^{NGFR}$ immunostaining was shown to increase the detection rate of microscopic PNI compared with H&E staining alone.[28] The authors suggested $p75^{NGFR}$ could serve as an alternative to S-100 or be included as part of an immunostaining

panel for PNI detection. Another recent study demonstrated that dual immunohistochemistry (IHC) staining with S-100 and AE1/3 increased detection of PNI in NMSC compared to H&E alone, however the improvement in detection was almost exclusively seen in SCC cases with small nerve PNI.[29] It was suggested that IHC staining helped distinguish true PNI from classical mimics, such as peri-tumour fibrosis. However, in this study only clinically suspicious cases were used giving an obvious selection bias. These special staining techniques may be useful in detecting or confirming incidental microscopic perineural invasion in primary lesions or in advanced tumour masses, however are usually not needed to histologically confirm large-nerve perineural spread. Perineural invasion is now a core item in national clinical guidelines for standardised reporting of cSCC and a staging determinant.[27,30] Use of IHC is not yet routine for detection of mPNI but is available and performed in some centres.

An important study by Frydenlund et al (2015) took 57 cSCCHN and 53 cSCC from other locations and analysed for perineural invasion and TrkA expression.[31] S-100 was used for nerve labelling and p63 for nuclear labelling of tumour cells in their novel double immunostaining protocol. The authors demonstrated an increase in detection of PNI in head and neck specimens from 11% to 23% compared to H&E alone, representing a 2.3-fold increase in detection. Panizza et al (2014) conducted the largest histological evaluation of cSCCHN with PNS to date, of 50 tumours from 49 patients.[20] Specialist dermato-pathologists characterised the tumour invasion pattern after assessment with both longitudinal and transverse sections, achieved by mounting dissected nerve segments into cassettes to preserve the respective axes. Consecutive processing of transverse and longitudinal sections allowed complete assessment of the nerve and maximally eliminated processing artefact. There was no evidence of skip lesions with perineural tumour spread contiguous in all cases. Coexistent perineural and intraneural invasion was the predominant pattern seen in 98% of cases.[20] This

finding suggests that tumour cells that have invaded and are traversing the perineural space are not confined to this space, but in almost all cases invade into the nerve fascicles. Alternatively, it could be considered that tumour cells undergo intraneural invasion first in the subcutis before spreading to the perineural compartment where they are confined by the perineural sheath. Either way, it is considered most likely that in cases of clinical perineural spread it is the intraneural involvement that causes the characteristic symptoms and signs.[20] In the aforementioned study, only 3.9% of specimens demonstrated epineural involvement, which is thought to reflect the multilayer barrier function of the perineurium beyond the superficial fascia, effectively limiting tumour cell migration beyond the nerve compartment into surrounding soft issue. The perineurium thus provides an adequate resection margin when tumour is confined to the nerve macroscopically.

2.3 Epidemiology of perineural growth

There is variation in reported rates of PNI and PNS across the literature, likely due to the absence of a standard working definition for each of these pathologies.[20,27] There is also likely variation in awareness levels and rates of detection across different geographical regions. PNI occurs in 2.5% to 14% of cases of cSCC, with most studies reporting rates < 5%.[32] Cutaneous SCCHN has a particularly high propensity for PNI, where it is an aggressive feature, portending an increased risk of locoregional recurrence and reduced disease-free survival.[33] In one series, 3-year disease-specific survival for cSCC with and without PNI was 64% and 91%, respectively.[34] Large studies by Goepfert et al (n=967) and Leibovitch et al (n=1177) firmly established the link between PNI and tumour recurrence, distant metastasis and reduced survival.[8] A study by Lin et al (2012) showed 5-year disease-free survival (DFS) of 78% with local failure of 40% and regional relapse of 29% for cSCC with PNI.[35]

In comparison, the incidence of large nerve PNS at our institution is 1% with other series reporting similar rates less than 5%.[36] It is proposed that the high incidence of cSCC in the chronically sun-exposed anterior face and the proximity of large nerves with rich ramifications, plays a significant part in their involvement.[37] Clinical PNS has worse prognostic influence than incidental PNI, partly because it can preclude obtaining adequate oncologic resection. Five-year local control rates are 25-38% versus 80-90% for clinical compared to incidental PNI following treatment with surgery and/or radiation therapy.[37] Although perineural spread is rare, given the high incidence of cSCCHN in Australia, it portends paradoxically significant morbidity and mortality.

Perineural invasion is also described in non-cutaneous malignancies, including head and neck, prostate, pancreatic, gastric and colorectal cancers (Table 1).[12] It has been reported in up to 80% of mucosal head and neck squamous cell carcinoma (HNSCC). Adenoid cystic carcinoma (ACC) of the salivary glands also has a particular propensity for nerve invasion, with up to 62% displaying perineural invasion.[38]

Table 1 Cancers in which perineural invasion (PNI) has been reported.[12]

Cancer type	Incidence PNI (%)
Pancreatic	Up to 100
Head and neck	**Up to 80**
Prostate	75-80
Biliary tract	90
Gastric	50-60
Colorectal	9-33
Cutaneous SCC	**2.5-14**

2.4 Current treatment approach to perineural spread

Cutaneous SCC with incidental PNI is treated with surgical excision, with consideration of adjuvant radiation therapy depending on the existence of other high risk features.[30] The current standard of care for clinical PNI or perineural spread is an appropriately designed en-bloc surgical resection with post-operative radiation therapy.[37] This approach has led to an almost doubling in survival rate.[34] Previously, for cSCC with clinical PNI treated with radiotherapy alone, 5-year DFS was 39%, with a pattern of predominantly local relapse. In comparison, 5-year locoregional control was 64% in a homogenous series of patients with MR imaging positive or histopathologically proven PNS treated with surgery and adjuvant radiation therapy.[37] However, significant morbidity can be associated with the often extensive surgical resection required. In advanced skull base disease, palliative radiation therapy is recommended, given the significant risk of leptomeningeal dissemination.

2.5 Future treatment options

Cetuximab is a chimeric (mouse/human) monoclonal antibody targeting the epidermal growth factor receptor (EGFR) that is a first-line treatment option in combination with radiotherapy for locally advanced cSCCHN.[39,40] Other monoclonal antibodies are in development or trial targeting a range of markers in advanced cSCCHN. However, there is currently no targeted therapy approved or in development for perineural spread as the molecular mechanisms have not been sufficiently elucidated. Targeted therapies may have applications in reducing the morbidity of surgical and radiation therapy, alleviating neuropathic pain, augmenting current therapeutic strategies and providing viable treatment options for currently palliative disease.

2.6 Molecular mechanisms of perineural spread

The mechanisms of perineural invasion and spread are poorly understood, especially in cSCC. Research has been conducted across a range of malignancies displaying PNI, particularly in prostate and pancreatic cancer. There is literature on mucosal head and neck squamous cell carcinoma (HNSCC) with some evidence to suggest that similar mechanisms may underlie invasion and spread along cranial nerves of cSCC in the head and neck region (cSCCHN).

A variety of investigative techniques and *in vitro* and *in vivo* models have been used to study this unique form of tumour spread. Biomarkers and mediators prominent in other malignancies have guided investigation thus far. A bias exists for drug targets with therapies already on the market or in clinical trial with the potential to be re-purposed.

2.6.1 Tumour-nerve microenvironment

The importance of the tumour microenvironment in facilitating advanced disease and nodal and distant metastasis is well understood. This environment comprises the extracellular matrix, the immune infiltrate and reciprocal interactions of these elements with invading tumour cells.

Particular characteristics of the nerve microenvironment are similarly theorised to contribute to and facilitate perineural invasion and spread. An increasing weight of evidence suggests it is the reciprocal interactions between tumour cells and neural tissue that culminates in perineural invasion (Figure 5). A phenotypic change in tumour cells is thought to facilitate an enhanced growth and survival response within the nerve microenvironment. Similarly, the tumour microenvironment promotes neurite outgrowth and infiltration into and around tumour.

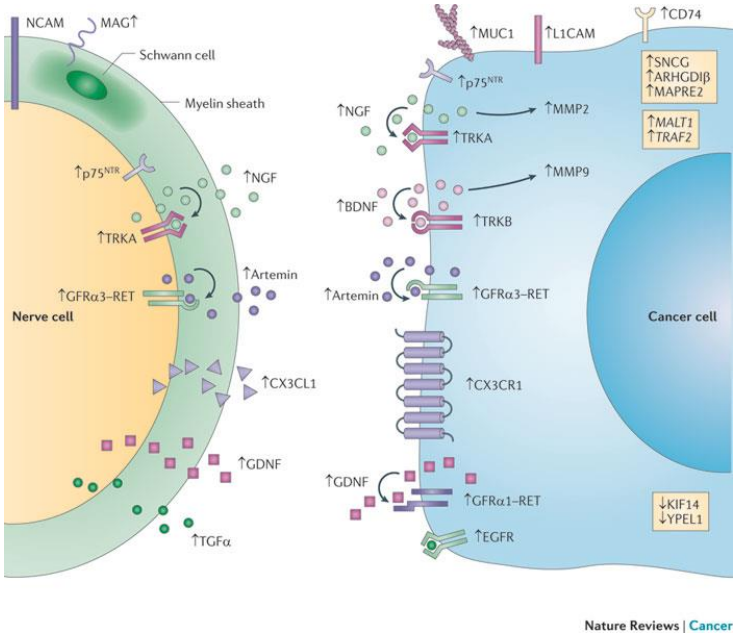

Figure 5 **Reciprocal interactions in the nerve-tumour microenvironment.** Up or down-regulated expression of gene products in pancreatic ductal adenocarcinoma with perineural invasion (PNI) showing how reciprocal interactions between tumour cells and the nerve microenvironment likely culminate in perineural invasion. Multiple signalling molecules from different signalling pathways are involved in the process. Neurotrophins include nerve growth factor (NGF) and brain-derived neurotrophic factor (BDNF) which bind to tropomyosin-receptor kinase A (TRKA) and TRKB, respectively, as well as the low-affinity neurotrophin receptor ($p75^{NTR}$). The secreted glial cell line-derived neurotrophic factor (GDNF) forms a complex with GDNF receptor-α1 (GFRα1) and rearranged during transfection (RET) receptor tyrosine kinase. Cell surface molecules implicated in PNI include mucin 1 (MUC1), myelin-associated glycoprotein (MAG), L1 cell adhesion molecule (L1CAM), neural cell adhesion molecule (NCAM) and the chemokine ligand 1-receptor (CX3CL1-CX3CR1) complex. Differentially expressed genes include mucosa-associated lymphoid tissue lymphoma translocation gene 1 (MALT1) and tumour necrosis factor receptor-associated factor 2 (TRAF2). Differentially expressed proteins include synuclein-γ (SNCG), RHO-GDP dissociation inhibitor-β (ARHGDIβ), microtubule-associated protein RP/EB family member 2 (MAPRE2), yippee-like 1 (YPEL1) and kinesin family member 14 (KIF14). The epidermal growth factor receptor (EGFR), transforming growth factor-α (TGFα) and matrix metalloproteinases (MMP) also play important roles within the microenvironment. Image adapted from Bapat et al (2011).[12]

A range of cell types and secreted proteins within and in proximity to the nerve sheath play are thought to play key roles. Schwann cells and fibroblasts are integral components of the nerve microenvironment, although their potential roles in PNI remain poorly defined. Endoneural macrophages were shown to be a prominent component of the perineural environment in both human PNI specimens and animal models of PNI.[41] Moreover, they are involved in reciprocal signalling *via* secretion of molecules, including glial cell-derived neurotrophic factor (GDNF), that induce perineural tumour cell growth. A recent study by Deborde et al (2016) revealed a sub-population of Schwann cells that was associated with tumour cells in mouse and human specimens of pancreatic adenocarcinoma with perineural invasion.[42] The authors went on to show with *in vitro* studies that Schwann cells induce cancer cell dispersion and neurite invasion in a contact dependent manner and that this is inhibited when neural cell adhesion molecule (NCAM) is depleted.[42] These findings highlight the active role the nerve microenvironment plays in the process of perineural invasion and spread, within a milieu of chemokines and other factors.

A similarly novel study by Chawla et al (2016) examined specifically the immune cells and molecules in the perineural tumour microenvironment.[43] Nearly 60% of the cohort had at least moderate lymphocytic infiltrate, comprising B and T cells, and including a sub-population of FoxP3 (forkhead box P3) positive natural regulatory T cells. In particular, positive staining for galectin-1, the prototypical galectin, a family known to be involved in immune mediation, was found to be a significant predictor of poor patient outcome.[43]

To date, a majority of research into the molecular mechanisms of perineural growth has focused on the neurotrophin family of peptides and their respective receptors, given their known roles in promoting the development and survival of the peripheral nervous system (Table 2). More

recently, several novel candidates have emerged. However, first it is important to consider the various models used by different research groups in characterizing PNI/PNS.

Table 2 Meta-analysis of neuropeptides in head and neck squamous cell carcinoma (HNSCC) using 16 independent studies. Meta-analyses were conducted as one-sample t-tests (significance p=0.05) to compare the expression of neurotrophins and neuropeptides in HNSCC and normal tissue samples. Adapted from Scanlon et al (2015).[44]

Full name (gene)	*N* (significant/non-significant studies)	*t*-test (df)	*P* value
Galanin (GAL)	16 (6/10)	2.6 (15)	0.01005
Brain-derived neurotrophic factor (BDNF)	16 (4/12)	1.789 (15)	0.025
Neural growth factor (NGF)	16 (3/13)	1.364 (15)	0.0963
Glial cell line-derived neurotrophic factor (GDNF)	12 (2/10)	1.0393 (11)	0.1607
Neurotrophin-3 (NTF3)	16 (2/14)	0.8783 (15)	0.1968
Neuropeptide Y (NPY)	16 (2/14)	0.8783 (15)	0.1968
Peptide YY (PYY)	16 (1/15)	0.2 (15)	0.4221
Vasoactive intestinal peptide (VIP)	16 (1/15)	0.2 (15)	0.4221

2.6.2 Modelling perineural growth

2.6.2.1 In vitro models

Despite the difficulties in modelling the complex system of perineural invasion, several *in vitro* models have been developed, which has allowed investigation of factors promoting PNI in a controlled experimental environment. Ayala et al (2001) were the first to develop an *in vitro* model by co-culturing human prostate cancer cells and mouse dorsal root ganglion (DRG) in Matrigel matrix (Figure 6).[45] Reciprocal interactions between the DRG and tumour cells were consistently demonstrated.[45,46] This 3-dimensional system allowed observation of growth of cancer cells towards the DRG and simultaneous outgrowth of neurites towards cancer cell colonies. In 2004, the same group went on to evaluate prostatic tumour PNI cells in human tissue microarrays.[46] Real-time quantitative polymerase chain reaction (PCR), immunohistochemistry and immunofluorescence were performed. It was found that prostate

cancer cells in the perineural environment displayed increased proliferation and reduced apoptosis in comparison to control cell lines. Proliferative index (PI) was higher in human cells at PNI sites and in the model when co-cultured with DRG. Subsequent profiling demonstrated differential expression of 15 genes, with upregulation of 3 genes involved in the anti-apoptotic nuclear factor kappa-light-chain-enhance of activated B cells (NFκβ) pathway in particular noted.[46]

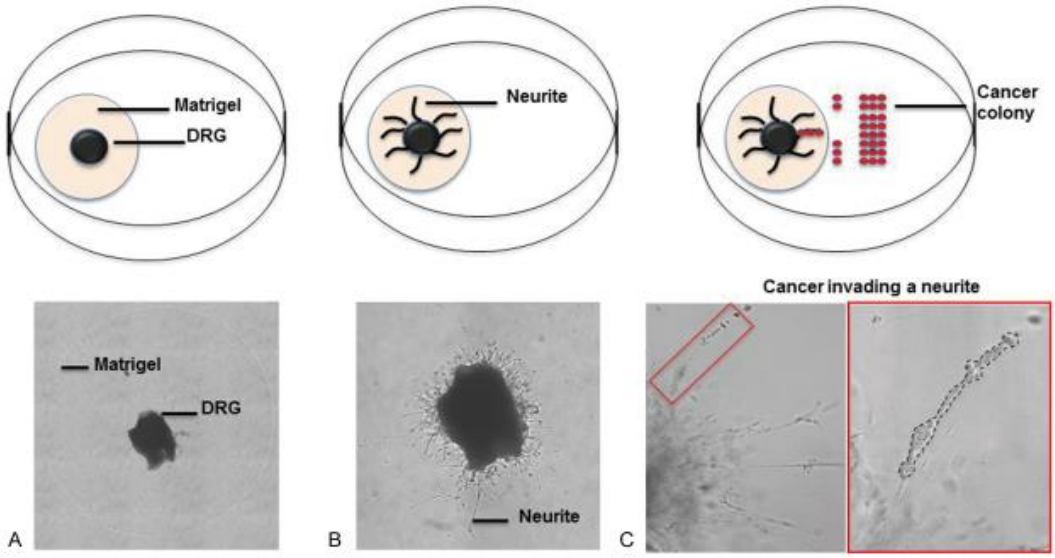

Figure 6 ***In vitro*** **mouse dorsal root ganglion (DRG) co-culture model**. Reciprocal interactions between cancer cells and outgrowing neurites have been observed using this model. Our collaborators at QIMR Berghofer showed that A431 cells have a high propensity for neural invasion using a similar model. Image adapted from Bakst and Wong (2016).[47]

2.6.2.2 Ex vivo models

An *ex vivo* model was previously developed to monitor perineural invasion and spread along surgically resected rat vagal nerves by a range of human pancreatic tumour cell lines.[48] The authors selected for nerve invasive cell line clones by placing dissected segments of rat vagus nerve in purpose-built nerve invasion chambers placed on tissue culture plates. Cell suspensions were poured into the chambers and cancer cells could migrate along the nerve towards the culture plate. Genome-wide transcriptional analyses were employed to identify the

consensus set of genes differentially regulated in highly nerve-invasive versus less nerve-invasive pancreatic tumour cell lines. The authors identified the involvement of kinesin family member 14 (KIF14) and Rho-GDP dissociation inhibitor beta, and correlated this with upregulation of mRNA levels in pancreatic cancer patients. Notably, these proteins play intrinsic roles in normal mechanics of cell migration. It is foreseeable that any such proteins would be upregulated in tumour cells with the demonstrated capacity of metastatic spread, perineural or otherwise, without this providing valuable insight into the actual drivers of perineural invasion and the mechanisms by which tumour cells enter and progress along the perineural space. However, such markers may be useful as prognostic factors allowing appropriate intensification or de-escalation of treatment in the clinic.

2.6.2.3 In vivo models

Several groups have used genetically engineered carcinogenesis-induced murine models to characterise the progression of pancreatic and prostate tumours that have a natural predilection for nerve invasion.[49] This ensures the nerve microenvironment remains intact as opposed to aforementioned models where PNI is facilitated or staged. These models have allowed effective study of tumour evolution in the context of the nervous system. However, the fundamental mechanisms of PNI remain uncharacterised. Orthotopic murine models exist for a wide range of malignancies, where tumour cells, are transplanted into the native organ of immunosuppressed mice. Specifically, pancreatic, prostate, salivary, head and neck and cSCC models have been used to investigate cancers that undergo PNI.[50]

In investigating cSCC with PNS our collaborators at QIMR Berghofer were the first to develop a live mouse model where human SCC cells are injected subcutaneously into the cheek of a nude immunosuppressed mouse (Figure 7).[51] Invasion and spread along the over-developed

mouse trigeminal nerve ensues in up to 40-50% of tumours.[51] There is potential for labelled tumour cells to be followed over time with imaging and/or serial frozen or formalin fixed sections as well as re-isolation of perineural tumour cells for genomic and proteomic analyses. This model also has significant potential for the future testing of targeted therapeutics.

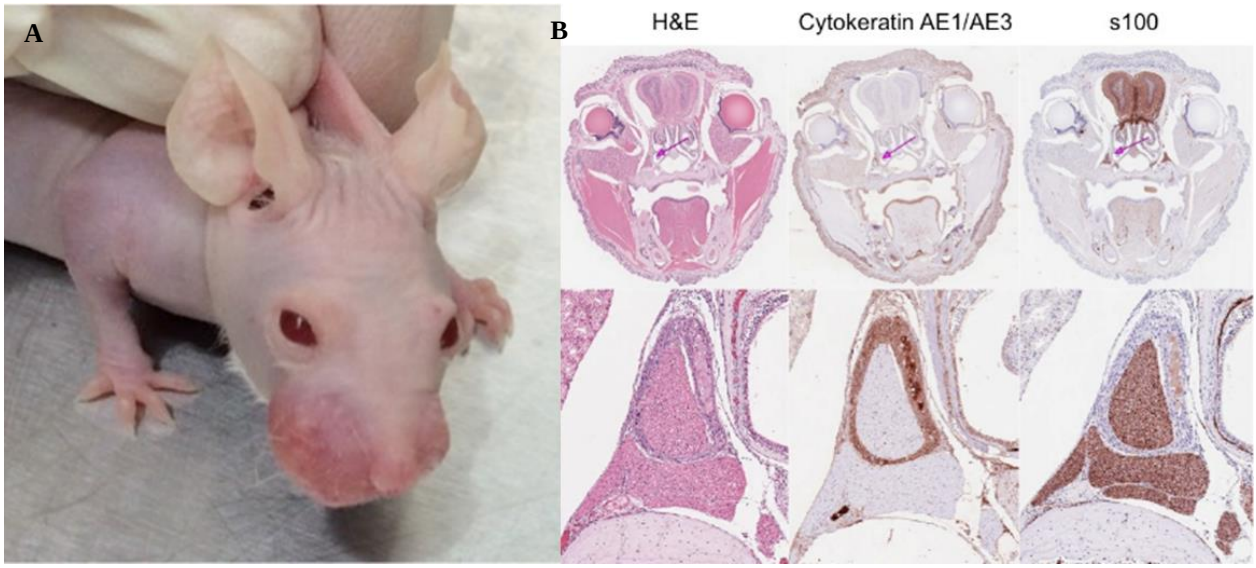

Figure 7 ***In vivo*** **subcutaneous mouse model of perineural spread.** Mouse inoculated with A431 cells develops cheek tumour with potential for invasion of maxillary division of trigeminal nerve (A). Histopathological analysis using haematoxylin and eosin and special immunohistochemical stains (pan-cytokeratin AE1/AE3 for epithelial tumour cells and S100 for myelin sheath) demonstrates perineural tumour spread (B). Image adapted from Gardiner et al (2016).[51]

A subcutaneous mouse transplantation model of perineural invasion of human pancreatic cancer was previously developed by Koide et al (2006).[52] The authors injected tumour cells in suspension subcutaneously on the midline dorsum of nude mice. At 6 weeks, the tumours were resected allowing microarray profiling to be performed. Another research group has developed an *in vivo* heterotopic model where tumour cells are injected directly into mouse sciatic nerve.[53,54] The ease of serial functional neurological and muscle bulk measures, as well as macroscopic and histologic evaluation is advantageous in following perineural spread. Moreover, magnetic resonance imaging can be performed to accurately quantify the degree of

sciatic nerve involvement. To date, only results with prostate and pancreatic cell lines have been published.

Most recently, Scanlon et al (2015) developed a novel chick embryo chorioallantoic membrane (CAM) model to investigate PNI in HNSCC cells.[44] In this *in vivo* model, adjacent rat DRG and labelled human HNSCC cells were introduced onto chorioallantoic membrane. The CAM is understood to mimic the pro-angiogenic microenvironment seen in tumourigenesis and nourishes both the DRG and tumour cells as nerve-tumour interactions are observed. Cell tracking was performed and the CAM harvested after 48 hours for imaging analysis of tumour spread and neurite outgrowth. The authors identified the ligand galanin and its receptor GALR2 to be novel candidates highly involved in the process of perineural invasion.[44]

2.6.3 Neurotrophins and the Trk receptor family

The neurotrophin family of growth factors is involved in development of the nervous system and is critical in peripheral nerve growth, maintenance and axon guidance. There is increasing literature to suggest that neurotrophins are involved in pro-survival signalling in many different forms of cancer.[55] Identified members of the family include the canonical nerve growth factor (NGF), brain-derived neurotrophic factor (BDNF), GDNF, neurotrophins 3 and 4 (NT-3, NT-4) and galanin. After protease cleavage, these molecules display variable high affinity binding to a family of receptor tyrosine kinases known as the Trk receptors. NGF has high affinity for TrkA, BDNF and NT-4 for TrkB and NT-3 for TrkC receptors, respectively. Phosphorylation leads to downstream signalling that modulates cell survival and proliferation. In neurons, signalling modulates axonal and dendritic outgrowth. Immature neurotrophins bind the $p75^{NGFR}$, a member of the death receptor superfamily, to which mature neurotrophins maintain a low affinity (low-affinity NGFR).

Much of the focus in elucidating the mechanisms underlying perineural invasion has centred on these neurotropic factors, given their undisputed prevalence in the nerve microenvironment. Findings have been somewhat inconsistent, however. A recently conducted meta-analysis compared expression of neurotrophins and neuropeptides between HNSCC and non-cancerous samples across 16 independent studies (Table 2). While not assessing tissue biopsies of perineural invasion or spread, the authors found that the neuropeptides galanin (GAL) and BDNF were significantly overexpressed whereas NGF, GDNF, NT-3 and other neuropeptides were not.[44]

2.6.3.1 NGF/TrkA and NGF/p75 receptor axes

NGF and its high and low affinity receptors are well studied in PNI. The NGF/TrkA high affinity receptor axis has been implicated in breast, prostate and pancreatic cancers with perineural growth and NGF is known to be over-expressed in HNSCC.[56,57] NGF was seen to be prevalent in both normal and tumorigenic prostate tissue in a study by Geldof et al (1998).[56] One study demonstrated higher intensity staining for NGF/TrkA in oral tongue SCC with PNI (n=21) compared to those without PNI (n=21).[57] In a retrospective analysis of adenoid cystic carcinoma (ACC), NGF/TrkA immunostaining was strongly correlated with PNI, while Myb and $p75^{NGFR}$ overexpression were not.[58] Dolle et al (2003) showed that nerve growth factor (NGF) is synthesized and released by breast cancer cells.[59] Moreover, inhibition of NGF or its receptor TrkA (with K-252a) significantly reduced the cancer cell growth, suggesting an autocrine feedback mechanism.[59] Targeting the NGFR and NFκβ pathways has also shown promise in a number of breast cancer cell line studies.[60-62] Locally injected anti-NGF antibodies have similarly demonstrated success in inhibiting animal models of pancreatic and prostate cancer.[59] Anolik et al (2015) reported a pattern of p75 staining in cSCC, which is also well recognised in oral and oesophageal SCC.[63]

Only two studies have looked at the role of TrkA in PNI in cutaneous SCC. The first study of cutaneous carcinoma with PNI compared immunohistochemistry of nine PNI-positive tumours (4 BCCs; 5 SCCs) with seven PNI-negative tumours (4 BCCs; 3 SCCs).[64] More intense staining for $p75^{NGFR}$ was qualitatively described in perineural portions of PNI-positive SCC tumours (80%) compared to PNI negative tumours. Moreover, staining for TrkA, B and C receptors was also more intense in PNI positive cSCC. However, small sample size, limited specificity of labelling antibodies and lack of quantitative evaluation limit conclusions from this study.

A more recent study by Frydenlund et al (2015) took 57 cSCCHN and 53 cSCC from other locations and analysed for PNI and TrkA expression using a novel double immunostaining (DIS) protocol.[31] While TrkA expression was more frequently observed in cSCCHN compared to other sites and correlated with high-risk variants in this group, no association with PNI was found.

2.6.3.2 NT-3/TrkC receptor axis

The previously described increased expression of Trk receptors in PNI-positive cutaneous SCC may suggest a role for NT-3 and NT-4 in perineural growth.[31] Previous studies in pancreatic ductal adenocarcinoma (PDAC) have revealed NT-3/4 overexpression in both tumour cells and nervous tissue compared to normal pancreatic tissue by mRNA analysis.[65] NT-3 blockade has also halted growth of prostate and pancreatic cancers in murine models.[66]

2.6.3.3 GDNF

The GDNF family includes neurturin, artemin, persephin and the namesake peptide GDNF. Secreted in the nerve microenvironment, binding occurs to specific GDNF receptors, which then cooperatively signal through membrane-bound rearranged during transfection (RET) receptor tyrosine kinases. GDNF has been extensively investigated in pancreatic cancer and also examined in bile duct carcinoma. Over-expression of GDNF and its RET receptor is seen in a number of neurotropic cancers and associated with progression in PDAC.[54] Cancer cells have been shown to migrate towards nerves via chemotaxis along a GDNF gradient in vitro.[53] Moreover, blockade of the RET receptor attenuates this effect. A recent study by Gao et al (2015) similarly demonstrated that artemin and its receptor, GDNF receptor-α1 (GFRα1), are overexpressed in PDAC and associated with neurotropy.[67] GDNF signalling axes may play an important role in PNI and spread.

2.6.3.4 Neural cell adhesion molecule

Neural cell adhesion molecule (NCAM) belongs to a family of adhesion molecules functioning in embryogenesis, cell growth and differentiation. The data for NCAM in the literature is inconsistently associated with perineural growth. In rectal cancer, NCAM is significantly associated with PNI.[68] Similarly, in one study of ACC, NCAM was highly expressed in 100% of tumours, regardless of PNI status. However, given the neurotropism ACC displays this is not an insignificant finding.[69] In another study (n=49), perineural invasion was more common in positive NCAM staining tissue.[70] The earliest cSCC study by Chen-Tsai et al (2004) was inconclusive, with 75% of cSCC expressing no NCAM at all.[64] A later study by Solares et al (2009) performed immunostaining, with an anti-CD56 antibody, in 14 cSCCHN with clinical PNI, 14 tumours without PNI and 4 normal nerves.[71] The authors found there to be no NCAM expression in any cSCCHN specimens, despite being strongly expressed in normal nerve tissue,

concluding no correlation of NCAM expression with perineural invasion in cSCCHN.[71] Other studies by Vural et al (2000) and McLaughlin et al (1999) did not differentiate between incidental and clinical PNI in demonstrating the converse finding.[72,73]

2.6.4 Chemokines

The directional nature of tumour cell perineural invasion makes chemotactic factors a logical avenue for investigation. A recent study showed that chemokine (C-C motif) ligand 2 (CCL2/CCR2) signalling mediated prostate cancer cell migration and PNI in an *in vitro* model.[74] In this study a proteomic profiler chemokine assay was utilised to screen for secreted factors in the nerve microenvironment. Knockout studies for CCL2 demonstrated that CCR2 activation facilitates perineural invasion. Furthermore, IHC revealed that 95% of prostate adenocarcinoma with PNI tissue specimens evaluated, exhibited CCR2 expression (n=20/21), supporting its potential as a future therapeutic target.[74] Another similar signalling pathway, chemokine (C-X3-C motif) ligand 1 (CX3CL1) binding CX3CR1 receptor, has demonstrated high expression in pancreatic and prostate cancers with PNI.[13,75] The CX3CR1 receptor is known to be heavily upregulated in malignant pancreatic epithelium. In binding its ligand, the transmembrane chemokine CX3CL1, which is expressed by neurons, exhibits intrinsic cell-adhesive properties. Overexpression of CX3CR1 has been linked to metastasis in both prostate and breast cancer. Marchesi et al (2008) went on to demonstrate that high CX3XR1 expression was associated with perineural invasion, and subsequent risk of local recurrence in pancreatic cancer specimens.[75] *In vitro*, CX3CL1 promotes chemotaxis of pancreatic cancer cell lines and *in vivo* potentiates nerve infiltration of pancreatic tumours, revealing another potential drug target.[75]

2.6.4.1 Galanin

A recent study by Scanlon et al (2015) rigorously investigated the role of galanin (GAL) in PNI and suggested the galanin receptor pathway as a novel therapeutic target for mucosal HNSCC with PNI.[44] The authors demonstrated that in HNSCC, galanin binds the GALR2 receptor, which is one of three known G-protein coupled receptors for galanin. Downstream signalling was shown to induce neurogenesis in adjacent nerves, thus facilitating PNI.[44] Using the novel *in vivo* CAM model discussed earlier, they were able to elegantly demonstrate the reciprocity of interactions at the nerve-tumour interface, as first described by Ayala et al (2001) with their prototypical *in vitro* DRG-Matrigel model of PNI.[45]

2.6.5 Ephrin/Eph receptor family

The erythropoietin-producing hepatocellular carcinoma (Eph) receptor family comprises 14 membrane-bound receptor tyrosine kinases (RTKs) in two receptor classes, class A and class B.[76] There are nine EphA (EphA1-8, Eph10) and five EphB (EphB1-4, EphB6) receptors that have been identified in humans.[77] These selectively interact with Eph receptor interacting proteins (ephrins) on neighbouring cell surfaces (Figure 8). Ephrins are named for their selective binding to either the A or B subfamilies, with EphA receptors binding ephrin-A ligands and EphB receptors binding ephrin-B ligands with high specificity. Notable exceptions are the EphA4 receptor, which can bind both ephrin A and B ligands, the EphB2 receptor, which can bind ephrin-A5 ligand, and the EphB4 receptor, which binds ephrin-B2 ligand exclusively. As both ligands and receptors are predominantly membrane-bound, Eph/ephrin interactions occur at sites of cell-cell contact or in plasma membrane clusters. Ligand binding triggers bidirectional kinase-dependent cytosolic signalling cascades.[78] Receptor-expressing cells undergo tyrosine kinase dependent forward signalling while reverse signalling occurs via Src family kinases in ephrin-ligand expressing cells.[78] Like other receptor tyrosine kinases,

on ligand binding, Eph receptors dimerise and undergo auto-phosphorylation with subsequent kinase activity. There are multiple downstream signalling effector pathways.

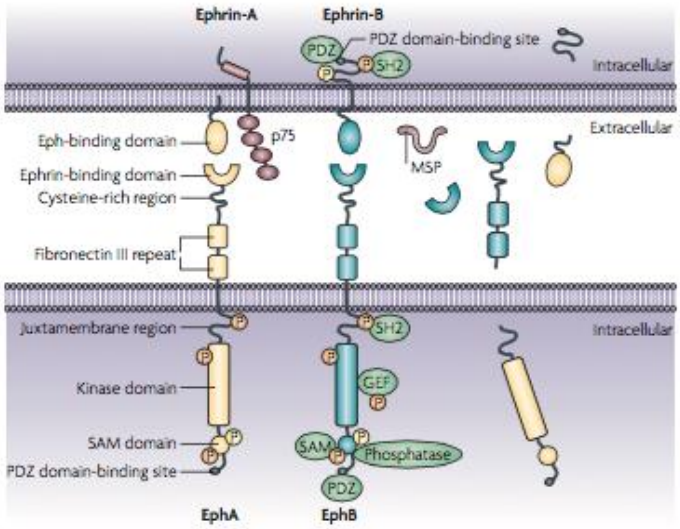

Figure 8 Eph receptors and ephrin ligand interactions of A and B classes involve bidirectional signalling. Ephrin binding induces Eph receptor clustering, autophosphorylation and downstream forward signalling. Transmembrane ephrin-B ligands and glycosylphosphatidylinositol (GPI)-linked ephrin-A ligands mediate reverse signalling upon binding to their respective membrane bound Eph receptors. Figure from Pasquale et al (2010).[78]

Eph/ephrin interactions have critical roles in developmental processes and normal adult physiology.[78] They are involved in regulating adhesion and migration at a cellular level, largely by modulating integrin signalling and binding of the ECM components laminin, collagen and fibronectin.[79] They have particularly important roles in neurodevelopmental processes, including axon guidance and neuronal circuitry.[80] They are also known to be important in normal human skin homeostasis, where EphA1, EphB3 and ephrin-A3 are expressed at high levels compared to other adult tissues.[77,81]

The Eph receptors/ephrins have also been implicated in tumourigenesis, progression and metastasis across a wide range of malignancies (Table 3).[82] However, their activities are evidently complex with both increased and decreased Eph receptor expression associated with cancer progression on review of the literature.[76] Mutations in Eph receptors are also likely to have a role in tumour development and progression. Eph receptors and ephrins are commonly expressed not only in cancer cells but also in the tumour microenvironment.[78] They potentially facilitate abnormal cell-cell communication between tumour compartments.[78]

Table 3 Erythropoietin-producing hepatocellular (Eph) receptor expression in various cancer types

Expression	**Eph receptor**	**Cancer type**
Upregulated	EphA2	Adenoid cystic carcinoma[83] Prostate cancer[84,85] Breast cancer[86,87] Melanoma[88] Glioblastoma[89,90] Gastric cancer[91]
	EphA3	Gastric cancer[92] Colorectal cancer[93]
	EphB2	Advanced cSCC[94] Glioblastoma[95-97] Cervical cancer[98] Breast cancer[99]
	EphB4	HNSCC[100] Non-small cell lung cancer[101] Breast cancer[99]
Downregulated	EphA1	NMSC[77]
	EphA2	Chemically induced murine SCC[102]
	EphA3	Renal clear-cell carcinoma[103]
	EphB2	Prostate cancer[104] Colorectal cancer[105,106] Gastric cancer[107] Transitional cell carcinoma[108]

Both EphA2 and EphB4 are seen to be upregulated in a wide range of cancers.[109] EphB4 was shown to be highly expressed in the majority of HNSCC tumours evaluated in a study by Ferguson et al (2014).[100] Conversely, the EphA1 receptor is downregulated in advanced cSCC and along with the EphB receptors is also downregulated in advanced colorectal cancer.[77,105] Notably, significant EphA1 downregulation was observed by Hafner et al (2006) in a study of 32 cutaneous SCCs compared to normal epidermis and appeared to correlate with tumour thickness.[77] With respect to the tumour microenvironment, both ephrinA1/EphA2 and ephrinB2/EphB4 signalling has been characterised in tumour vasculature.[78]

Moreover, EphB2 was shown to be overexpressed in human cSCC compared to premalignant lesions and normal skin in a study by Farschian et al (2015).[110] Knockdown of EphB2 signalling resulted in down-regulation of genes associated with cell invasion, including matrix metalloproteinases MMP1 and MMP13, and inhibited progression and invasion of human SCC cell lines. This is early evidence of the role of EphB2 in aggressive advanced cSCC and suggests a possible therapeutic target. EphB2 may well be over-expressed in the subset of advanced cSCC with perineural spread and certainly warrants further investigation in this sub-population.

A study by Shao et al (2013) recently implicated EphA2/ephrinA1 in adenoid cystic carcinoma of the salivary gland.[83] Increased levels of mRNA and expression of product proteins EphA2 and ephrinA1 was seen in ACC tissue compared to normal gland tissue by immunoprecipitation, PCR and IHC. This correlated with clinical tumour-node-metastasis (TNM) staging, vascular invasion and perineural invasion. In one instance, nerve invaded by ACC cells showed ephrinA1 staining with weak EphA2 staining also observed. Together, these

findings suggest a possible role of EphA2/ephrinA1 interactions in perineural invasion of ACC.[83]

The Eph/ephrin signalling pathway is a current research focus in the development of targeted therapies to either interfere with tumour promotion or enhance tumour suppressor effects.[78] It is also becoming clear that Eph/ephrin signalling may play a role in resistance to anti-cancer therapies. In breast cancer tumour xenograft studies, EphA2 expression is associated with resistance to tamoxifen (anti-oestrogen receptor antibody) and Herceptin (anti-HER2 receptor antibody).[111] Several clinical trials with anti-Eph receptor agents are currently underway, including an EphA2 inhibitor (Dasatinib) in various solid tumours and an anti-EphB4 agent (XL647) in non-small cell lung cancer (NSCLC).[111]

Little is known about Eph/ephrin expression in the perineural compartment or tumour cells invading the perineural space. Invasion of tumour cells and subsequent spread along the perineural space is probably cell-cell contact dependent. Interestingly, EphB/ephrinB, particularly EphB1/ephrinB2, interactions have also been implicated in neuropathic pain caused by cancer, inflammation and nerve injury.[112] In a rodent model, EphB receptor inhibition has been shown to alleviate neuropathic pain.[112]

Given the demonstrated importance in neurodevelopmental processes, normal skin physiology, the balance between tumour suppression and tumour progression and neuropathic pain, the Eph/ephrin pathway is a candidate signalling axis for investigation in perineural invasion and spread of cSCCHN. Certainly, there is a gap in knowledge regarding this family of RTKs in perineural spread of carcinoma. Dysregulation of cell-surface ligand/receptor expression in

tumour cells and/or the nerve-tumour microenvironment may potentially facilitate infiltration of the perineural space and subsequent progression.

2.6.6 ErbB receptor family

The ErbB family is a group of homologous transmembrane RTKs comprising EGFR (HER1, ErbB1), HER2 (ErbB2), HER3 (ErbB3) and HER4 (ErbB4). Each receptor has an extracellular ligand-binding domain, a transmembrane region and an intracellular cytoplasmic domain which includes a tyrosine kinase residue (Figure 9).[113] These receptors are activated by growth factors such as the epidermal growth factor (EGF) and related ligands. Receptor activation by ligand binding leads to homo- or heterodimerisation and trans-phosphorylation of corresponding tyrosine kinase domains. This leads to activation of well characterized intracellular signaling pathways involved in cell proliferation, survival, differentiation and migration (Figure 9).[113]

EGFR is the prototypical RTK and is activated by its ligand EGF and other closely related growth ligands. HER2 has a non-functional ligand binding domain and thus exists in a constitutively activated conformation, making it the preferred dimerization partner for other receptors.[114] HER3 has a kinase domain dependent on phosphorylation with another ErbB receptor and is thus considered an impaired RTK.[114]

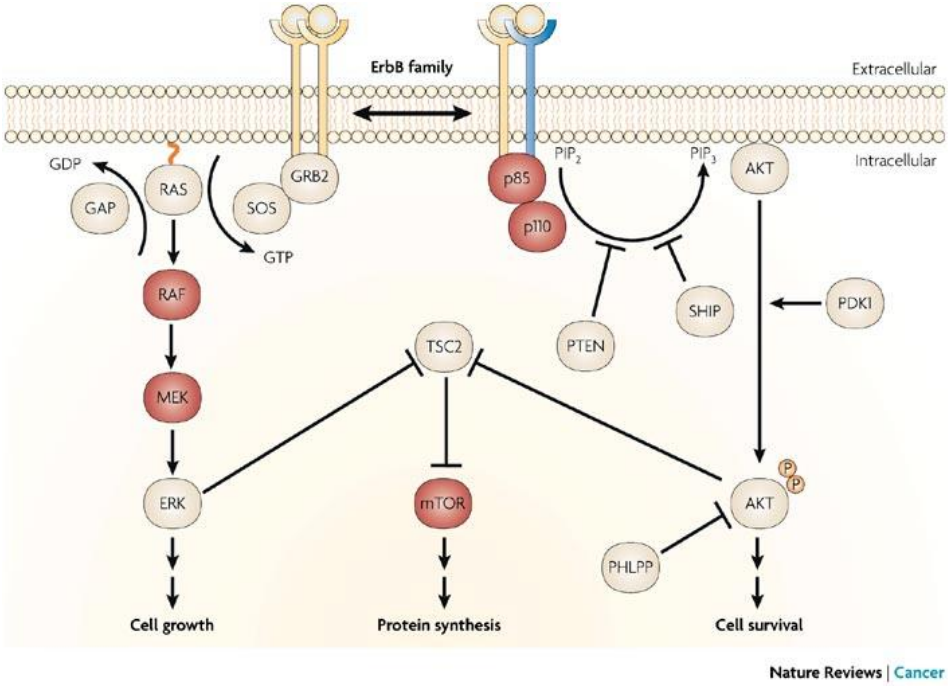

Figure 9 Downstream signaling pathways of activated ErbB receptor tyrosine kinases. Stimulatory (open) and regulatory (closed) arrows are shown. Mitogen-activated protein kinase (MEK), extracellular signal-regulated kinase (ERK), tuberous sclerosis complex 2 (TSC2), mechanistic target of rapamycin (mTOR), PH domain and leucine rich repeat protein phosphatases (PHLPP), Ptdlns(3,4,5)P3-dependent protein kinase (PDKI), SH2-containing inositol phosphatase (SHIP), phosphatase and tensin homolog (PTEN), son of sevenless (SOS), guanosine triphosphate (GTP), guanosine diphosphate (GDP), growth factor receptor-bound protein 2 (GRB2), GTPase-activating protein (GAP). Figure from Sharma et al (2007).[115]

Downstream signaling pathways include the phosphatidylinositol 3-kinase (PI3K)/Akt pathway and the Ras/Raf/MEK/MAPK (mitogen activated protein kinases) pathway.[116] Ligand-induced activation leads to clustering of the receptors into clathrin coated pits which invaginate to form vesicles, a process catalyzed by dynamin, a large GTPase.[117] Thus, dynamin mediates internalization of activated ErbB receptor complexes to the early endosome, where receptors are either recycled back to the cell surface or proceed to lysosomal degradation. Contrary to previous understanding, activation of intracellular signaling pathways

occurs from both the plasma membrane and the endocytic compartment with qualitative differences in signaling recently described.[118] Thus, receptor trafficking is now recognised to be important in modulating downstream signaling.

The dysregulation of ErbB receptor trafficking is associated with tumorigenesis and tumour progression across various malignancies. Some mechanisms well characterized in different tumour types include receptor over-expression and activating mutations in receptors leading to aberrant tyrosine kinase signaling.[113] Overexpression of EGFR is commonly seen in HNSCC, NSCLC and colorectal cancer (CRC) and is most often secondary to gene amplification and results in prolonged signaling even with low ligand concentrations. HER2 overexpression is commonly observed in breast and gastric cancers.[119] One other mechanism by which ErbB receptors potentiate cancer is through activating mutations which allow escape from normal regulation. The EGFRvIII mutation leads to a truncated receptor lacking a functional ligand binding domain.[115] Effects are twofold, the receptor is constitutively phosphorylated leading to constant activation of MAPK and PI3K/Akt pathways and secondly there is no catalyst for internalization allowing prolonged signaling. This mutation is commonly seen in NSCLC but is not significant in mucosal HNSCC.

2.6.6.1 EGFR expression in cSCCHN

EGFR overexpression is documented in approximately one third of epithelial malignancies across head and neck, colorectal, breast, ovarian, prostate, bladder and lung cancers.[120] In cutaneous SCC, EGFR over-expression is reported in approximately 35% of primary cSCC and up to 58% of advanced local cSCC or nodal metastatic disease (Table 4). To our knowledge, no previous study has examined EGFR expression in perineural spread of cSCCHN at the protein level. In unpublished data from our own laboratory, 48% of cutaneous

SCC (n = 58/120) were EGFR over-expressing using secondary immunofluorescence techniques (verbal communication, Dr Fiona Simpson, 2016). Perineural spread is an advanced subset of cSCCHN and of note from the literature it is apparent that as disease stage for cSCC increases, positivity for EGFR also increases. Regardless, there is a significant gap in our understanding of EGFR and other ErbB receptor expression in perineural spread cSCCHN.

Table 4 EGFR positivity reported in primary and nodal metastatic cSCCHN

Study	Stage	Primary	Nodal metastasis
Canueta et al (2016)	Primary cSCC	35% (n=33/94)	n/a
Sweeney et al (2012)	Recurrent cSCC (stage III/IV)	56% (n=28/50)	58% (n=7/12)
Ch'ng et al (2008)	Primary cSCC +/- nodal metastasis	36% (n=9/25)	47% (n=7/15)

2.6.6.2 Targeted therapies to the ErbB family

It is unsurprising that the ErbB receptor family has been the focus of novel cancer therapeutic development for some years. Strategies have included immunotherapy using monoclonal antibody therapies (mAbs) which target the patient immune system against tumour cell specific antigens. Small-molecule tyrosine kinase inhibitors (TKIs) have also been developed and are approved in several malignancies (Figure 10).

There are four FDA-approved therapeutic mAbs available in the clinic including both anti-EGFR (cetuximab, panitumumab) and anti-HER2 (trastuzumab, pertuzumab) drugs. Trastuzumab (Herceptin) was the first to be approved for use in HER2 positive metastatic breast cancer and is now also used in high-risk non-metastatic HER2 positive tumours.[121] More recently it was approved for HER2 positive metastatic gastric or gastroesophageal junction cancer.[121] A benefit in patients has only been shown where tumours are demonstrably

HER2 positive. HER2 positive status is associated with aggressive disease and worse patient outcomes in breast and gastric cancer. Trastuzumab is thought to inhibit downstream signaling, induce antibody-dependent cell cytotoxicity (ADCC) and reduce receptor shedding.[122] It also has been shown to work synergistically with some chemotherapy regimens.

Cetuximab (Erbitux) was the first anti-EGFR therapy to reach the market in 2004 as an approved treatment for metastatic colorectal cancer patients with EGFR positive tumours, as a single agent or in combination with chemotherapy.[123] Patients with KRAS mutant tumours or an unknown gene status are not treated with cetuximab, as several sub-group analyses have shown a survival disadvantage in this group.[123] It is also now approved as a first line therapy for locally or regionally advanced HNSCC in combination with radiotherapy, for recurrent or metastatic HNSCC in combination with chemotherapy or in disease progression on standard platinum based regimens.[124]

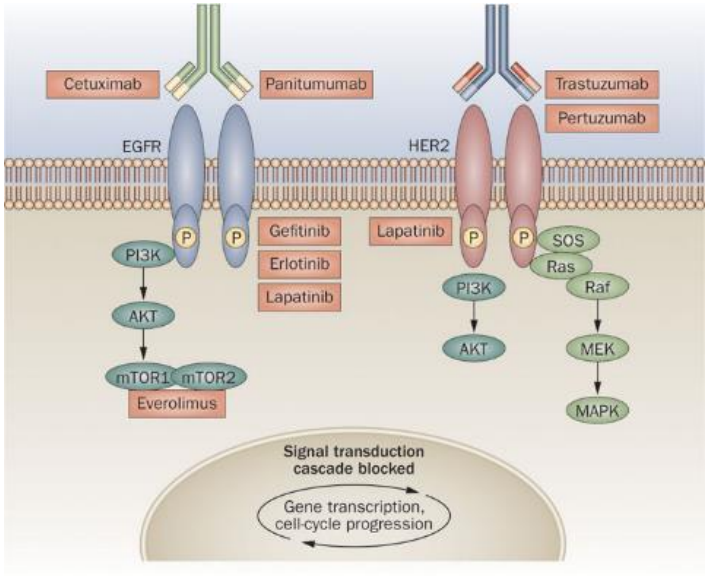

Figure 10 **Targeted therapies against the ErbB receptor family.** Anti-EGFR monoclonal antibody therapies include cetuximab and panitumumab and anti-HER2 monoclonal antibodies include trastuzumab and pertuzumab. Gefitinib and erlotinib are small molecule tyrosine kinase inhibitors

which act on the intracellular domain of EGFR, while lapatinib acts on both the EGFR and HER2 receptors to inhibit receptor tyrosine kinase signaling. Everolimus is an inhibitor of mammalian target of rapamycin (mTOR). Figure from Okines et al (2011).[125]

Anti-cancer immunotherapy is now understood to work both directly and indirectly; directly by inhibiting downstream cell signaling and indirectly by inducing antibody-dependent cell cytotoxicity (ADCC).[126] For example, the chimeric IgG1 cetuximab, through high affinity binding to EGFR, prevents true ligand binding and receptor dimerization, thus inhibiting downstream signaling. Such binding also promotes receptor internalization. Moreover, by binding FcγRIII on natural killer (NK) cells, cetuximab induces ADCC.[127] Classical ADCC involves activation of NK cells, most commonly via their cell surface Fc receptor CD16, also known as FcγRIII, which binds the Fc region of IgG coating the tumour cell, resulting in tumour cell lysis. This has been shown to be an important mechanism of action for Cetuximab and several other therapeutic monoclonal antibodies. Trastuzumab has similar actions in that it binds the extracellular domain of ErbB2 preventing dimerization with other ErbB receptors and promotes downregulation via endocytosis. It also induces ADCC via the FcγRIII receptor on NK cells.[128]

Given the proven role of ErbB receptors in cancers at various sites, including head and neck and cutaneous carcinomas, we postulate a possible role in perineural spread of carcinoma. To our knowledge there has been no study to date examining the role of receptor tyrosine kinases, including the ErbB and Eph receptor families, in perineural spread of cSCCHN.

2.6.7 Genetic profile of cSCCHN with and without PNS

With the advent of next generation sequencing technology, genetic profiling of many cancers has been undertaken. In cSCC there is a massive mutational burden, making identification of

driver genes difficult and translation from genomics to the clinical setting slow.[129-131] There has been significant work looking at progression of AK to cSCC and recognition that like other malignancies, this is a multi-hit process requiring several accumulated genetic and epigenetic alterations in key pathways to culminate in invasive SCC.

The majority of published research in genomic studies of cSCC has revealed and focused on mutations in tumour protein 53 (TP53), NOTCH, RAS, EGFR, SRC-family kinase (SFK), cyclin-dependent kinase inhibitor 2A (CDKN2A), NFκβ and transforming growth factor beta (TGF-β).[132] One of the major recognised cellular drivers of SCC is loss of function of the tumour suppressor gene TP53. Data supports a strong correlation between solar ultraviolet radiation (UVR) and mutational burden in the p53 gene with up to 90% of squamous cell carcinomas exhibiting p53 mutations.[131,133,134] It is thought that UV radiation has direct effects at the TP53 locus with mutations affecting cell cycle regulation and allowing clonal expansion to occur.[134,135] Members of the mitogen activated protein kinase (MAPK) family are also thought to play a significant role in in cSCC.[136]

The EGFR has also been implicated in the carcinogenesis of cSCC at the genetic level. EGFR is known to be constitutively activated in a subset of invasive cSCC and is an important emerging drug target.[133] Homo- or heterodimerisation induced by ligand binding or directly by UVR results in auto phosphorylation of the intracellular tyrosine kinase, activating downstream signalling and promoting cell proliferation, migration, survival and suppression of differentiation.[135] On the other hand, mutations in the EGFR are not known to play an important role in the carcinogenesis or progression of cSCC, as they are at some other sites.

In a recent mutational analysis, Pickering et al (2014) identified 23 candidate driver gene mutations after whole genome sequencing of 39 cases of advanced cSCC.[132] The authors concluded that the mutational signature of advanced cSCC is similar to mucosal HNSCC and dominated by tumour suppressor genes, with 8 of the top mutated genes shared between these tumour types. Similarly, an earlier study by Dooley et al (2003) found genetic profiles between oral SCC cell lines and facial cutaneous SCC cell lines to be highly similar across 23 biomarkers.[137] NOTCH1 and NOTCH2 were both significantly mutated with NOTCH2 positively associated with PNI in this study.[137]

More recently, Li et al (2015) undertook genomic analysis of 29 cases of nodal metastatic cSCC, performing targeted sequencing of 504 cancer-associated genes.[138] The authors focused on identifying clinically significant genomic alterations and found phosphatidylinositol-4,5-bisphosphate 3-kinase catalytic subunit alpha (PIK3CA), fibroblast growth factor receptor 3 (FGFR3), BRAF and EGFR to be potential therapeutic targets.[138] Although informative for our study, nodal metastasis and perineural disease are not inherently related, with only 5.8% of patients with perineural spread presenting with concomitant nodal disease at our institution.[22] While perineural spread is a form of tumour metastasis, we consider it to be distinct from haematogenous or lymphatic dissemination with similarly distinct molecular profile. However, both forms of tumour spread represent aggressive forms of the same underlying malignancy and it is important to consider significant alterations in the nodal metastatic cohort. Interestingly, EphA7 and EphA3/4 were significantly over-expressed in nodal metastatic cSCC in 27% and 20% of specimens, respectively. EphA1, EphA2 and EphB1 were less commonly overexpressed with an incidence of 10% overexpression reported for each receptor.[138]

Comparable results were seen in more recent genomic profiling by Al-Rohil et al (2016) of 122 cSCC cases looking at both primary (63%) and metastatic (37%) lesions.[139] Across these samples they identified a total of 1120 genomic alterations with 88% of cSCCs harbouring at least one clinically relevant genomic alteration (CRGA) for which there is an anticancer drug already on the market or in clinical trial. The most common CRGA was in NOTCH1 (43%) with PTCH, ATM, ErbB4 (HER4), NF1, ErbB2 (HER2), PIK3CA, CCND1, EGFR and FBXW7 over-expression recorded in 5-11% of specimens for each marker.[140]

To date, there have been very few gene-profiling studies to identify driver genes involved in perineural invasion or spread. Using microarray expression analysis to analyse more than 20,000 genes, Mays et al (2015) identified 24 differentially expressed genes between specimens of cSCC with and without microscopic PNI, none of which before had been implicated in perineural disease.[141] However, unfortunately they were unable to identify any biological pathways associated with these differentially expressed genes by gene ontology enrichment analysis. The authors did highlight the possible role of down-regulation of the tumour suppressor gene TXNIP in aggressive PNI, given a > 2-fold reduction was observed in PNI positive specimens. However, this reinforces the necessity and value in focusing on clinically relevant and druggable biomarkers and pathways.

Our collaborators at the Queensland Institute of Medial Research (QIMR) have undertaken whole genome expression profiling of cSCCHN without PNI versus microscopic PNI versus clinical PNS.[142] This study identified a wide range of genes that were differentially up or downregulated across the groups. Several statistically and biologically significant differentials were identified, including downregulation of transglutaminase 3 (TGM3) and up-regulation of lysyl oxidase like 2 (LOXL2) and EphA3 in the perineural spread cohort (Figure 11). TGM3

and LOXL2 were selected for further study in the subcutaneous mouse model, however due to small numbers and variable tumour growth no significant conclusions could be drawn.[51,142] Generous provision of the raw microarray data allowed differential expression levels of Eph receptors and ephrin ligands to be specifically reviewed as part of this thesis (Table 5). In addition to up-regulation of EphA3, EphA4 and EphA5 were elevated without reaching statistical significance. Downregulation of EphA1 as well as EphB1 and EphB6 was also observed in perineural spread cSCCHN compared to control cSCCHN.

Gene	Function
ASPRV1 aka TAPS	Critical for homeostasis of epidermis; its expression correlates with keratinocyte differentiation
CST6	Tumor suppressor gene; loss associated with invasiveness in breast, prostate ca & melanoma
TGM3	Catalyses cross linking of proteins; significantly downregulated in various cancers
SOX21	Pro-apoptotic; blocks Sox1 which keeps stem cells in immature & proliferative state
SPINK7	Tumor suppressor gene; regulates migration/invasiveness of cells in esophageal ca
DSG1	Transmembrane component of desmosome (cell-cell junction); down regulation associated with worse prognosis in HNSCC

Gene	Function
FOXC2	correlates with lymph node mets in bowel CA, oesophageal SCC prognosis, basal-like breast CA, Involved in transition to metastasis
LOXL2	Involved in transition to metastasis, head and neck, breast CA and oesophageal mets
ATF3	Activating transcription factor, promotes tumour progression, high in tumour stroma correlates with aggressiveness of cSCCs
EPHA3	TSG yet upregulated in head and neck SCC and HCC and breast CA, Higher in colorectal CA mucosa
MDK	growth factor which promotes angiogenesis, cell migration and cell growth, assoc with desmoid tumours, laryngeal SCC
FN1	Involved in cell adhesion, migration and metastasis

Figure 11 Main target genes identified as downregulated (left panel) or upregulated (right panel) in perineural spread cSCCHN compared to cSCCHN without perineural invasion. Gene microarray analysis was performed at QIMR Berghofer by Dr Glen Boyle in collaboration with Prof Ben Panizza, who generously provided this image.[142] Function of each gene is briefly described. Ca, cancer; HNSCC, head and neck squamous cell carcinoma.

Table 5 Data extracted from gene microarray analysis of cSCCHN with and without perineural spread for ephrin ligand/Eph receptor gene expression.

Gene	**Regulation**	**Absolute FC**	**P-value** (Mann-Whitney)
EphA3	Up*	6.31	0.001
EphA5	Up	1.80	0.001
EphA4	Up	1.02	0.013
EphB6	Down*	4.28	0.004
EphA1	Down*	3.92	0.001
EphB1	Down*	3.59	0.009
EFNB3	Down	2.70	0.019
EFNB1	Down	2.61	0.017
EFNB2	Down	1.93	0.007

*Indicates statistically significant differential gene expression, defined as > 3-fold absolute fold change and p-value < 0.01 (Mann-Whitney).

Subsequent pathway analysis by our collaborators revealed genetic signatures representative of activation of the p53 pathway in cSCCHN with perineural spread compared to cSCCHN without perineural involvement.[142] The authors proceeded to examination of p53 at the protein level by immunohistochemistry, which revealed an absence of normal p53 staining in all tumours with PNS and a preponderance of a diffuse over-expression pattern. Although this did not correlate with a difference in p53 mutation number or position there was a significant differential observed in regulators of p53 stability, activity and degradation consistent with dysregulation of the p53 pathway in cSCCHN with perineural spread.[142]

2.6.8 Other molecular biomarkers

Aside from this single study looking at genetic alterations in perineural spread cSCCHN there is a paucity of data on the expression profile of important cancer biomarkers in perineural spread cSCCHN. The p53 pathway clearly warrants further investigation in perineural spread, building on the earlier work of our colleagues.[142] p16 is another well recognised cell cycle regulator that is implicated in carcinogenesis and tumour progression that has not previously

been examined in perineural spread cSCCHN. It is also widely used as a surrogate marker of high risk human papilloma virus (HPV) infection in the cervix and oropharynx. Ki-67 is histopathological marker of cellular proliferation with the calculated proliferation index (PI) often correlating with clinical disease course in carcinomas. It is an emerging biomarker for tumour stratification and prognostication, particularly in breast cancer. Despite potentially important implications, to our knowledge no previous studies have examined the expression profiles of these biomarkers in perineural spread of cSCCHN.

2.6.8.1 p53 pathway

The TP53 gene is the most frequently mutated gene in human cancer. It has been labelled the "guardian of the genome" and is the prototypical tumour suppressor gene acting through various anti-cancer mechanisms, including activation of DNA repair apparatus, arrest of the cell cycle and initiation of apoptosis in the setting of irreparable genetic damage.[143,144] Many studies have investigated the significance of TP53 mutations in the prognosis and treatment of tumours at various sites. Mutations in cutaneous carcinoma occur early and often with no definite prognostic correlation in the literature.[145] The presence of a TP53 mutation is known to confer poor prognosis in colorectal, lung, prostate, and breast cancer.[144] At other sites, genetic alterations have been associated with treatment resistance. Given the significant labour and time cost involved in nucleotide sequencing, p53 IHC has become a surrogate marker utilised in clinical and research laboratories.[146] This has been based on the premise that wild-type p53 has a short half-life and is generally detectable only at low levels by IHC. Conversely, mutated p53 has a prolonged half-life and nuclear accumulation facilitates immunohistochemical detection. A consensus of studies regard strong and diffuse immunolabeling as abnormal and suggestive of a missense TP53 mutation while completely negative staining implies a non-immunoreactive truncated protein, likely secondary to a

nonsense mutation.[147] In the absence of a TP53 mutation a weak or focally positive immunoreaction is most commonly observed. In a study of ovarian carcinomas, combining the two immunohistochemical patterns associated with mutations correctly identified TP53 mutations in almost all cases.[148] A similar study was undertaken in colorectal adenocarcinoma, where three distinct patterns of p53 protein expression were observed: complete negative immunostaining, restricted expression characterised by focal positive staining and diffuse over-expression characterised by diffuse strongly positive staining.[147]

As discussed earlier, recent data published by our collaborators attempted to correlate immunohistochemical staining patterns of p53 expression in perineural of cSCCHN with mutational analysis data. The authors observed three distinct patterns as described by Nyiraneza et al (2011), and that compared to incidental PNI or tumours with no PNI, cSCCHN with PNS was significantly more likely to exhibit a strongly positive diffuse over-expression pattern.[147] Their study went on to suggest a probable role for the p53 pathway in the process of perineural spread. The results of the analysis showed signatures of gene expression representative of activation of p53 in tumours with PNI compared to tumours without, with regulators of p53 degradation, stability and activity significantly altered. Although at the gene loci analysed there was no difference in TP53 mutation or location, immunohistochemistry revealed a diffuse over-expression pattern or negative staining to be most common. We sought to build on this novel data by completing p53 immunohistochemistry in our cohort of perineural spread cSCCHN and pooling data for analysis.

2.6.8.2 p16 tumour suppressor gene

p16 is a cyclin-dependent kinase inhibitor encoded by the CDKN2A gene involved in regulation of the cell cycle.[149] This tumour suppressor gene is frequently mutated or deleted

in a wide range of cancers. The encoded $p16^{Ink4a}$ protein is activated during cell cycle progression upon the release of retinoblastoma protein (pRB) from the transcription factor E2F. The p16 protein is integral in the negative feedback loop which maintains the balance between cell proliferation and cell cycle arrest by inhibiting progression from G1 to S phases.[149] Up to 50% of human malignancies show p16 inactivation or downregulation, including head and neck carcinomas.[149,150] Conversely, some tumour sub-types display significant p16 overexpression which can be detected immunohistochemically. Most notably, HPV associated tumours have high rates of p16 over-expression such that p16 positivity is regarded as a surrogate marker for the presence of high-risk HPV genotypes.[149,151] For example, in the cervix, persistent high risk HPV infection leads to production of viral E6 and E7 oncoproteins that dysregulate the cell cycle by disrupting binding of pRB to E2F. This releases p16 from its negative feedback control leading to hyperproliferation and a paradoxical increase in p16 expression.[149]

p16 has been explored as a biomarker in several other cancers. HPV is responsible for an increasing percentage of oropharyngeal HNSCC, while not appearing to play an important role at other mucosal sites in the upper aerodigestive tract.[152,153] In recent clinical data from our institution, 79% of oropharyngeal SCC was p16 positive by immunohistochemistry (verbal communication, Ben Panizza, 2016). HPV related oropharyngeal SCC is highly radiosensitive and thus p16 over-expression confers a recognised prognostic benefit in this setting.[154]

Non-HPV related p16 overexpression has been observed in other malignant tumours and has also been associated with transformation from pre-malignant lesions.[149] Overexpression in malignant tumours is thought to represent an attempt to arrest the uncontrolled proliferation secondary to failure of the Rb pathway. As alluded to earlier, escape from this regulatory

pathway can be secondary to viral infection, gene mutations or other yet uncharacterised mechanisms. Certainly, restoration of p16 tumour suppressor functionality remains a viable anti-cancer strategy under investigation at other sites. Moreover, regardless of the mechanism, p16 has demonstrated utility as an independent prognostic marker outside the head and neck. In colorectal adenocarcinomas and breast carcinomas, p16 over-expression in a subset of tumours has been repeatedly shown to correlate with unfavourable clinical features.[149]

A proportion of cSCC are positive for p16 immunohistochemistry, however solar UVR can equally be responsible for mutation and dysregulation of expression of this cell cycle protein. Low risk HPV DNA has been detected in cSCC however there is not an increased prevalence of known high-risk sub-types.[155] It remains unclear whether chronic HPV infection plays a significant causal role in the carcinogenesis of cSCC or whether the virus is simply a bystander. In primary cSCC the role of p16 staining as a surrogate marker for HPV infection and/or as a prognostic factor is not clear. Hodges et al (2002) demonstrated increasing p16 expression in the progression from AK to CIS to SCC.[156] Later studies have shown that p16 status in cSCC does not correlate with the presence of HPV DNA and therefore, like most of the mutational burden, may be secondary to UV mediated DNA damage. However, in the setting of metastatic cervical nodal SCC of unknown origin, p16 immunohistochemistry is considered in many centres a useful adjunct in differentiating between an occult mucosal or occult cutaneous primary lesion.[157] There is recent literature looking at p16 expression in cervical lymph nodes of known cutaneous origin. A recent study by McDowell et al (2016) evaluated p16 immunohistochemistry in 143 cSCCHN lymph node metastases to the parotid gland.[158] The authors performed HPV RNA in situ hybridisation (ISH) in a subset of 59 patients to detect high-risk HPV sub-types. Of the cohort, 31% had positive and 15% weak p16 expression, with 54% exhibiting no staining. Overall and disease-free survival were not correlated with p16

status. Equally, there was no correlation of p16 status with high-risk HPV sub-type. Another study by Beadle et al (2013) found p16 expression to be relatively common in lymph node-positive cutaneous head and neck SCC and similarly recommended against use of p16 as an independent indicator of an occult oropharyngeal primary.[159] An earlier study by Compton et al (2011) evaluated HPV status using both fluorescence in situ hybridisation (FISH) and p16 status, reporting 28% of metastatic lymph nodes from occult primary tumours to be HPV positive.[160] There remains a paucity of data and no systematic review has been performed to date.

To our knowledge, $p16^{Ink4a}$ expression has not previously been examined in cSCCHN with PNS. We hypothesise that viral or UVR associated dysregulation of the p16 pathway may be a contributing driver for perineural invasion. The hypothesis that chronic viral infection, either with HPV subtypes or other viruses, may predispose to or facilitate perineural invasion and/or spread is novel although plausible. Infection and associated inflammation may affect the integrity of the perineural sheath and space. A subset of HPV-associated mucosal HNSCC tumours have a significant inflammatory infiltrate compared to HPV negative tumours.[161,162] A recent study by our collaborators has similarly demonstrated the presence of a significant inflammatory infiltrate in the setting of perineural spread cSCCHN.[43] Potentially chronic HPV infection and an increased inflammatory infiltrate associated with certain cutaneous SCCs might explain at least some of the tendency for particular tumours to undergo perineural invasion and spread. A pathogenic role for neurotropic viruses, such as the human herpesviruses, has also not been considered previously but is beyond the scope of our current study and certainly an avenue for future research. Regardless of the putative underlying mechanism, defining the expression profile of p16 in perineural spread cSCCHN may assist

our understanding of the disease process or with further clinical correlation reveal a novel prognostic factor.

2.6.8.3 Ki-67 proliferation index

The Ki-67 antigen is a non-histone nuclear protein involved in the early steps of RNA synthesis.[163] Its exact role remains uncharacterised however appears important in cell division, with expression varying through the phases of the cell cycle. It is not expressed during the resting G0 phase but is expressed during replication, peaking at mitosis. The MIB-1 antibody can be used to detect the Ki-67 antigen on formalin fixed paraffin embedded (FFPE) tissue sections and calculate the percentage of cells with strong nuclear positivity and thus actively undergoing mitosis.[164] This Ki-67 score is known as the proliferation index (PI) and has been evaluated across a range of malignancies as a marker for aggressive disease and poor clinical outcome. The utility of Ki-67 as a biomarker in breast cancer has been most extensively investigated, with a proliferation index > 10-14% conferring higher risk.[165] Per consensus guidelines published in 2009, Ki-67 score is used to classify tumours as low (<15%), intermediate (15-30%) or highly (>30%) proliferative.[166] It is this and other biomarkers in breast cancer that determine whether multi-drug therapy is indicated. A high PI has also been correlated with survival outcomes in prostate, brain and neuroendocrine tumours.[167,168]

Limited studies have looked at proliferation index in cSCC. On the spectrum of actinic keratosis to carcinoma in situ (CIS) to invasive SCC, proliferation index has been shown to increase.[169] In one recent study, all cases of cSCC were positive for Ki-67 expression with a mean PI of 85%.[169] Another study which evaluated Ki-67, p53 and p16 in 10 cases of invasive SCC, showed one case to have a PI > 30% while three cases had a PI 5-30% and the remaining six cases had PI < 5%.(170) No previous studies have investigated this biomarker in perineural

spread of cSCCHN, likely because it has not previously been considered a highly proliferative process. However, without data on mitotic rate or Ki-67 index this remains supposition. The paradigm to date has very much focused on tumour cells traversing the space in a directional manner rather than simply proliferating within the perineural compartment. Although many cases present with slowly progressive clinical disease, other cases are rapidly progressive towards the brain stem or can be locally aggressive as in the setting of peripheral recurrence. There is *in vitro* data reporting proliferation index in the DRG-tumour co-culture model, where it was shown that neurites induce proliferation of SCC cell lines.[46] It is a logical extension to address this evident gap in the literature by examining Ki-67 expression in tissue sections of cSCCHN with PNS and correlating the proliferation index with existing clinicopathological factors and other potential biomarkers of interest.

3.0 Clinical significance and rationale

The molecular mechanisms underlying perineural spread of cSCCHN are poorly understood and there has thus been no advances in development of targeted therapy. Adequate oncologic resection and adjuvant radiation therapy can add significant morbidity to an already morbid, and if left untreated, ultimately fatal, disease process. The lack of clinically relevant biomarkers limits our ability to risk stratify and prognosticate patients and de-intensify therapy when appropriate.

Immunotherapy is the current frontier in cancer treatment. Therapeutic antibodies have the advantage of blocking the transduction of pro-tumour signalling and localizing and amplifying the host immune response to tumour. A range of therapeutic antibodies are in clinical use or under development for a variety of malignancies. These antibodies, most frequently of the IgG class, bind their specific antigen or receptor molecule, thus interfering with cell signal

transduction and the processes of cell growth, migration and proliferation. It is now well understood that anti-tumour effects are also a function of the antibody Fc domain mediated induction of effector functions, which can include complement-dependent cytotoxicity (CDC), antibody-dependent cell-mediated cytotoxicity (ADCC) and antibody-dependent phagocytosis.[124] Antibodies also provide an opportunity to target other anti-tumour treatments, such as radiation, drugs and toxins, to tumour cells through conjugation. Locating druggable antigens that are largely tumour specific or selective allows such targeted therapy to occur while minimising harmful side effects.

The balance of RTK activity plays a critical role in tumorigenesis, progression and metastasis in a variety of cancers. We hypothesise that one or more of these membrane receptors is implicated in the perineural spread of carcinoma. If so, the availability of existing monoclonal antibody therapies would make for a readily exploitable target. The EGFR is an established therapeutic target in breast, colon and head and neck cancers with use of the chimeric IgG1 antibody cetuximab. Similarly, panitumumab is a humanised anti-EGFR monoclonal antibody approved in pancreatic and colorectal cancer.[124] Trastuzumab is a humanised IgG1 targeting the HER2 receptor approved in breast and now gastric and gastro-oesophageal cancer. Further highly specific monovalent and multivalent antibodies targeting Eph receptors and other members of the ErbB family are in development and clinical trial.

To our knowledge this is the first study to examine the role of RTKs in the molecular mechanisms underlying perineural invasion and spread in cSCCHN. In applying immunohistochemistry and immunofluorescence techniques and high-resolution imaging we hope to identify markers and pathways associated with perineural spread to shed light on therapeutic targets. Moreover, this is the first body of work to examine the expression profile

of well-recognised cancer biomarkers, including the cell cycle regulators p16 and p53, and the proliferation marker Ki-67, in perineural spread cSCCHN. Specifically this work builds on gene expression analysis and recently published data suggesting aberration of the p53 pathway in perineural spread.[142] Findings may have implications for treatment and prognostication of advanced cSCCHN with PNI as well as other neurotropic malignancy, including pancreatic, gastric, colorectal and prostate cancers. Specific treatment of perineural invasion and spread would improve patient survival and quality of life.

4.0 Hypothesis

Study of the pattern of expression and cellular localisation of receptor tyrosine kinases and other cancer biomarkers will contribute to understanding the molecular mechanisms underlying perineural spread of carcinoma. We hypothesise that dysregulation of receptor tyrosine kinase trafficking plays a role in perineural spread cSCCHN as in other forms of squamous cell carcinoma. Identification of such proteins may allow re-purposing and/or novel development of targeted therapies including immunotherapy. Correlation of biomarkers with clinical factors may allow patient prognostication and rationalisation of therapy in the future.

5.0 Aims

1. To define the level and cellular distribution of Eph and ErbB receptor tyrosine kinases on SCC cell lines; and
2. To define the level and cellular distribution of Eph receptors and ErbB receptors in human tissue specimens of perineural spread cSCCHN; and
3. To determine the expression profile of the proliferation marker Ki-67 and cell cycle regulators p53 and p16 in perineural spread cSCCHN

6.0 Materials and methods

6.1 Antibodies

Primary antibodies used in this study are tabulated below with concentrations used for various applications (Table 6). Commercial primary and secondary antibodies were purchased from sources as indicated. Pre-dilute clinically approved antibodies for immunohistochemistry for HER2, Ki-67 and $p16^{Ink4a}$ were used as per manufacturer protocols on automated platforms. HRP conjugated secondary antibodies for Western blot were diluted to 1/10,000. Alexa Fluor™ fluorophore conjugated secondary antibodies for cell and tissue immunofluorescence experiments were diluted to 1/200. The Ventana Discovery anti-HQ HRP detection system was used for immunohistochemistry performed on the Ventana Discovery Ultra platform (Ventana Medical Systems, Inc. USA) at the Translational Research Institute Core Histology Facility.

Table 6 Antibodies used in experimental work

Antibody	**Clone**	**Source**	**IgG**	**WB Conc.**	**Cell IF Conc.**	**Tissue IHC/IF Conc.**	**Optimised retrieval/incubation conditions and time**
β-tubulin	2-28-33	Invitrogen	Mouse	1/10,000	n/a	n/a	n/a
EphA2	D4A2	CST	Rabbit	1/1000	1/200	Serial dilutions*	n/a
EphA3	L-18 polyclonal	Santa Cruz	Rabbit	1/200	1/50	n/a	n/a
EphB1	Q-20 polyclonal	Santa Cruz	Rabbit	1/1000	1/50	n/a	n/a
EphB2	AF467	R&D	Goat	1/500	1/20	Serial dilutions*	n/a
EphB4	D1C7N	CST	Rabbit	1/1000	1/640	Serial dilutions*	n/a
S100	Z0311	DAKO	Rabbit	n/a	n/a	1/1000	CC1 32/Ab 12
AE1/AE3	MAB3412	Chemicon	Mouse	n/a	n/a	1/500	CC1 32/Ab 24
EGFR	31G7	Life Technologies	Mouse	1/1000	n/a	1/100	P2 16/Ab 60
HER3	DAK-H3-IC	DAKO	Rabbit	1/1000	n/a	1/100	n/a
HER2	4B5	Roche	Rabbit	n/a	n/a	Pre-dilute	CC1 32/Ab12
$p16^{Ink4a}$	E6H4	Roche	Mouse	n/a	n/a	Pre-dilute 1/2	CC1 32/Ab 8
MIB-1	M7240	DAKO	Mouse	n/a	n/a	Pre-dilute	CC1 32/Ab 32

p53	CM5p	Leica Biosystems	Mouse	n/a	n/a	1/200	Citrate

Antibodies are monoclonal unless otherwise specified. Optimised antigen retrieval time/primary antibody incubation time are indicated in minutes. Antigen retrieval solutions on the automated platform were CC1 (cell conditioner 1), CC2 (cell conditioner 2) and P2 (protease 2). Citrate buffer (pH 6.0) was used for heat retrieval of p53 antigen on the bench. All antigen retrieval was performed at 98°C. Ab, primary antibody incubation time. *Serial dilutions were performed with variable antigen retrieval and antibody incubation for these un-optimised antibodies (see Table 14 in Results).

6.2 Tissue acquisition

Tumour samples were collected from patients with large nerve perineural spread of cSCCHN treated surgically at the Princess Alexandra Hospital (PAH), Brisbane. Biopsy of the involved nerve was performed by the treating surgeon. Institutional ethics approval is in place (HREC/03/QPAH/197). Specimens were de-identified at the point of collection. A unique identifying code was assigned to each specimen and maintained in a secure database to allow subsequent review of the formal histopathological report and extraction of relevant clinical data. Specimens were FFPE and uniformly sectioned to 5µm. In all cases a routine haematoxylin and eosin (H&E) stain was performed on 1-2 sections of the research block to histologically confirm the presence of SCC with perineural spread within the block. Not all subsequent serial sections contained nerve tissue but sufficient SCC was present for analysis and considered representative of tumour that had undergone perineural spread. Specimens without evidence of perineural spread in the research block or sufficient tumour present in serial sections were excluded from this study.

Twenty-one tissue biopsies were collected from the PAH over an 18-month period. A further 18 blocks of confirmed PNS from cSCCHN (collected 2003-2011 at the Princess Alexandra Hospital under the same institutional ethics approval) were generously provided by our collaborators at QIMR. These blocks had previously been retrieved from QLD pathology archives and subject to independent histopathological review. Routine H&E stains were performed to ensure sufficient tumour remained in each block for analysis.

6.3 Immunohistochemistry

IHC was performed on the Ventana Discovery Ultra auto-staining platform (Ventana Medical Systems, Inc. USA). Protocol optimisation was performed using appropriate positive control human tissue for each antibody. Antigen retrieval was enzymatic for EGFR and heat retrieval

with CC1 retrieval solution (pH 8.0) for other antigens. Primary antibody concentrations for IHC are reported in Table 6 and incubation was 1 hour at 36°C unless otherwise specified. The Ventana anti-HQ HRP detection system was used with pre-dilute IgG anti-mouse or anti-rabbit HRP-conjugated secondary antibodies incubated for 1 hour at room temperature (RT) unless otherwise specified. Colour development with DAB reagent and haematoxylin counter-stain were also automated on the staining platform. Slides were mounted and cover-slips applied by the TRI Histology Core Facility staff. Negative controls included omission of the primary antibody (secondary only control) and tissue negative for the protein of interest. A positive FFPE tissue control was included in each run to ensure reproducibility of staining.

6.3.1 EGFR immunohistochemistry

For the EGFR, in brief, specimens were dewaxed and pre-treated with Protease 2 enzyme retrieval solution for 16 minutes at 36°C. Primary antibody was manually applied to the slide at a volume of 100uL and at recommended concentration of 1/100 diluted in Ventana antibody diluent solution (Ventana Medical Systems, Inc. USA). Incubation was at 36°C for 1 hour as per manufacturer recommendation and an anti-mouse HQ HRP detection system was used. DAB and haematoxylin counterstain were applied. Positive control was EGFR positive mucosal HNSCC.

Interpretation of EGFR immunohistochemistry was performed by two independent medical pathologists using two standardised scoring systems. Firstly, a clinically validated staining index, as described in Hirsch et al (2003), was calculated for each specimen by multiplying the percent (%) of stained tumour cells by average staining intensity graded from 0 to 4, giving an index between 0 and 400.[171] For the purposes of this score, positive tumour cell staining was defined as any IHC staining of tumour cell membranes above background level, whether complete or incomplete circumferential staining. By this scoring system, EGFR positivity is defined as a staining index score ≥200. The second scoring system used was the widely accepted histopathological four-point intensity score, where specimens are graded as negative (0), weakly positive (1+), moderately positive (2+) or strongly positive (3+) (Table 7). To receive a positive score, ≥10% tumour cells must exhibit strong membranous staining. By this method, moderately and strongly positive specimens are considered EGFR over-expressing. In subsequent analysis, only tumours that were positive by both scoring methods were considered positive for EGFR over-expression.

Table 7 Histopathologic scoring system for membrane receptor expression

Staining	Description	Score
Negative	No membrane staining is detected	0
Weakly positive	Faint, partial staining of the membrane in any proportion of the tumour cells	1+
Moderately positive	Weak to moderate complete staining of the membrane, in at least 10% tumour cells	2+
Strongly positive	Strong, complete staining of the membrane in at least 10% tumour cells	3+

6.3.2 HER2 immunohistochemistry

For HER2, pre-dilute clinical antibody was purchased and staining performed per manufacturer recommendations for the Ventana Discovery Ultra platform (Ventana Medical Systems, Inc. USA). In brief, specimens were dewaxed and pre-treated with CC1 retrieval solution (pH 8.0) for 32 minutes at 95°C. Primary antibody was incubated at 36°C for 12 minutes and an anti-rabbit HQ HRP detection system was used. DAB and haematoxylin counterstain were applied. Positive control was a 4-in-1 HER2 cell line control slide supplied by the manufacturer, depicting four cell lines with the range of staining intensity, and an independent HER2 positive breast cancer tissue control gifted by the PAH pathology laboratory. Specimens were scored in parallel to the 4-in-1 control slide with the standard four-point intensity score applied to membrane receptors, where specimens where graded 0 to 3+. To receive a positive score, ≥10% tumour cells must exhibit strong membranous staining (Table 7).

6.3.3 p53 immunohistochemistry

p53 immunohistochemistry was performed by the QIMR Berghofer Histology Facility using previously published methodology.[142] Appropriate positive and negative controls were included in each run. In our study, we performed immunohistochemistry for 10/20 specimens. The remaining 10 specimens had previously been immunostained at the same facility and the results published.[142] The raw data was generously provided by the authors for inclusion in this thesis and subsequent analyses and are attributed as such.

In brief, tissue sections were de-waxed, rehydrated and incubated in 2% hydrogen peroxide for 10 minutes. Antigen retrieval was performed in 10 mM citrate buffer for 8 minutes at 121°C. Sections were cooled, washed in TBS and blocked with Background Sniper (Biocare Medical, Concord, USA) for 15 minutes at RT. The p53 primary antibody (clone CM5p, Novacastra,

Nussloch, Germany) was then applied overnight at RT, and MACH1 Universal Polymer (Biocare Medical) applied for 45 min for detection. Sections were counterstained in haematoxylin, washed in water, dehydrated, cleared with xylene and mounted.

Immunohistochemistry was assessed according to the method described by our collaborators at QIMR Berghofer based on earlier analyses published by Nyiraneza et al (2011).[142,147] Only nuclear staining was scored and tumours were deemed positive if any positive nuclear staining was observed or negative if none was observed. There was no cut-off value. The pattern of positive staining was qualitatively assessed as "diffuse positive over-expression" or "focal positive expression." This allowed pooling of data with previous results from our collaborators, ensuring data for our entire cohort was available for subsequent analysis.

6.3.4 p16 immunohistochemistry

p16 immunohistochemistry was kindly performed by staff at the clinical pathology laboratory at the Princess Alexandra Hospital on a Ventana Benchmark Ultra platform. The clinically validated pre-dilute CINtec p16 antibody (E6H4, Roche) was used as per manufacturer recommendations. In brief, heat induced epitope retrieval was performed with CC1 retrieval solution (pH 8.0) for 32 minutes. Primary antibody was incubated for 8 minutes at 36°C. A Ventana Optiview detection kit was used and haematoxylin counterstain performed. Positive control was p16 positive tonsil SCC.

The method of scoring used by McDowell et al (2016) in their study of p16 status in nodal metastatic cSCCHN was applied in our study.[158] Both the intensity and proportion of positive tumour cell staining was assessed. The stain intensity was scored on a 4-point scale: 0 (no staining), 1 (weak), 2 (moderate) or 3 (strong). The proportion of tumour cells staining positive was scored as a percentage (0-100%). There is no universally accepted definition for p16 positivity in cSCCHN and this has not previously been assessed in perineural spread. We utilised the cut-off employed by Beadle et al (2013) and McDowell et al (2016) in the context of recent studies of nodal metastatic cSCCHN.[159,172] This is the same cut-off used in clinical pathology laboratories when assessing oropharyngeal HNSCC for p16 status (verbal communication, Ian Brown, 2016). p16 positivity is defined as an intensity score of 2-3 present in ≥70% of tumour cells. Negative staining was defined as no staining in any tumour cells. Specimens with any other degree of staining were classed as weakly positive.

6.3.5 Ki-67 proliferation index

Ki-67 immunohistochemistry was performed by at Envoi Specialist Pathologists using an MIB-1 antibody on their clinical autostaining platform. A control tissue slide with positive staining breast carcinoma cells and negative adipose tissue was included in each run. A single representative tumour-rich high powered field image was taken by an independent medical pathologist. The staining ratio appeared relatively uniform across individual specimens and the most tumour-rich hotspot was photographed for analysis. Interpretation of Ki-67 staining is difficult and prone to inter-observer variability. We combated this by utilising two scoring methods, a manual cell count and automated image analysis software. The proliferation index or proportion of Ki-67 positive cells, defined as strongly positive nuclear staining, was determined by counting all tumour cells within the field (≥ 50 tumour cells in all cases). Images with diffuse tumour were secondarily analysed using ImmunoRatio, a publicly available web application for quantitative image analysis, to externally validate the manual cell count results.[173] This plugin calculates the percentage of cells with a positively stained nuclear area using a colour deconvolution algorithm for distinguishing DAB and haematoxylin staining components. This automated method has been validated by several authors in breast and neuroendocrine tumours and compares favourably to manual methods.[164,173,174] There was a high degree correlation between the two methods in those specimens with diffuse tumour present, allowing the average of the two scores to be calculated. In several specimens, a low number of tumour cells and an abundance of stromal and inflammatory elements, an inherent anatomical feature of perineural spread, limited application of the image analysis software, which significantly underestimated the proportion of positive staining. In these few cases the manual cell counts were used alone. The optimal Ki-67 cut-off for prognostic assessment is unknown, and values ranging between 15-30% have been suggested previously in breast carcinoma. Some authors have suggested using the median value of Ki-67 labelling index as a cut-off within a series.[164,173] In consultation with an independent medical pathologist, cut-offs of 15% and 30% were used to define three groups for qualitative reporting: low, intermediate and highly proliferative (verbal communication, Ian Brown, 2016). For the purposes of quantitative statistical analysis, we applied a cut-off value of 30% to differentiate low and highly proliferative groups.

6.4 Cell Culture

All cell lines were mycoplasma tested and verified mycoplasma free. Fixed human adult keratinocytes (HEKa) were obtained as a gift from Dr Glen Boyle (QIMR Berghofer,

Australia). A431, COLO16, SCC15 and HeLa tumour cell lines were obtained from the American Type Culture Collection (ATCC). A transformed KJD cell line (human keratinocytes infected with SV40 virus) was obtained as a gift from Professor Nicholas Saunders (UQDI, Australia). Tumour cell lines were maintained in Dulbecco's Modified Eagle's Medium: Nutrient Mixture F-12 (DMEM-F12) (Life Technologies, Gibco) supplemented with 10mM HEPES, 10% heat-inactivated foetal bovine serum (FBS) and 2mM of L-Glutamine (Life Technologies, Gibco). Cells were grown in a humidified incubator with 5% CO_2 concentration at 37°C.

6.5 SDS page and Western blot

Cell lysates were prepared at 4°C with lysis buffer (1/1000 protease; 1/1000 phosphatase) and stored at minus 80°C. Cell lysates were sonicated and a Pierce BCA Protein Assay Kit (Thermo Scientific) was used per manufacturer recommendations to determine protein concentrations. Samples were diluted with H_2O and x5 loading buffer to standardise protein concentration to 1mg/ml. Equal volumes (18µL) of standardised samples were separated on 10% SDS-PAGE gel and transferred to methanol-activated PVDF membranes by electrophoresis. A pre-stained molecular weight marking ladder was run on each gel. Membranes were blocked in x1 TBST (20mM Tris-HCl, pH 7.4/137mM NaCl/0.1% Tween® 20) with 5% w/v nonfat dry milk for 40 minutes with gentle shaking. Primary antibodies were diluted in 5% w/v BSA, x1 TBST at recommended concentrations and incubated overnight at 4°C with gentle mixing. Beta-tubulin was used as a loading control. Membranes were washed x 3 with TBST before 1 hour incubation at RT with horseradish peroxidase (HRP) conjugated secondary antibodies diluted to 1/10,000 in 5% w/v BSA, x1 TBST. Final washes were in TBST x 3 then TBS x 2 for 5 minutes each. Proteins were visualized using enhanced chemiluminescence (ECL) reagents as per manufacturer guidelines and images acquired using Image-Lab Software (Life Science, New South Wales).

6.6 Cell immunofluorescence

Cells were plated on coverslips in 12-well plates to be approximately 80% confluent on the day of labelling. Cells were fixed with 4% paraformaldehyde (PFA) in PBS before permeabilization with 0.01% Triton TX-100 for 10 minutes at RT. Cells were blocked with a solution of 1% bovine serum albumin (BSA) and 4% horse serum in PBS for 15 minutes at RT. Cells were labelled with primary antibody at RT for 1 hour at titrated concentration in blocking solution. An Alexa fluorophore-conjugated secondary antibody was then applied at a

concentration of 1/200 in blocking solution for 1 hour at RT (α-mouse-Alexa 555, α-rabbit-Alexa 488 or α-goat-Alexa 594 were used depending on the primary antibody IgG). Coverslips were mounted in ProLong Gold (Invitrogen) on Superfrost slides. Confocal image acquisition was performed within 48 hours. The HeLa cell line was included as an expected negative control for each anti-Eph receptor antibody as this cell line is reported to express very little to no detectable levels of Eph receptor (The Human Protein Atlas, www.proteinatlas.org).[175] Secondary only negative controls were also included for each antibody. Antibody specificity was assessed by Western blot prior to immunofluorescence studies.

6.7 Tissue immunofluorescence

Human tumour specimens were FFPE then serial sectioned at 5μ onto positively charged Superfrost slides as previously described. Sections were dewaxed by heating in a 37°C oven for 30 minutes and soaking in xylene for 10 minutes. Rehydration in serial dilutions of EtOH at 100% for 5 minutes and 90%, 80%, 60% and 40% for 1 minute each was undertaken before soaking in H_2O for 5 minutes. Heat-induced epitope retrieval (HIER) or enzymatic antigen retrieval was performed specific to the primary antibody. For HIER either 10mM sodium citrate buffer (pH 6.0) or 10mM/1mM Tris-EDTA buffer (pH 9.0) were used. Retrieval solution was brought to boiling in a microwave oven before slides were submerged for a total of 2 minutes with temperature maintained between 90-98°C. Slides were washed in PBS x 2 for 5 minutes each. Tissue sections were ringed with a wax pen and incubated in a blocking buffer (BB) of 1% BSA, 4% horse serum, 0.1% Triton X-100 in PBS for 1 hour at RT. Primary antibody was diluted in BB with Triton and incubated overnight at 4°C. The next morning slides were warmed to RT for 15 minutes before washes in BB for 5 mins x 3 then application of an IgG specific Alexa fluorophore-conjugated secondary antibody (1/200) for 1 hour at RT in the dark. Slides were protected from ambient light from this point onwards. Wash in BB x 3 was performed prior to DAPI counter-stain at 1/10,000 for 10 minutes at RT. Sections were washed briefly with PBS and ddH_2O before being coverslip mounted with ProLong Gold. Slides were stored in the dark at 4°C until image acquisition was performed.

6.8 Microscopy

Cell immunofluorescence experiments were analysed using a Zeiss 510 Meta laser scanning confocal microscope with x25 and/or x63 oil objective lenses. Emission wavelengths of 405nm, 488nm and 555nm were used for blue, green and red fluorescence, respectively. Images were acquired using Zen 2009 software (Carl Zeiss Microscopy, Germany). Images

were analysed using Adobe Photoshop and Image J 1.48 for Mac OS X 10.7. Tissue immunofluorescence images were acquired on an Aperio FL Scanner (Leica Biosystems, IL, USA) at x20 magnification at the QIMR Berghofer Core Imaging Facility. Images were analysed in WebScope and minimally adjusted for brightness and contrast parameters to enhance visualisation of staining patterns. Appropriate positive and negative controls were imaged and analysed with identical parameters. In select cases high resolution images were acquired at x20 and x40 magnification with the Olympus FV1200 confocal microscope at the TRI Microscopy Core Facility using FV10i software (Olympus Microscopy, USA). Brightfield microscopy was used to visualise immunohistochemistry results. Slides were scanned with an Aperio slide scanner and digital slides viewed with OlyVIA software for scoring (Olympus Microscopy, USA).

7.0 Results

7.1 Cell line data

7.1.1 Eph and ErbB receptor expression in SCC cell lines

We aimed to assess expression of Eph and ErbB receptors in SCC cell lines. Western blots were performed for EphA2, EphA3, EphB1, EphB2, EGFR and HER3 receptors across four SCC cell lines and one human epidermal keratinocyte cell line. A431 is a human cutaneous carcinoma cell line derived from an epidermoid carcinoma in an 85 year old patient and is known to be highly EGFR over-expressing.[176] The COLO16 cell line was first derived from a metastatic cutaneous SCC in a 59 year old patient.[177] KJD is a keratinocyte cell line produced by transforming normal keratinocytes with the SV40 virus (KJD-1/SV40) and were prepared by and received as a gift from the Saunders laboratory (UQDI, Australia).[178] Together these three cell lines represent a spectrum of cutaneous SCC. The SCC-15 cell line (ATCC No. CRL-1623) is derived from a tongue SCC in a 55-year-old patient, representing mucosal HNSCC. Primary human epidermal keratinocytes were received as a gift from the Boyle laboratory (QIMR Berghofer, Australia) as a normal epithelial control cell line. To our knowledge, there are no established cell lines derived from perineural spread cSCCHN.

Representative Western blots for Eph and ErbB receptors in human epidermal keratinocytes and SCC cell lines are depicted (Figures 12, 14). All blots were performed in triplicate and histograms quantifying the results have been first normalised to β-tubulin as loading control and then normalised to HEKa expression, as the control cell line, to obtain a uniform y-axis.

Results were then averaged to depict mean signal intensity and standard deviation in arbitrary units (Figures 13, 15). Appropriate molecular weight bands were identified for EphA2 (125 kDa), EphA3 (135 kDa), EphB1 (130 kDa), EphB2 (130 kDa), EphB4 (135 kDa), EGFR (175 kDa) and HER3 (185 kDa) in each of the SCC cell lines and HEKa cell line indicating at least baseline level expression across these benign and malignant epithelial cell lines. Single high intensity bands at the appropriate molecular weight were seen for the EphA2 (125kDa) and EphB4 (135kDa) receptors using Cell Signalling Technology (CST) antibodies, confirming the specificity of the antibodies and the expression of the receptor in each of the cell lines examined. Similarly, an appropriate band was detected for the EphB2 (130kDa) receptor using an R&D Systems antibody. Although appropriately sized bands were detected for EphA3 (135kDa) and EphB1 (103kDa) using Santa Cruz Biotechnology (SCBT) antibodies, there was significantly more background staining on the blots despite identical conditions. Furthermore, the presence of lower molecular weight bands on the blots in both instances suggests either non-specific binding of the primary antibody or alternatively the presence of splice variants or protein cleavage products for these proteins.

The degree of Eph receptor expression qualitatively appears variable across the cell lines when examining the blots in combination with the loading control β-tubulin (Figure 12). Quantitative analysis confirmed that on average, expression of EphA2 receptor was higher in SCC cell lines compared to HEKa cells across the board, but particularly elevated in the A431 cell line with a >1.5 fold-change. Increased expression of the EphB2 was more significant with all SCC cell lines exhibiting high expression levels relative to normal keratinocytes with the A431 cell line again showing the most significantly elevated protein levels. Relatively high EphB4 expression was observed in COLO16 cells but was no different in other SCC cell lines when normalised to the loading control and HEKa cell line. EphA3 and EphB1 receptor expression was relatively stable across the malignant and control cell lines.

Qualitative and quantitative expression of the EGFR was examined across the cell lines with a commercial antibody (clone 31G7, Life Technologies) (Figures 14, 15). EGFR expression in known highly over-expressing A431 cells was as expected significantly higher than all other cell lines, with a near 50-fold increase. Expression in COLO16 and SCC-15 cell lines was also increased relative to normal epidermal keratinocytes by 2-3-fold. The SV-40 virus immortalised KJD cell line had low EGFR expression comparable to the control HEKa cells. HER3 expression demonstrated a similar pattern across the cell lines although with less marked

fold-changes observed. A431, SCC-15 and COLO16 cell lines had an approximately 6-fold, 4-fold and 2-fold change respectively compared to HEKa cells. Again, the transformed KJD cell line had a low expression of this RTK which was comparable to untransformed HEKa cells.

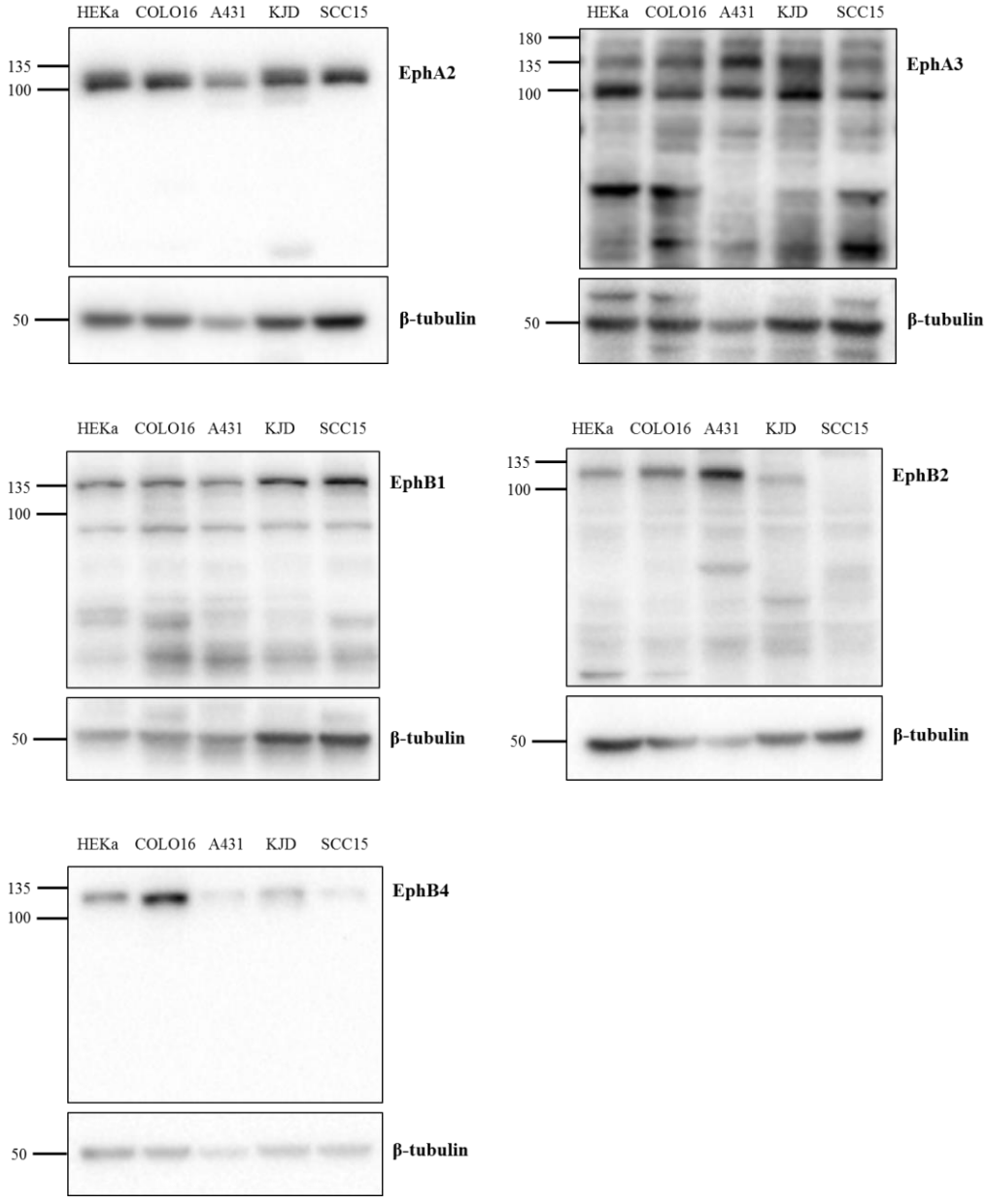

Figure 12 Western blot analysis of EphA2 (125kDa), EphA3 (135kDa), EphB1 (130kDa), EphB2 (130kDa) and EphB4 (135kDa) receptor expression in HEKa, COLO16, A431, KJD and SCC15 cell lines. 18µg of whole cell protein lysates were separated on 10% SDS-PAGE and immunoblotted for the protein of interest. Experiments were performed in triplicate. Blots were re-probed for β-tubulin which served as a loading control reference protein. Representative images are shown.

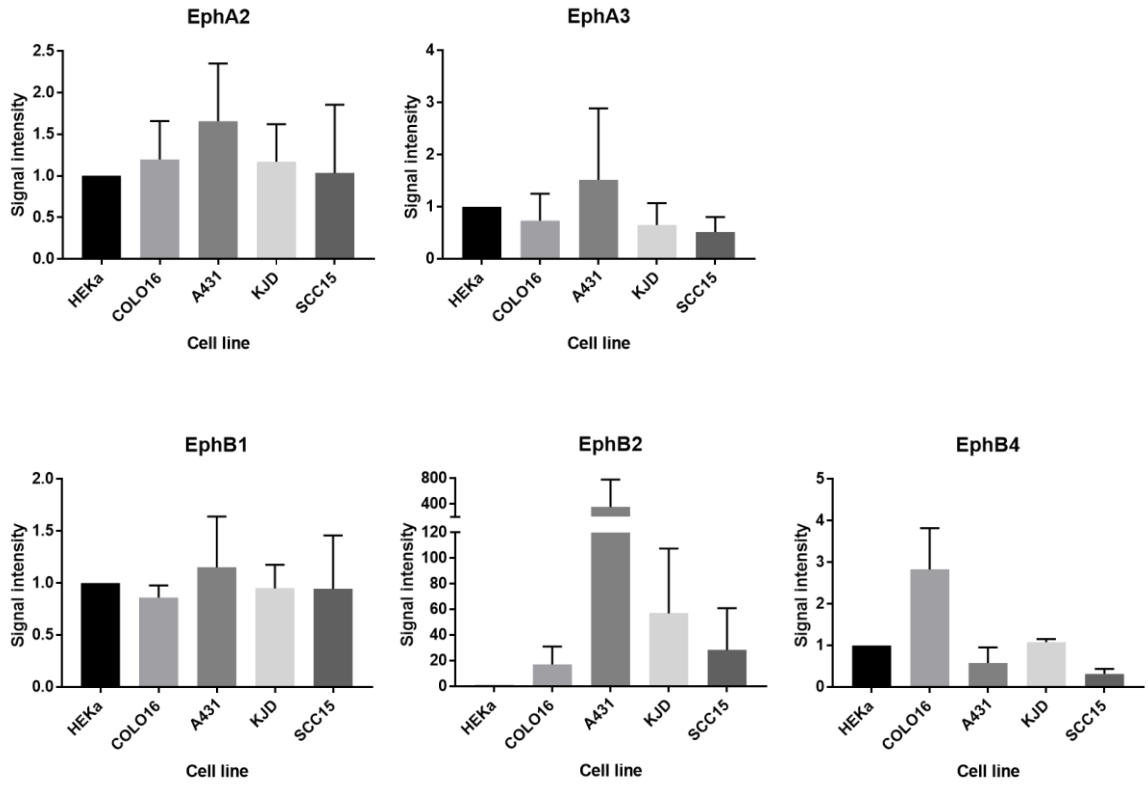

Figure 13 Quantified Western blot analysis of Eph receptor expression in HEKa, COLO16, A431, KJD and SCC15 cell lines. Western blots were performed in triplicate. Western blot bands were quantified using ImageLab (Bio-Rad) and the signal normalised to β-tubulin as a loading control and then to HEKa expression as a normal epithelial cell line. Mean and standard deviation are depicted with signal intensity expressed in arbitrary units.

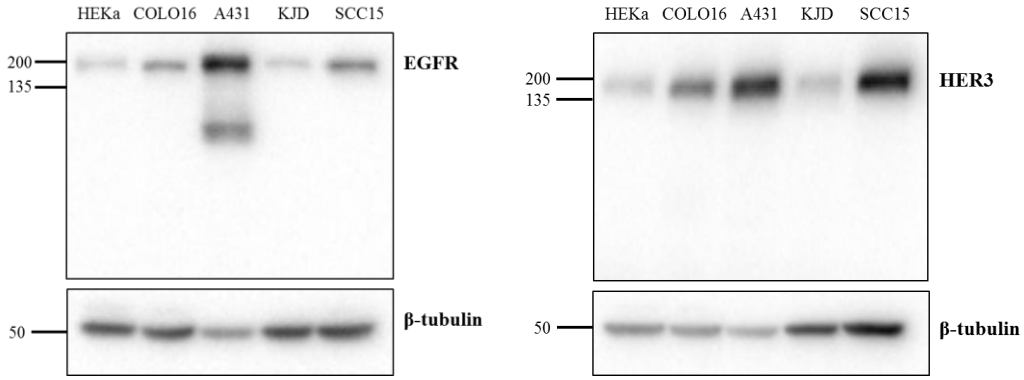

Figure 14 Western blot analysis of EGFR (175kDa) and HER3 (185kDa) expression in HEKa, COLO16, A431, KJD and SCC15 cell lines. 18µg of whole cell protein lysates were separated on 10% SDS-PAGE and immunoblotted for EGFR (A) and HER3 (B), respectively. Experiments were performed in triplicate. Blots were re-probed for β-tubulin which served as a loading control reference protein. Representative images are shown.

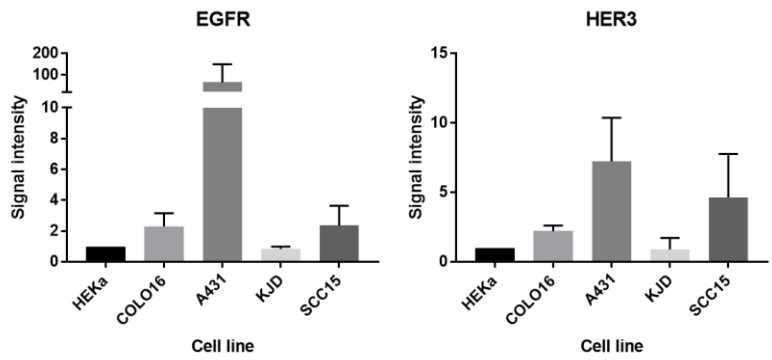

Figure 15 Quantified Western blot analysis of EGFR (A) and HER3 (B) receptor expression in HEKa, COLO16, A431, KJD and SCC15 cell lines. Western blots were performed in triplicate. Western blot bands were quantified using ImageLab (Bio-Rad) and the signal normalised to β-tubulin as a loading control and then to HEKa expression as a normal epithelial cell line. Mean and standard deviation are depicted with signal intensity expressed in arbitrary units.

7.1.2 Eph receptor localisation in SCC cell lines

Following assessment of antibody specificity by Western blot and initial quantified expression analyses, cell immunofluorescence was employed to localise Eph receptor expression at a subcellular level across the cell lines. Increasing evidence suggests that it is not simply receptor level of expression but cellular localisation of the receptor that is important in tumour biology and targeting treatment. EGFR and HER3 localisation studies have previously been performed by our laboratory and others so these experiments were not undertaken. However, given the minimal data on expression of Eph receptors in SCC cell lines, we labelled for each of EphA2, EphA3, EphB1, EphB2 and EphB4. We were unable to complete immunostaining for EphB1 and EphB2 staining on KJD or SCC-15 cell lines due to a limited supply of the respective monoclonal antibodies. A secondary only negative control was included in each experiment and images acquired under identical conditions. The HeLa cell line (ATCC CCL-2) was used as a further negative control for EphA and EphB receptor antibodies as this cell line expresses very little to no detectable levels of these receptors.

A summary table of cellular localisations of Eph receptors in human epidermal keratinocyte (HEKa) and tumour cell lines (COLO16, A431, KJD, SCC15) is included below (Table 8). Corresponding figures depicting representative images are included in Appendix A. All cell immunofluorescence was performed in duplicate in each of two separate experiments. Cellular localisation has been reported based on the predominant staining pattern observed: cytoplasmic

punctate endosomal staining (C) or membranous cell surface staining (M), and intensity qualitatively graded as 1+ to 3+ where positive staining was observed. In our study we have categorised predominant punctate cytoplasmic staining as endosomal staining. Work was completed with specimen sections available and remaining sections will be analysed by co-localisation with endosomal markers to validate endosomal staining.

Consistent with immunoblot results EphA2 had high levels of expression across all cell lines with strongly positive plasma membrane staining and minimal cytoplasmic expression observed. Relatively more intense staining was observed in tumour cells lines consistent with upregulation of the receptor at the cell surface. EphA3 had consistent levels of cytoplasmic expression across the cell lines with minimal plasma membrane staining detected. EphB1 expression was similarly localised to endosomes within the cytoplasm with greater staining intensity observed in the COLO16 cell line compared to the HEKa and A431 cell lines. Notably, EphB2 predominantly localised to the cell membrane in COLO16 and A431 cell lines whereas in control HEKa cells it was largely cytoplasmic in expression, suggesting relocation or trapping of the receptor at the cell surface in the malignant cell lines. EphB4 expression was similarly intensely membranous in the COLO16 and KJD cell lines. Interestingly, minimal to no detectable EphB4 in the A431 cells or normal keratinocytes. These findings are consistent with the preceding Western blot analyses.

Table 8 Predominant localisation of Eph receptors in human cell lines by immunofluorescence

Cell lines	**Keratinocyte**	**Squamous cell carcinoma**				**Control**	Corresponding figures (Appendix A)
Localisation	**HEKa**	**COLO16**	**A431**	**KJD**	**SCC15**	**HeLa**	
EphA2	M+	M++	M++	M+++	M+++	Neg	A1
EphA3	C++	C++	C+	C+++	C+	Neg	A2
EphB1	C+	C++	C+	n/p	n/p	Neg	A3
EphB2	C+	M+	M+	n/p	n/p	Neg	A4
EphB4	Neg	M++	Neg	M+	Neg	C+	A5

Key: M = predominantly plasma membrane staining; C = predominantly cytoplasmic staining; graded 1-3 (+, ++, +++); n/p = not performed; Neg = negative (minimal or no detected expression)

7.2. Tissue data

7.2.1 Clinicopathological factors

A total of 21 research biopsies were collected from surgical resections of patients with suspected perineural spread of cSCCHN over an 18-month period. All specimens were FFPE as previously described. The formal histopathological report and clinical data were reviewed for each patient. On formal histopathology 2 patients were found to have perineural spread of melanoma, 1 patient had adenoid cystic carcinoma and 1 had no tumour in the specimen and were thus excluded from the study. One patient had perineural invasion at the advancing tumour front but no large nerve perineural spread while 1 patient had indiscriminate invasion of structures including nerve tissue. Both were excluded from this study of clinical perineural spread. The 15 remaining patients had histologically confirmed perineural spread of cSCCHN documented in the formal pathology report. Review of 1-2 H&E stained transverse and/or longitudinal sections was performed for each research block to confirm the presence of sufficient tumour for experimentation. In 5 research blocks, insufficient tumour cells were identified on serial sections to facilitate immunostaining for proteins of interest. Thus, these blocks were excluded from the study. This left a total of 10 research specimens collected within our study timeframe with histologically confirmed cSCCHN with PNS within the research block for our study.

To increase the size of our cohort, a further 18 research blocks were generously provided by our collaborators at QIMR Berghofer, having been previously collected under the same institutional ethics approval between 2003-2011. These blocks had previously been retrieved from QLD pathology archives and subjected to independent histopathological review to confirm perineural spread cSCCHN. Data has previously been published for this cohort by our collaborators.[142] Repeat H&E section and pathologist review was performed which revealed insufficient tumour remaining in the block for 6/18 specimens, leaving 12 additional research specimens for our study. Two specimens could not be re-identified meaning we were unable to independently review the formal pathology reports and clinical data could not be extracted. These patients were excluded from this study, leaving us a total of 20 specimens for this study. Clinicopathological factors and biomarker expression status, as determined by immunohistochemistry, are documented below (Table 9).

Of the 20 specimens, one did not have differentiation specified in the formal report and we were unable to retrieve the block from archive to make an equivalent assessment. Of 19 specimens, 8 (42%) were poorly differentiated; 10 (53%) were moderately differentiated and 1 (5%) was well differentiated. With respect to the primary lesion, 55% (11/20) had an

identifiable primary while in 2 cases (10%) the primary could not be assessed and in 7 cases (35%) the primary was unknown (i.e. there was no history of a likely index lesion). The median time from symptom onset to diagnosis of perineural spread in our cohort was 4 months (range, 1-60 months), with a mean of 10.7 months.

Table 9 Histopathological data and biomarker expression profile by immunohistochemistry

Perineural spread		**Primary lesion**			**Biomarkers in PNS**		
Block ID	**Diff.**	**Identifiable**	**Diff.**	**Time to diagnosis**	**Ki-67 PI (%)**	**p16**	**p53**
56	mod	yes	poor	8	35.8	pos	neg*
57	mod	yes	poor	1.5	20.4	neg	diffuse*
62	mod	T0	n/a	2	22.7	weak	focal*
63	poor	yes	mod	3	23.1	pos	focal*
67	well	yes	well	2	22.7	weak	diffuse*
69	mod	yes	mod	42	19.5	neg	neg*
70	poor	yes	mod	5	32.9	weak	diffuse*
71	mod	TX	n/a	6	38.3	pos	diffuse*
72	mod	yes	poor	16	18.8	neg	diffuse*
73	poor	T0	n/a	7	12.2	weak	neg*
T2	mod	yes	n/s	1	13.2	weak	focal
T6	poor	TX	n/a	2.5	35.1	neg	diffuse
T10	poor	T0	n/a	12	15.4	weak	focal
T13	poor	T0	n/a	2.5	32.1	pos	diffuse
T21	poor	T0	n/a	2	55.4	weak	focal
T22	n/s	T0	n/a	60	19.3	pos	diffuse
T26	poor	yes	well	24	31.8	neg	diffuse
T27	mod	yes	n/s	1	35.5	pos	diffuse
T28	mod	T0	n/a	3	34.8	weak	focal
T31	mod	yes	mod	13	45.0	weak	focal

All reported cases (n=20) had clinical perineural spread of cSCCHN prior to resection and confirmed perineural spread cSCCHN on formal pathology. All research blocks had tumour in serial sections on assessment by two independent medical pathologists. Diff, differentiation grade; PNS, perineural spread; PI, proliferation index; time to diagnosis, time to diagnosis of perineural spread from symptom onset; well, well differentiated; mod, moderately differentiated; poor, poorly differentiated; T0, unknown primary; TX, primary not assessable; n/s, not specified; n/a, not applicable. *indicates p53 immunohistochemistry staining data published by Warren et al (2016) and used with permission.[142]

7.2.2 Expression of cell cycle molecular biomarkers in cSCCHN with PNS

A proportion of tumour cells in all specimens had nuclear positivity for Ki-67 expression, with a range of calculated proliferation indices (Table 9). The mean Ki-67 proliferation index was 28.2% and the median value 27.5% (range, 12.2% to 55.4%). Using a 3-tiered grading system a high proliferation index (>30%) was observed in half the cohort, a moderate proliferation index (15-30%) in 8 specimens and a low proliferation index (< 15%) in 2 specimens (Table 10). As per previously published studies, with a mean and median value approximating 30% we used this as single-point cut-off to differentiate two groups (<30%, lowly proliferative; ≥30%, highly proliferative) for the purposes of statistical analysis. Representative images of Ki-67 staining and ImmunoRatio analyzed pseudo-images are shown (Figure 16).

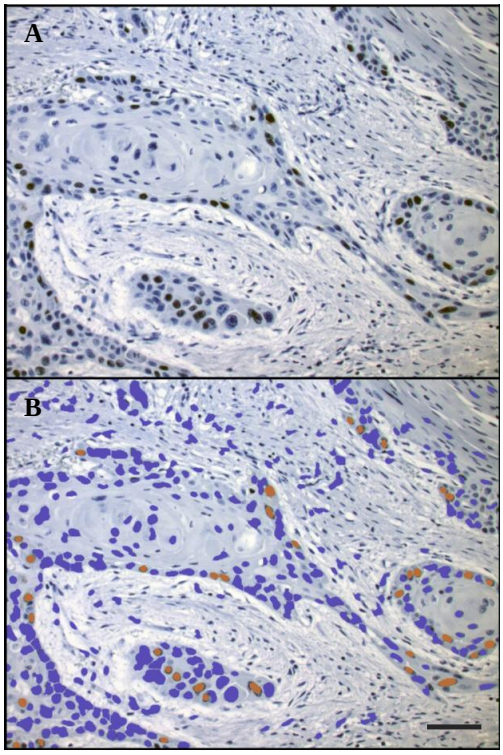

Figure 16 Immunohistochemical detection of Ki-67 protein in cSCCHN with PNS. Representative image of Ki-67 nuclear staining (brown) is shown for a specimen of perineural spread of cSCCHN. The proliferation index (PI) is calculated by the number of positively stained tumour cells divided by the total number of tumour cells in the field. (A) Top panel shows the original representative high powered field image taken by an independent pathologist. Manual count of tumour cells yielded a PI of 22.7%. (B) Lower panel shows the pseudo-image constructed by the ImmunoRatio colour deconvolution algorithm to facilitate automated calculation of proliferation index.(173) ImmunoRatio calculated PI was 5% in this case. Given the abundance of stromal elements in this specimen, the manual cell count was used for subsequent analysis. Scale bar: 200µm.

Table 10 Ki-67 proliferation index calculated by immunohistochemistry

Grade	Ki-67 proliferation index	cSCCHN with PNS (n=20)
Low	< 15%	2 (10%)
Intermediate	15-30%	8 (40%)
High	> 30%	10 (50%)

Of the combined cohort (n=20) of perineural specimens for which p53 data was available, half had diffuse positive over-expression, 7/20 (35%) had focal positive expression and 3/20 (15%) were negative for p53 expression by immunohistochemistry (Table 11). Representative images of the staining patterns in cSCCHN with PNS are shown (Figure 17).

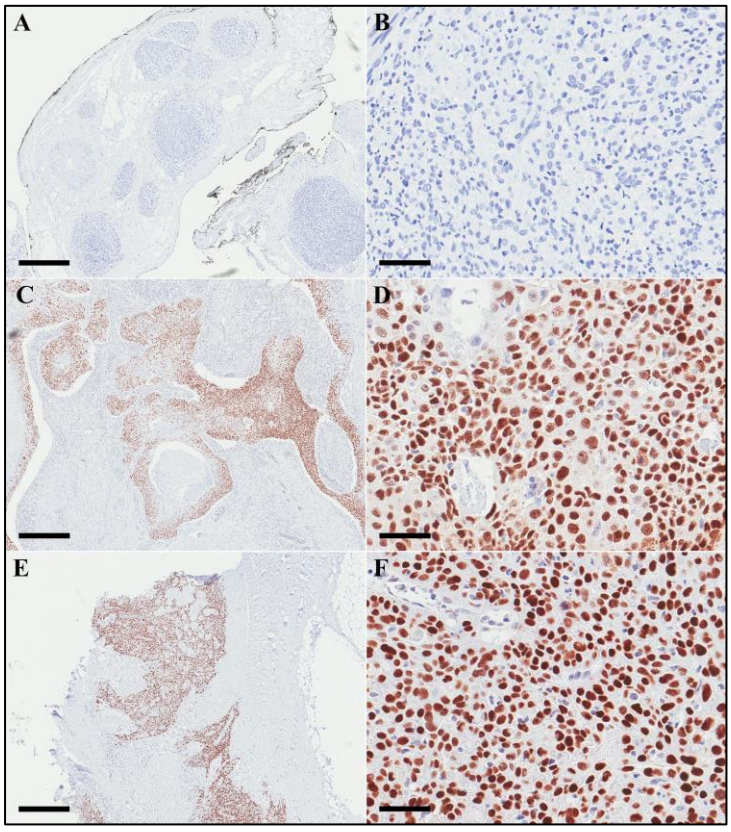

Figure 17 Immunohistochemical detection of p53 protein in cSCCHN with PNS. Representative images of p53 staining are shown at low (left panel, 40x) and high (right panel, 400x) magnification with nuclear p53 visualized in red. (A/B) negative pattern of p53 expression (no expression visualized in any tumour cell nuclei); (C/D) focal positive pattern of expression (strong expression within restricted areas of tumour in background of negative or weakly positive nuclei); (E/F) diffuse positive pattern of over-expression (very strong positivity throughout the tissue). Scanned images used with permission from the Boyle laboratory.[142] Scale bars: A, C, E are 500µm (40x); B, D, F are 50µm (400x).

Table 11 p53 expression pattern by immunohistochemistry

p53 staining pattern	**cSCCHN with PNS (n=20)**
Negative	3 (15%)
Focal/restricted expression	7 (35%)
Diffuse over-expression	10 (50%)

Positive staining for p16 was observed in 15/20 (75%) of specimens with 5 (25%) showing negative staining for p16. However, only 6/20 (30%) reached the threshold for positive p16 status (2-3+ staining in ≥ 70% tumour cells) with the remaining 9/20 (45%) specimens displaying only weakly positive staining below the threshold (Table 12). Representative images of p16 staining are shown (Figure 18).

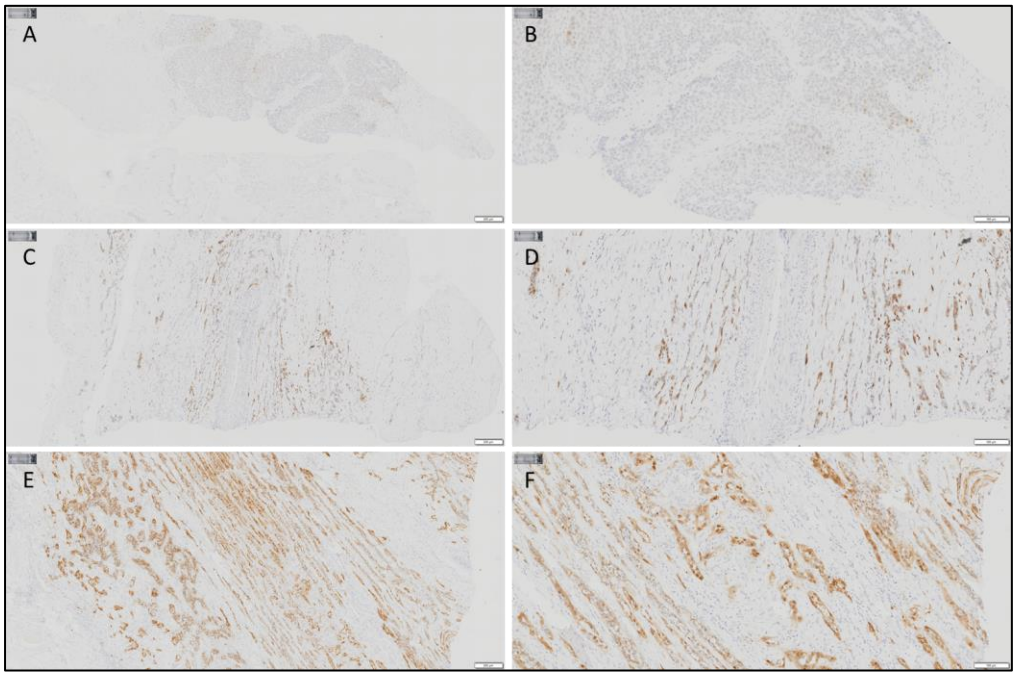

Figure 18 Immunohistochemical detection of p16 protein in cSCCHN with PNS. Representative images of p16 staining are shown at low (left panel, 10x) and high (right panel, 4x) magnification with nuclear p16 visualized in red. (A/B) negative staining; (C/D) weakly positive staining; (E/F) strongly positive staining meeting threshold criteria (nuclear staining intensity grade 2-3 in ≥ 70% of tumour cells). Scale bars: A, C, E are 200µm (10x); B, D, F are 100µm (4x).

Table 12 p16 expression status by immunohistochemistry

p16 status	**cSCCHN with PNS (n=20)**
Negative (no staining)	5 (25%)
Weakly positive (below threshold)	9 (45%)
Strongly positive (≥70% cells intensity 2-3)	6 (30%)

7.2.3 EGFR is over-expressed in perineural spread cSCCHN with variable localisation

Given the high specificity of the anti-EGFR antibody and a plausible potential role for EGFR in perineural spread of cSCCHN, this candidate drug target was selected for further analysis at the tissue level using immunohistochemistry. A total of 20 specimens of histologically proven PNS of cSCCHN were available. EGFR immunohistochemistry was performed as previously described and scoring was conducted by two independent pathologists (Table 13). Where scores differed, a consensus score was reached. Two scoring systems were used in parallel to reduce potential bias. High quality specific and reproducible staining was achieved with intensity graded 0 to 3+ or 0 to 4, respectively. The percentage of positively stained tumour cells was also recorded to allow calculation of the staining index as previously described. Representative images of positive EGFR staining in perineural spread cSCCHN are shown (Figure 19). Sectioning resulted in a combination of longitudinal and transverse sections relative to the nerve fascicles (Figure 20). Both perineural and intraneural tumour cells were observed to stain strongly positive for the EGFR (Figure 20).

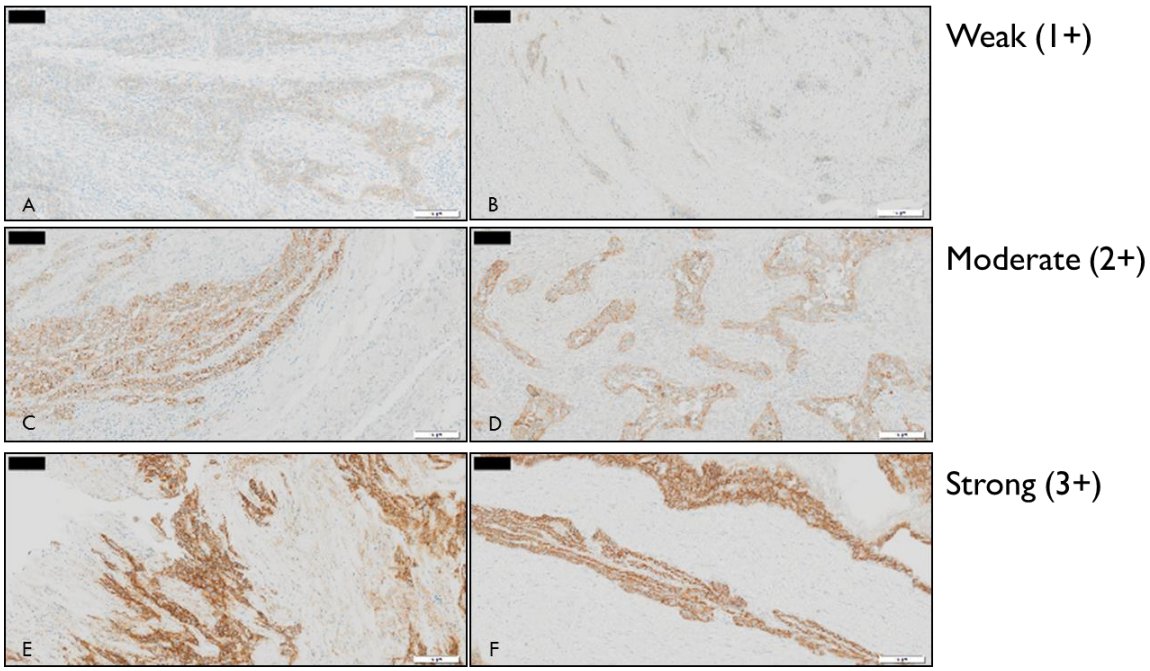

Figure 19 Immunohistochemical detection of EGFR in perineural spread of cSCCHN. Representative images of EGFR immunohistochemistry showing weakly (1+), moderately (2+) or strongly (3+) positive staining of formalin fixed paraffin embedded 5µm tissue sections of perineural spread of cSCCHN. Primary antibody was mouse anti-EGFR (clone 31G7, Life Technologies) with a rabbit anti-mouse HQ HRP detection system and DAB reagent used on the Ventana Discovery Ultra automated staining platform. Representative images at 10x magnification of 1+ (A, B), 2+ (C, D) and 3+ (E, F) positive staining are shown. Moderate or strongly positive staining represents over-expression of the EGFR using this standardized scoring method. Scale bars: 100µm.

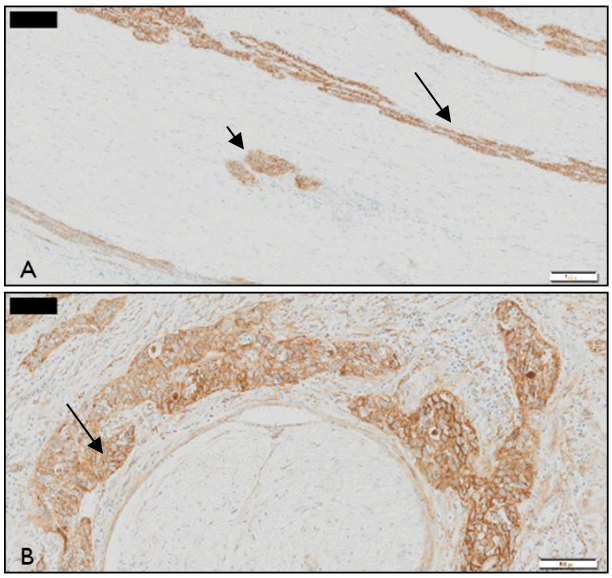

Figure 20 EGFR immunohistochemistry on perineural spread cSCCHN in longitudinal and transverse sections. This figure depicts strongly positive (3+) perineural (arrow) tumour cell staining in longitudinal (A) and transverse (B) sections of perineural spread cSCCHN. In longitudinal section (A) positive staining of intraneural (arrowhead) tumour cells is also seen. Primary antibody was mouse anti-EGFR (clone 31G7, Life Technologies) with a rabbit anti-mouse HQ HRP detection system and DAB reagent used on the Ventana Discovery Ultra automated staining platform. Scale bars: 100μm.

Of 20 specimens, 18 (90%) scored ≥ 200 for the staining index, consistent with EGFR over-expression. These specimens all also scored positive with the standard 0-3+ histopathological score (Figure 21).

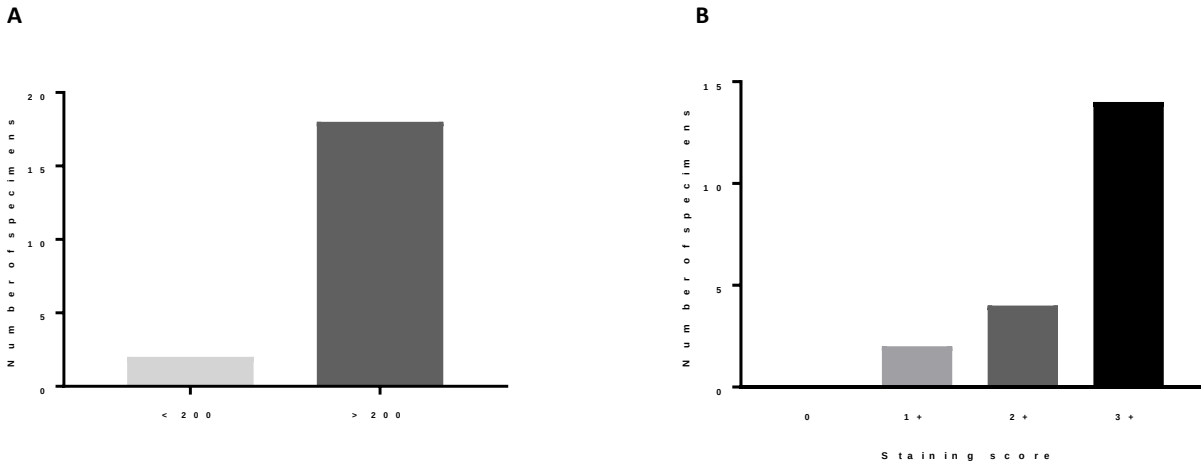

Figure 21 Results of two methods of scoring EGFR immunohistochemistry in perineural spread of cSCCHN. There was good correlation between the scoring systems with 18/20 (90%) specimens scored positive for EGFR over-expression using (A) a clinically validated staining index (% positive cells × staining intensity (0-4)) and (B) a standard histopathological score (0-3+).

For the 18 specimens scored positive for EGFR over-expression by both scoring methods, we went on to characterise subcellular localisation of the receptor using secondary immunofluorescence. Immunohistochemistry was of sufficiently high quality to allow preliminary assessment of predominantly plasma membrane staining compared to cytoplasmic compartment staining in the specimens, which was scored independently by a medical pathologist and the principle investigator. Secondary immunofluorescence was then conducted on the bench for all positive cases to validate the preliminary findings and allow high resolution imaging. Fluorescently labelled slides were scanned in their entirety at 20x magnification and images analysed using ImageScope software by the principle investigator in consultation with the supervising cell biologist. Where higher resolution imaging was required, image acquisition was performed with a confocal microscope at 40x magnification. Two patterns were differentiated: circumferential plasma membrane staining, consistent with cell surface expression, and cytoplasmic punctate staining, consistent with endosomal expression. All specimens positive for EGFR over-expression exhibited strong plasma membrane staining (n=18/18, 100%). Half (n=9/18, 50%) had concomitant cytoplasmic staining while 9/18 (50%) had strong circumferential plasma membrane staining in a "cobblestone pattern" with little to no detectable cytoplasmic expression by secondary immunofluorescence (Figure 22). Raw data (Table 13) and representative images of secondary immunofluorescent staining for EGFR in PNS of cSCCHN are shown below (Figures 23, 24).

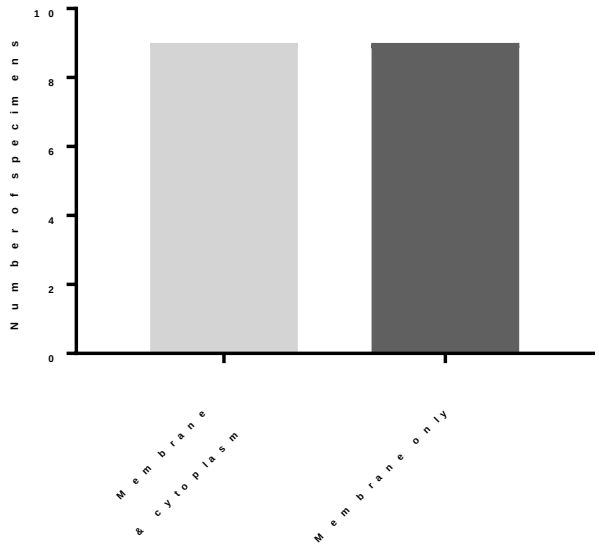

Figure 22 EGFR subcellular localisation assessed by secondary immunofluorescence. Plasma membrane staining was observed in all specimens (n=18). Detectable concomitant cytoplasmic

staining was only observed in 50% (9/18) of specimens with the other 50% appearing to have exclusive plasma membrane localisation of the EGFR.

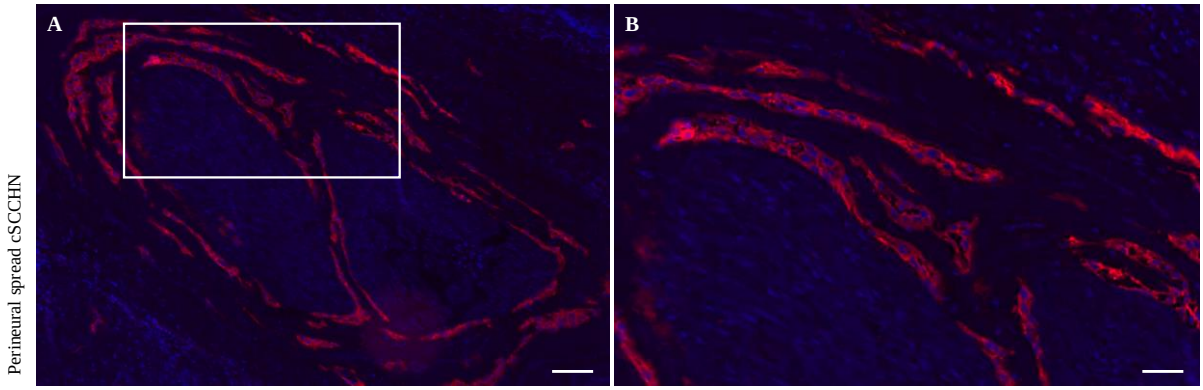

Figure 23 Secondary immunofluorescence staining for EGFR in FFPE tissue of perineural spread of cSCCHN. Primary antibody was anti-EGFR (31G7) and secondary antibody Alexa-555 (red) conjugated anti-mouse IgG. Nuclei were counter-stained with DAPI (blue). Image acquisition was with an Aperio FL Scanner (Leica Biosystems, IL, USA) at 20x magnification. Images were viewed using WebScope software. Left image is at 10x and right image is at 20x magnification (of white boxed area). Scale bars: 200µm (left) and 100µm (right).

Table 13 EGFR staining index, score and localisation assessed by immunostaining in perineural spread cutaneous squamous cell carcinoma of the head and neck

	Staining index			**IHC**	**EGFR**	**Localisation**	
ID	Proportion (%)	Intensity	Index	**Score**	**Status**	Membrane	Cytoplasm
56	90	3	270	2	+	yes	yes
57	40	1	40	1	-	n/a	n/a
62	90	4	360	3	+	yes	no
63	60	1	60	1	-	n/a	n/a
67	100	3	300	3	+	yes	no
69	70	3	210	2	+	yes	yes
70	100	3	300	3	+	yes	yes
71	70	4	280	3	+	yes	no
72	80	3	240	3	+	yes	yes
73	80	3	240	3	+	yes	yes
T2	90	3	270	3	+	yes	yes
T6	100	3	300	2	+	yes	yes
T10	90	3	270	2	+	yes	no

T13	100	4	400	3	+	yes	yes
T21	100	4	400	3	+	yes	no
T22	100	3	300	3	+	yes	no
T26	90	4	360	3	+	yes	no
T27	90	4	360	3	+	yes	no
T28	100	4	400	3	+	yes	yes
T31	80	4	320	3	+	yes	no

n/a = not applicable (immunofluorescence was only performed for immunohistochemically positive specimens)

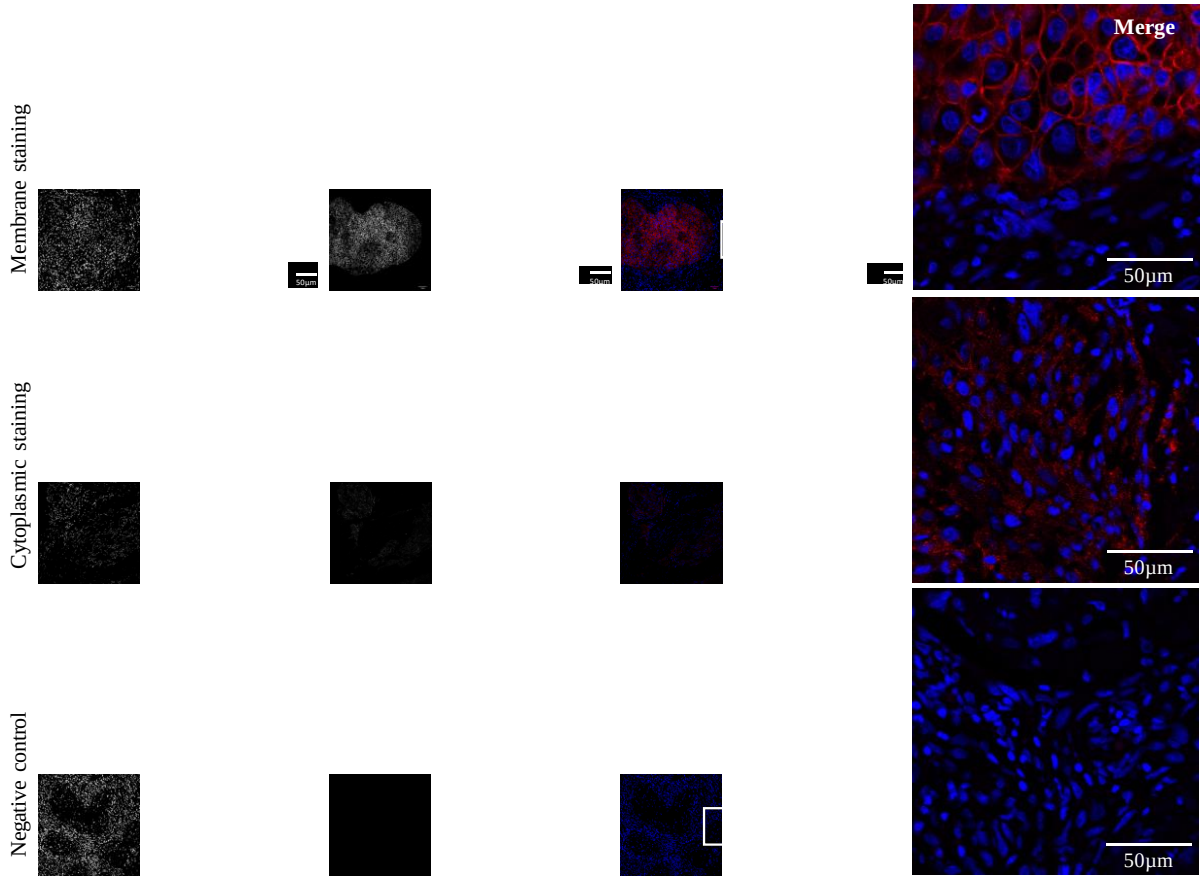

Figure 24 Confocal imaging of secondary immunofluorescence for EGFR in FFPE tissue sections of perineural spread of cSCCHN. Primary antibody was anti-EGFR (31G7) secondary conjugated anti-mouse Alexa-555. Nuclei were counter-stained with DAPI (blue). Images are displayed from left to right as isolated blue channel (DAPI), isolated red channel, merged image at 20x and merged image at 40x magnification (area highlighted by white box). Images were analysed using ImageJ software. Top panel shows plasma membrane staining, middle panel shows punctate endosomal staining within the cytoplasm and lower panel is secondary only negative control on mucosal HNSCC tissue. Scale bars: 50µm.

7.2.4 Perineural spread of cSCCHN has low expression of HER2

Immunohistochemistry for HER2 was similarly performed on the 20 tumour specimens meeting inclusion criteria. Known HER2 positive breast carcinoma and a 4-in-1 manufacturer supplied cell line control slide were used as positive controls and included in each run to ensure reproducibility of staining. A standardized IHC scoring method was used (Table 7). No specimens had detectable HER2 membrane expression by immunohistochemistry (Figures 25, 26). Given the absence of detectable antigen immunofluorescent studies were not performed.

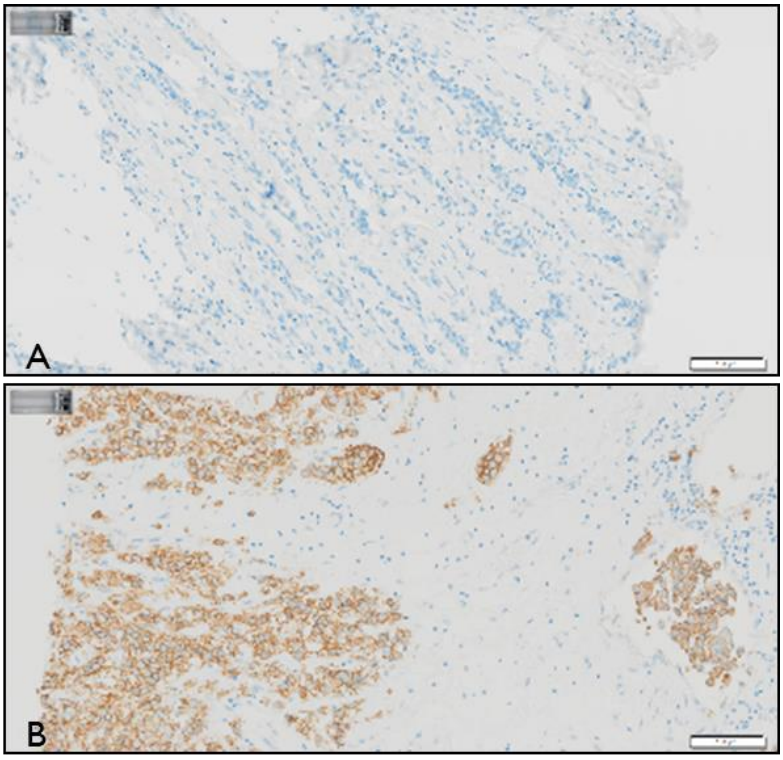

Figure 25 Immunohistochemistry for HER2 protein in formalin fixed paraffin embedded 5-micron tissue sections of perineural spread of cSCCHN. Representative images are shown at x10 magnification. (A) HER2 positive breast carcinoma was used as a positive control. (B) None of 20 perineural spread cSCCHN specimens were positive for HER2 staining in our cohort. The primary antibody was a clinically validated rabbit anti-HER2 (clone 4B5) monoclonal antibody with a goat anti-rabbit HQ HRP detection system and DAB reagent on the Ventana Discovery Ultra automated staining platform. Scale bars: 100μm.

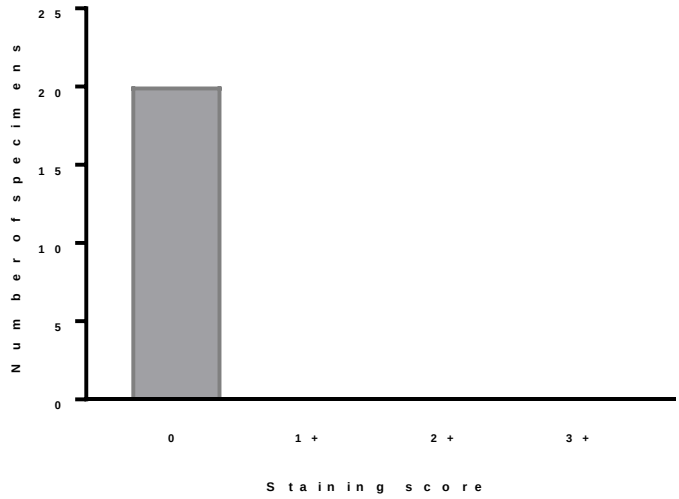

Figure 26 Results of scoring HER2 staining on perineural spread of cSCCHN. None of 20 specimens had detectable HER2 antigen by immunohistochemistry in our cohort.

7.2.5 Further optimisation of tissue immunostaining for HER3 and Eph receptor proteins is required in FFPE tissue

Given the high specificity of antibodies to the EphA2, EphB2 and EphB4 receptors and their variable expression and localisation patterns across the previously examined SCC cell lines, we proceeded to optimisation experiments for immunostaining protocols with these antibodies. Given the notable positive and negative findings with EGFR (ErbB1) and HER2 (ErbB2), respectively, we also aimed to achieve tissue staining for HER3 across our cohort. Given questionable specificity of the EphA3 and EphB1 antibodies available to us and no significant variation in expression level or localisation observed in SCC cell lines compared to the HEKa cell line, no tissue work was pursued with these antibodies.

The Human Protein Atlas database (www.proteinatlas.org) was used to review expression of each target receptor across a range of normal and malignant tissue.[175] Together with manufacturer recommendations, this information was used to select appropriate positive control tissues for optimisation experiments. Available selected tissues were generously gifted by the PAH pathology laboratory from their control stock and are tabulated below (Table 14).

Secondary immunofluorescence was first performed at the bench using the previously described method. Antigen heat retrieval was performed using a microwave oven with retrieval

solution specific for the antibody as per the manufacturer datasheet (Table 14). Both acidic (citrate, pH 6.0) and basic (EDTA, pH 8.0) retrieval solutions were trialled for the EphB2 receptor antibody. Serial dilutions of the primary antibody were based on the recommended starting concentration for immunohistochemistry (Table 14). Primary antibody incubation was overnight at 4°C while an appropriate Alexa fluorophore conjugated secondary antibody (anti-rabbit or anti-goat) was diluted 1/200 and incubated in the dark for 1 hour at RT. Appropriate secondary only negative controls were included in each experiment. Image acquisition with confocal microscopy revealed no specific fluorescent labelling above background across the selected tissues for each of the four receptors.

To ensure these negative results were not a consequence of failings in our laboratory HIER method or high background due to autofluorescence, we attempted immunohistochemistry for EphA2, EphB4 and HER3 on the automated Ventana Discovery Ultra platform. An anti-goat HQ HRP detection system was not available for the Ventana platform at our institute, thus no further experiments were attempted with the anti-EphB2 antibody. Target retrieval solution was again based on the antibody datasheet recommendations at incubated for standard on the automated platform, 32 and 64 minutes, respectively. Serial dilutions across three positive control tissues were performed (Table 14). Brightfield microscopy revealed no positive staining across these tissues for the three antibodies.

Given the inability to achieve positive staining in FFPE control tissues with anti-Eph receptor antibodies, we sought advice from collaborators with experience in this field. Verbal communication with the Boyd laboratory at QIMR Berghofer, who work extensively with the ephrin/Eph receptor family, confirmed that staining in FFPE tissues with the current generation of anti-Eph receptor antibodies is inconsistent and unreliable. Certainly, the standard approaches to optimisation of both immunofluorescence and immunohistochemistry we employed on archival pathology tissue were unsuccessful. Given limited tissue availability and cost constraints a decision was made to pause further attempts at optimising anti-Eph receptor immunostaining and continue to focus experimental tissue work on the ErbB receptor family.

As reported earlier, immunohistochemistry for both EGFR and HER2 with commercially available antibodies was successfully optimised on the Ventana automated platform, with highly specific and reproducible staining achieved. Conversely, there is a lack of standardised immunohistochemistry based methods for detection of HER3 in FFPE tissue. A recent study

compared four commercially available HER3 antibodies and concluded that the monoclonal DAKO (DAK-H3-IC clone) is the only reliable currently available antibody for translational research.[179] The authors observed reproducible circumferential plasma membrane staining in 80% of HER2 positive breast cancers when immunohistochemistry was performed on a DAKO autostainer.[179] Using this antibody on the automated Ventana research platform at our institute, with comparable basic antigen retrieval (CC1 pH 8.0), we were unable to attain positive staining in our small sample (n=2) of HER2 positive breast carcinoma or other potential positive control tissues at recommended dilutions of 1/50 and 1/100 (Table 14). Given tissue and cost constraints we were not able to proceed with further optimisation experiments at this time. This is an area for future research and certainly worth pursuing with DAKO retrieval solution and autostaining apparatus with a wider selection of HER2 positive breast cancer specimens as positive controls.

Table 14 Optimisation immunostaining experiments for monoclonal antibodies to proteins of interest

Antibody	**Serial dilutions**	**Antigen retrieval**	**Positive control**
EphA2	1/50, 1/100, 1/200	EDTA (pH 8.0) CC1 (pH 8.0)*	Breast Ca Colorectal Ca/colon Gastric Ca/stomach
EphB4	1/100, 1/250, 1/500	Citrate (pH 6.1) CC2 (pH 6.0)**	
EphB2	1/20, 1/50, 1/100	EDTA (pH 8.0) Citrate (pH 6.0)	Colorectal Ca/colon Gastric Ca/stomach Cutaneous SCC
HER3	1/50, 1/100	EDTA (pH 8.0) CC1 (pH 8.0)*	Melanoma Breast Ca (HER2+) Colorectal Ca/colon

* CC1 (Ventana cell conditioner 1 target retrieval solution, pH 8.0); **CC2 (Ventana cell conditioner 2 target retrieval solution, pH 6.0). Ca, cancer; SCC, squamous cell carcinoma; EDTA, ethylenediaminetetraacetic acid.

7.2.6 Multiplex immunofluorescent labelling is a viable research strategy for investigating perineural spread of carcinoma

As part of this thesis, double immunofluorescent labelling was performed in perineural spread cSCCHN. Pathology standard pan-cytokeratin (AE1/AE3) and anti-S100 antibodies were used to demonstrate labelling of epithelial tumour cells and nerve sheath myelin, respectively. The previously described secondary immunofluorescence method was applied with the two primary antibodies incubated concurrently overnight and two different Alexa fluorophore conjugated

secondary antibodies, anti-mouse Alexa-555 and anti-rabbit Alexa-488, incubated for 1 hour at room temperature. To our knowledge, this is the first double immunofluorescent staining reported in perineural spread of carcinoma (Figure 27). Previously double immunohistochemistry techniques have been applied with a view to increasing the detection of microscopic perineural invasion. This technique demonstrates that multiplex fluorescent labelling can be achieved with suitable high-specificity antibodies in this disease process. Such a technique is aptly suited to future experimental work given the anatomy of perineural spread and the importance in examining all components of the nerve-tumour microenvironment in dissecting the underlying mechanisms of invasion and spread.

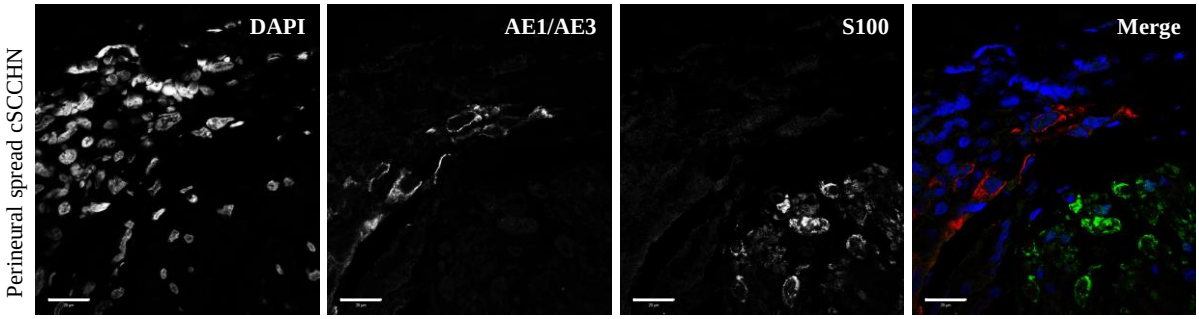

Figure 27 Confocal imaging of double immunofluorescent staining of FFPE tissue sections of perineural spread cSCCHN. Primary antibodies were AE1/AE3 pan-cytokeratin (red) and anti-S100 (green) for epithelial tumour cells and myelin sheath, respectively. Secondary anti-mouse Alexa-555 (red) and anti-rabbit Alexa-488 (green) antibodies were used, respectively. Nuclei were counter-stained with DAPI (blue). Representative image of perineural spread cSCCHN in transverse section at x63 magnification is displayed from left to right as isolated blue channel (DAPI), isolated red channel (AE1/AE3), isolated green channel (S100) and merged colour image. Scale bar: 20μm.

7.2.7 Biomarker profile and correlations in perineural spread of cSCCHN

It is integral to consider the complete molecular profile of a malignant process, not just individual receptors or drug targets in isolation. EGFR over-expression and receptor localisation are compared for p16 status, p53 staining pattern and Ki-67 proliferation index (PI) in tables below (Tables 15, 16). Contingency table analysis in GraphPad Prism software was performed using two-tailed Chi-square analysis (significance, $p<0.05$) to examine possible correlations between these categorical variables. Specifically, we examined whether EGFR over-expression (positive, n=18 or negative, n=2) or EGFR staining pattern (plasma membrane only, n=9 or other staining pattern, n=11) were related to any of the three biomarkers assessed

by immunohistochemistry. Due to low numbers, for analysis by expression pattern, EGFR negative specimens (n=2) were combined with the group with concomitant plasma membrane and cytoplasmic expression (n=7), which was then compared as a single group to the plasma membrane only expression group (n=9). Each biomarker was then categorized into two clinically significant groups: p16 status was categorized as either positive or negative (negative and weak positivity groups combined), p53 staining pattern was categorized as abnormal (negative or diffuse positive over-expression) or normal (focal positive expression) and Ki-67 PI re-categorized as lowly (<30%) or highly (>30%) proliferative.

There was no statistically significant correlation between EGFR status and p16 status (p=0.52), p53 staining pattern (p=0.64) or PI (p=0.14) (Table 15). Similarly, there was no statistically significant relationship between EGFR staining pattern and these variables (p16, p=0.77; p53, p=0.42; PI, p=0.65) (Table 16). These analyses are largely limited by the small sample size and a larger data set is be required for more meaningful correlations to be examined. Moreover, once sufficient follow-up data is available, Kaplan-Meier survival analyses could be performed with rigorous univariate and multivariate analyses for these biomarkers and other clinicopathological factors.

Given the variability in p16 status and p53 staining pattern, we also examined the relationship between these two variables, given the suggestion of possible distinct underlying mechanisms. There was no statistically significant relationship observed (p=0.63). We also performed Pearson coefficient linear regression analysis to assess correlation between Ki-67 proliferation index, a molecular biomarker for aggressiveness, and time from symptom onset to diagnosis of perineural, a clinical marker for aggressiveness. Low numbers limit conclusions however there was a trend towards correlation without reaching statistical significance in our cohort (p=0.29).

Table 15 Comparison of EGFR over-expression status and biomarker profile

Biomarker		**EGFR positive**	**EGFR negative**	**p-value**
p16 status	Positive	5 (27.8%)	1 (50%)	0.52
	Negative	13 (72.2%)	1 (50%)	
p53 pattern	Abnormal (negative or diffusely positive)	12 (66.7%)	1 (50%)	0.64
	Normal (focally positive)	6 (33.3%)	1 (50%)	
Ki-67 PI	Low (< 30%)	10 (55.6%)	0 (0%)	0.14
	High (> 30%)	8 (44.4%)	2 (100%)	

Chi-square analysis with two-sided p-value (n = 20, significance $p<0.05$). EGFR positive (n = 18) and negative (n = 2) refers to over-expression assessed by immunohistochemistry. PI, proliferation index.

Table 16 Comparison of EGFR localisation pattern and biomarker profile

Biomarker		**Plasma membrane only**	**Other pattern or no over-expression**	**p-value**
p16 status	Positive	3 (33.3%)	3 (27.3%)	0.77
	Negative	6 (66.7%)	8 (72.7%)	
p53 pattern	Abnormal (negative or diffusely positive)	5 (55.6%)	8 (72.7%)	0.42
	Normal (focally positive)	4 (44.4%)	3 (27.3%)	
Ki-67 PI	Low (< 30%)	4 (44.4%)	6 (54.6%)	0.65
	High (> 30%)	5 (55.6%)	5 (45.5%)	

Chi-square analysis with two-sided p-value (n = 20, significance $p<0.05$). PI, proliferation index. EGFR localisation assessed as either plasma membrane only (n = 9) or other pattern (negative or concomitant cytoplasmic staining, n = 11).

8.0 Discussion

8.1 Eph and ErbB receptor expression is variable across SCC cell lines

We examined expression of Eph and ErbB receptors across 4 representative SCC cell lines relative to a normal keratinocyte cell line. Expression of most Eph receptors/ephrin ligands is low in normal adult tissues compared to embryonic development where Eph/ephrin signalling is critical to a number of processes.[77] As described earlier, the dysregulation of expression of these RTKs is complex and observed in a wide range of malignancies.

In normal human epidermal keratinocytes, EphA1, EphA2 and EphA4 are increasingly expressed with differentiation while EphA3 and EphB2 are expressed at very low levels.[180] Ligand activation of EphA2 has been shown to promote differentiation and adhesion via desmoglein 1.[181] EphB2 also promotes differentiation but through reverse signalling in normal skin.[182] Limited research has been conducted in cSCC tissue or cell lines. In chemically induced cutaneous mouse carcinoma, knockout of EphA2 was associated with tumour progression, suggesting a potential tumour suppressor role in normal keratinocytes. Similarly, downregulation of EphA1 has previously been observed in NMSC.[77]

In our study, one HEKa cell line, three cSCC cell lines and one oral cavity SCC cell line were examined qualitatively and quantitatively for Eph receptor expression by Western blot and cell immunofluorescence. Western blot analysis confirmed at least low level expression for EphA2, EphA3, EphB1, EphB2 and EphB4 across the 5 cell lines. However, level and localisation of Eph receptor expression was variable and appeared to possibly be co-related to ErbB receptor expression. The significant membranous EphB2 expression in COLO16 and A431 cell lines we observed by immunofluorescence and immunoblotting supports recently published data that suggests a role for EphB2 in potentiating UVR induced cSCC. In the recent study by Farshchian et al (2015), tumour microarray (TMA) analysis revealed upregulation of EphB2 and EphA4 in primary and metastatic cSCC cell lines compared with HEKa cell lines.[94] Eight SCC cell lines were established from surgically removed primary or metastatic cSCC and upregulation of EphB2 was verified by next generation sequencing and reverse transcriptase PCR. Evaluation of human cSCC tumours on TMAs revealed positive tumour-cell specific EphB2 staining on the cell surface and/or in the cytoplasm of both invasive cSCC and CIS. Subsequent knock-down experiments were performed demonstrating that EphB2 regulates proliferation, migration and invasion of cSCC cell lines *in vitro* and in a xenograft model.[94]

The cytoplasmic expression we observed in normal HEKs suggests relocation or trapping of the EphB2 receptor at the cell surface as a malignant phenotype. However, the very high EphB2 receptor level in A431 cells on quantitative Western blots compared to the qualitative plasma membrane over-expression observed by immunofluorescence suggests at least a level of endosomal expression in the A431 cell line. Conversely, the KJD cSCC cell line did not appear to express EphB2 at significant levels at the plasma membrane by immunofluorescence. This cell line is transformed by a virus (SV40) and not derived from solar UVR exposed human skin, thus a dissimilar receptor profile is not unexpected. Similarly, this may account for the low receptor tyrosine kinase expression observed in the KJD cell line across the board, including the other Eph receptors, EGFR and HER3. Our data supports the notion that virus induced cancers may not be dependent or as dependent on receptor tyrosine kinase signalling.

The role of EphA2 as a tumour suppressor gene in skin cancer suggested by previous studies in mice is somewhat challenged by our data. The globally high levels of EphA2 expression across the SCC cell lines in our study would suggest overexpression as a key mechanism in concordance with recent clinical data associating EphA2 with tumour progression and poor survival.[84,183,184] A recent systematic review found EphA2 overexpression to be significantly correlated with poor overall survival in patients with various human carcinomas.[185] In our study, all four tumour cell lines had significant plasma membrane expression of EphA2 on immunofluorescence. Immunoblotting results were largely consistent with these findings. A relative discrepancy between the strong membranous staining observed in the SCC15 and A431 cell lines and the much higher quantitative EphA2 expression by Western blot in the A431 cells can be explained by likely changes in epitope accessibility between denatured samples for Western blot compared to native structure in immunofluorescence studies. Moreover, Western blot assesses the entire protein complement whereas immunofluorescence is used to visualise subcellular patterns of protein expression, particularly plasma membrane staining. While our initial attempts at optimisation of immunohistochemistry and immunofluorescence for the EphA2 receptor in tissue were unsuccessful, ongoing improvements in the utility of monoclonal antibodies available for research applications may allow us to re-examine EphA2 and other Eph receptors in perineural spread tissue in future work. Our laboratory also has a banked collection of specimens of actinic keratosis (AK), CIS and invasive cSCC and anticipate further study of EphA2 expression in this spectrum of primary carcinoma.

The observation of high EphB4 expression in COLO16 cells relative to the A431 cell line,

could possibly reflect lower plasma membrane expression of EGFR and HER3 in the COLO16 cell line. In the absence of dominant RTK signalling from ErbB family members, other surface receptors may be upregulated and potentiate kinase signalling. Our data revealed no significant patterns for the EphA3 or EphB1 receptors by immunoblotting or immunofluorescence. However, review of the Western blots suggests that these two antibodies were much less specific with significant background staining and multiple bands present. Based on our data a role for EphA3 and/or EphB1 in cutaneous carcinoma and its forms of metastasis can certainly not be excluded. Expression profiling of a large cohort of cSCCHN with perineural spread found a > 6-fold upregulation of the EphA3 receptor, thus further investigation is warranted.

The cross-talk between membrane receptors in malignancy is an emerging area of research. Tumour heterogeneity is recognised as a key factor in tumour initiation, progression and resistance to therapy. For example, ligand-independent activity of EphA2 has been implicated in multiple cross-talks with EGFR and vascular endothelial growth factor (VEGF) pathways to promote migration, invasion and metastasis.[186] A recent study explored the cross-talk between the EphA2 and EGFR pathways in colorectal cancer.[187] Dual EphA2 and EGFR over-expression had prognostic significance in patients with increasing disease stage and was associated with cetuximab resistance in stage IV patients, independent of KRAS mutation status. These results suggest EphA2 as a complementary biomarker to EGFR and as a possible mechanism of resistance to existing monoclonal antibody therapy. An earlier study in HNSCC suggested STAT-related profiles, including EphA2 status, predicted patient response to targeted treatments in locally advanced disease.[188] EphA2 and EphB2 gene expression were assessed on HNSCC tumour tissues with high EphA2 expressing tumours having higher response to combination cetuximab/radiotherapy and longer progression-free survival. Clearly, more work is required to define the exact mechanisms involved at different tumour sites, but given the observed expression in cSCC and HNSCC cell lines, the EphA2 pathway and its interactions with ErbB receptor signalling remains a candidate axis for future research at the cellular and tissue level in perineural spread cSCCHN.

Although it is difficult to draw significant conclusions from largely qualitative cell line data, the representative cell lines we studied would appear to demonstrate that solar UVR induced, as opposed to virus transformed, SCC cell lines are more dependent on kinase signalling whether via ErbB receptors or Eph receptors. It is likely the balance of receptor expression and activity within each RTK family, and even the balance of the total complement of receptor

tyrosine kinases, that determines the malignant cell phenotype and potential for invasion, metastasis and/or perineural spread. Moreover, further understanding of the variable localisation of these receptors at steady and dynamic states will contribute to understanding the downstream pathways, targeting treatment and overcoming resistance. There is no doubt that RTKs have a significant role to play in cSCC and probably in perineural spread of the same. Eph expression and regulation is probably interdependent on other underlying tumour drivers, whether ErbB tyrosine kinase signalling or disruption of the p53 pathway.

Future studies with a perineural carcinoma cell line would be advantageous but there are obvious anatomical and technical challenges involved in establishing such a cell line. Alternatively, knock-down studies using the *in vitro* DRG tumour co-culture model may be informative regarding the role Eph and ErbB receptor signalling and cross-talk plays in the nerve-tumour microenvironment.

8.2 cSCCHN with perineural spread over-expresses EGFR which represents a potential therapeutic target

We comprehensively examined EGFR expression and localisation in this relatively large series of perineural spread cSCCHN. Acquisition of sufficient tumour samples for meaningful analysis remains challenging given this is a relatively rare condition. At our tertiary institution in Queensland, Australia, we arguably see the highest number of cases per year of perineural spread cSCCHN of any centre worldwide due to the extraordinarily high incidence of NMSC. Of these approximately 25 cases per year are amenable to surgical resection. The inherent anatomy of perineural spread of carcinoma adds another level of difficulty. Research biopsies were not uncommonly found to lack sufficient tumour cells in serial sectioning for rigorous immunostaining experiments, unlike in diffuse solid tumour types. However, excellent recruitment over several years meant that 10 new samples in addition to 10 archived samples were available for our study, a relatively large and representative cohort for this disease.

On review of the literature, EGFR overexpression is reported in up to 35% of primary cSCC and up to 58% of advanced, recurrent or nodal metastatic disease.[189,190] EGFR overexpression is documented in approximately one third of epithelial malignancies across colorectal, breast, ovarian, prostate, bladder and lung cancers.[191] In mucosal HNSCC it is well recognised that EGFR is highly expressed in 80-100% of tumours.[191,192] To our knowledge, this is the first study to look at EGFR expression in perineural spread of cSCCHN.

In our cohort, EGFR over-expression was observed in 90% (18/20) of specimens. The rate of over-expression appears significantly higher than that reported in primary cSCC lesions. Canueta et al (2016) recently evaluated a series of 94 cSCC with only 33 (35%) reported as having high EGFR expression on immunohistochemistry, although at least low level EGFR was detectable in 85 (90.4%) cases.[193] EGFR over-expression was associated with Ki-67 proliferation index, TNM stage and nodal progression in this study. An earlier study by Ch'ng et al (2008) found a similar rate with 9/25 (36%) primary cSCC not associated with metastasis displaying EGFR overexpression.[190] The authors went on to look at nodal metastatic disease derived from 15 of these tumours and observed EGFR overexpression in 7/15 (47%). The highest rate of expression was seen in a sub-group analysis of just the primary lesions associated with metastasis (n=11/14, 79%). Although EGFR over-expression was prognostic for metastasis on multivariate analysis (p=0.05), over-expression was not conserved in metastatic lesions in 53% of cases. FISH analysis revealed EGFR over-expression was independent of gene amplification or mutation however localisation studies were not performed. Possibly, trapping of EGFR on the plasma membrane is an inciting or driving event in invasion and lymphatic dissemination, although the receptor may not play a critical role in established metastatic disease.

Outside this study, there is a consistent general trend towards increasing level of EGFR expression in more aggressive or metastatic lesions reported in the literature. Maubec et al (2005) looked at EGFR and HER2 expression in a series of 13 metastatic recurrent SCC of the skin with 2 primary lesions also studied.[189] Weak HER2 expression was detected in 4/13 (31%) specimens with only 2/13 (15%) displaying membrane positivity, and only in a small proportion of well-differentiated tumour cells. Using the now widely-standardized staining criteria for HER2 applied in our study, none of these specimens would have reached the threshold for positivity. On the other hand, strong plasma membrane staining for EGFR was reported by the authors in 13/13 (100%) metastatic lesions. They noted that 80% cells stained positive at 3+ intensity in every specimen, with a general comment that staining was strongly membranous and a single representative image shown. There is no comment on whether the IHC scoring was performed by an experienced medical pathologist and whether they were blinded to the study hypothesis. The authors used similar methodology with an identical anti-EGFR mouse monoclonal antibody (31G7) at 1/100 and scored the percentage of positively-stained cells per high-power field and intensity of staining as values 1+ to 3+. However, the

identical scoring attributed to all 13 metastatic lesions and 2 associated primary lesions (+++, 80%) raises a concern. One other study examined both primary and metastatic cSCC lesions in 5 patients and reported overexpression in 4/5 (80%) metastatic cases with corresponding but much lower intensity staining in the primary tumours.[194] A different mouse monoclonal antibody (H11) was used in this study. Krahn et al (2001) looked at co-expression patterns of EGFR, HER2, HER3 and HER4 in a small series of 5 cSCC lesions by mRNA analysis.[195] In cSCCs, 40% exhibited triple expression of EGFR/HER2/HER3 compared to 26% of normal skin samples.

In unpublished data from our own laboratory, only 48% of cutaneous SCC (n = 58/120) were EGFR over-expressing on immunofluorescence studies (verbal communication, Fiona Simpson, 2016). Perineural spread is considered to be advanced disease and of note from the literature it is apparent that as disease stage increases, positivity for EGFR also increases. The finding that 90% of perineural spread cSCCHN over-expresses EGFR suggests that the EGFR in some way confers the potential for perineural invasion and spread. Certainly it remains unclear whether our finding simply is representative of the aggressive subset of tumours that undergo perineural spread or is indicative of a specific underlying mechanism. However, the finding that half of over-expressing specimens (9/18) appear to have relocation or trapping of the receptor on the cell surface, suggests dysregulation of receptor trafficking may be a significant mechanism. This finding also indicates that perineural spread is not a molecularly homogenous condition. There is significant tumour heterogeneity within the perineural spread cSCCHN cohort which has definite implications in targeting therapy.

Subcellular localisation of the EGFR receptor is variable between specimens as demonstrated by our combined immunohistochemical and immunofluorescence approach, with 50% of EGFR over-expressing specimens in our series (9/18) having concomitant cytoplasmic staining consistent with internalised EGFR on endosomes. Previous live uptake experiments by our laboratory in HNSCC has demonstrated various subtype patterns where, in response to EGF ligand stimulation, EGFR may be polarised on the membrane or internalised on endosomes.[135] Earlier work in our laboratory, with the closely related HER2 receptor, has demonstrated the significance of tumour heterogeneity in terms of subcellular localisation of receptors targeted therapeutically. The EGFR normally internalises by ligand-induced endocytosis and thus in post-fixation steady state staining, such as shown by IHC, we would expect all positive tumour cells to show a degree of cytoplasmic staining. Thus, it is unusual that 50% of specimens show

only marked cell surface labelling with the characteristic cobblestone pattern. The escape of RTKs from internalisation and degradation has been suggested to be a new hallmark of cancer.[196] Tumour heterogeneity and dysregulation of receptor trafficking are now considered the most likely culprits for high rates of treatment failure and resistance development. For example, monotherapy with anti-EGFR antibodies has produced only modest response rates of 5-15% in mucosal HNSCC in clinical trials.[197] Numerous different mutations lead to this phenotype of RTK escape and it will be of great interest to further examine whether such a high rate of RTK escape is a driving factor and amenable therapeutic target in perineural spread cSCCHN. This phenotype alone may represent a major mechanism of cSCC invading and tracking along the perineural compartment.

However, dysregulation of EGFR trafficking is unlikely to be the only driving mechanism implicated in the process. As is described in cSCC, dysregulation of other pathways, including the p53 pathway, may make a significant contribution. Further studies are needed to better elucidate the molecular biology and correlate clinicopathological factors with EGFR status and expression pattern. Irrespective, EGFR expression may constitute a useful biomarker that could be used to predict disease behavior and allow patient stratification.

Although there are certainly limitations in immunohistochemical detection and scoring of protein markers, by performing secondary immunofluorescence with highly specific monoclonal antibodies, we have internally validated our findings. We also aimed to limit bias by utilising two different scoring methods performed by two independent medical pathologists blinded to the study hypotheses. The advent of new techniques, such as in fluorescence situ hybridisation and gene mutation analysis, raises the potential for new complementary approaches to analysing potential drug target expression in future experiments.

We did not perform testing on the index primary lesions in this series and acknowledge that this may have been informative. However, as reported in previous studies, up to 20% of PNS have no history of a primary lesion while in another approximately 20% cases it is impossible to identify the likely primary in the context of a history of multiple cutaneous malignancies in patients with widespread UVR induced field change. The most recent analysis of our institutional database show that 42% patients have an unidentifiable primary.[142] As expected, this was a consistent finding in our cohort where 45% had an unidentifiable or un-assessable index lesion. In future work, it would be useful to access tissue for those identifiable likely

primary lesions to assess whether EGFR status and other biomarkers correlate between the primary and subsequent perineural disease. However, we expect this may have limited clinical application given the large numbers with an unidentifiable primary. Resources may be better dedicated to other promising avenues of research.

The logical next step to build on our finding of EGFR overexpression is application to the *in vitro* and *in vivo* models of perineural spread discussed earlier. Recent findings by our collaborators at QIMR demonstrate that the A431 cell line has a strong propensity for perineural invasion.[51] This research group utilized a popular *in vitro* DRG co-culture model and has also developed and optimized an *in vivo* murine model whereby tumour cells are injected subcutaneously into the cheek of Balb/c nude mice (Figure 7).[51] The whisker region is richly innervated by the maxillary division of the trigeminal nerve and models the proximity of the human division to high-risk mid-face cSCC. This is thought to be a higher fidelity model as it avoids direct injection of tumour cells into the nerve sheath, replicating the disease natural history in humans. In their *in vitro* study the highest rates of neurite outgrowth and tumour cell invasion were observed for the parenteral A431 cell line. Knockdown studies for LOXL2 and TGM3 did not significantly alter neurotropism. After initial optimization of cell injection counts, 6 of 7 (86%) mice injected with parenteral A431 cell line developed PNI. However, none developed perineural spread away from the main tumour bulk in the timeframe of mouse survival post tumour cell inoculation, in the setting of rapid primary tumour growth. On the other hand, no incidental PNI or PNS was observed histologically in any of the mice with tumours derived from the COLO16 cell line.[51] Further studies are underway to optimize the cell number injection required to allow sufficient time for perineural spread to occur before mandated euthanasia due to primary tumour bulk (verbal communication, Dr Glen Boyle, 2016). Potentially, there may be a role for primary tumour excision to allow sufficient time for perineural invasion and spread to occur and thus replicate the natural history of perineural spread in humans.[51]

The A431 cell line is known to express abnormally high levels of EGFR in culture and our work and that of many others supports this at a gene and protein level.[176] Given the increased levels of EGFR expression demonstrated in human specimens of perineural spread by our work, and our collaborators experience with this cell line *in vivo,* we suggest that it may be the EGFR receptor and/or RTK downstream signaling that facilitates perineural invasion in the first instance, as observed in the model, and then subsequent spread, as seen in our tissue work.

Regardless, EGFR overexpression appears to be a consistent feature implicated in the process. We anticipate further experimentation with the A431 cell line in the xenograft model including further knockdown studies. Alternatively, ethical approval could be sought for trial of an anti-EGFR monoclonal antibody in mice with perineural spread. Radiological investigations may need to be validated to replace histopathological confirmation of perineural spread in this setting.

EGFR is not currently considered a useful biomarker or prognostic factor in cutaneous SCC. Although it may be associated with an increased metastatic potential in some lesions, its expression does not appear to be conserved once metastasis has occurred.[190] Current response rates to EGFR monoclonal therapy in metastatic cutaneous SCC remain extremely poor.[198] However, our data suggests a potential role for EGFR in perineural spread and reveals a novel therapeutic target and possible biomarker in this subset of disease. In future, EGFR may be used to identify those primary lesions with an increased propensity to access and propagate along the perineural compartment. Knowledge of a patients EGFR status in combination with the presence of other adverse features such as the presence of microscopic PNI on original pathology and location on a high risk area (e.g. mid-face, forehead or lower lip) could inform follow-up protocols post primary resection. Such patients could be considered high risk for perineural spread and appropriate close clinical follow-up instituted, with a low threshold for MR neurogram to evaluate the trigeminal and/or facial nerves. Evaluation of index lesions, other clinicopathological factors and survival outcomes would be of benefit.

8.3 HER2 does not play a significant role in perineural spread of cSCCHN

In the era of development of multivalent antibodies, it may be suboptimal to identify a single receptor tyrosine kinase as a potential drug target, even in a disease process where there is currently no targeted therapy. A known mechanism of tumour resistance to current monoclonal antibody therapies is tumour evasion by activation of other kinase signalling pathways.[126] Thus, there is current focus on combination therapeutics targeting either proteins within the same family or between families in a range of malignancies.[199] Advances in antibody engineering technology has facilitated such approaches and several bispecific antibodies are currently in early clinical trial. Recently, the superiority of a tetraspecific antibody to individual monospecific antibodies was demonstrated in a heterogenous tumour population.[200] Beyond inducing antibody dependent cell cytotoxicity by recruiting FcγR positive immune cells, some

research groups have looked at targeting the immune system against cancer by designing dual antibody constructs that cross-link tumour cells and T cells via their CD3 receptors.[199]

In terms of the ErbB family specifically, where the HER2 receptor is completely dependent and the HER3 is a partially impaired RTK, preventing heterodimerisation is a key strategy. Dual targeting of EGFR and ErbB2 pathways has been shown to have synergistic effect on cancer cell proliferation and migration in *in vitro* models with human cancer cell lines.[201] Lapatinib is a dual TKI that targets both EGFR and HER2 and has progressed to clinical trial in breast cancer.[202] Targeting the four members of the ERRB family in HNSCC with a mixture of six antibodies (pan-HER) has also recently been shown to reduce cell proliferation in vitro and achieve superior growth delay in a murine model compared to cetuximab or vehicle control.[203]

Thus, given that HER2 is the preferred heterodimerisation partner for other members of the ErbB family, including EGFR, we sought to characterise HER2 expression in perineural spread to complement our finding of significant EGFR overexpression. None of 20 specimens stained positive for HER2 using a high affinity antibody. Although limitations in immunohistochemistry do exist, HER2 interpretation is subject to standardised guidelines and highly reproducible.[204] The 4B5 anti-HER2 antibody we used has been shown to have excellent sensitivity, specificity and inter-laboratory reproducibility for the detection of HER2 status in breast cancer.[205] However, HER2 was not detectable by IHC in any of the 20 specimens of perineural spread. We conclude that HER2 does not play a significant role in perineural spread of cSCCHN and does not represent a potential therapeutic target in this unique form of tumour metastasis.

On review of the literature, there are few previous studies investigating the role of HER2 in squamous cell carcinoma. One study looked at co-expression patterns of ErbB receptors in NMSC and found HER2 to be ubiquitously expressed in all tested tissue from a mixed cohort of normal skin, BCCs and SCCs (n=56).[195] In a later study of 13 metastatic cSCC, HER2 was weakly expressed in 31% with a membrane expression in only 2 (15%) cases.[189,195] Similarly, ErbB2 status in mucosal HNSCC has not been well studied. In a recent study only 2/42 (5%) laryngeal SCCs and 2/94 (2%) oral cavity SCCs were positive for ErbB2 (HER2) over-expression on immunohistochemistry.[206] Earlier studies have reported an inverse relationship between EGFR and HER2 expression although this was not observed by Maubec et al (2005)

in metastatic cSCC and the absence of HER 2 positivity in our cohort precluded this assessment.[189]

The lack of HER2 expression in these tumours mechanistically is likely to lead to higher EGFR activation as EGFR will homodimerize in the absence of its preferred heterodimeric partner. Under usual circumstances EGFR activated complexes are down-regulated by internalisation and degradation. Our results suggest that in half of the samples of perineural spread, EGFR has escaped this pathway and in the absence of HER internalisation via other routes, such as the clathrin-independent carriers (CLIC)/glycosylphosphotidylinositol-anchored protein enriched compartments (GEEC) endocytosis pathway, EGFR degradation will not occur. This balance of receptor expression and downstream signalling consequences is an area for future exploration in perineural spread. Nonetheless, given our result and others in both cutaneous and HNSCC, it appears that HER2 is not central to the mechanism of perineural spread. Certainly, HER2 absence or low level of expression precludes drug targeting whether as a monotherapy or combination therapeutic. It is also unlikely to emerge as a valuable biomarker in future.

8.4 HER3 and Eph receptor expression remains poorly defined in perineural spread cSCCHN and immunohistochemistry requires further optimisation

HER3 expression is poorly understood in cSCCHN and not characterised at all in perineural spread. In one study of SCC of the cervix (n=78), immunohistochemistry for HER1-HER4 revealed overexpression in 63% for HER1, 22% for HER2, 74% for HER3 and 80% for HER4.[207] Overexpression of HER2 and HER3 was associated with worse prognosis.(207) HER3 has previously been investigated in cSCC but observed to have consistently low level expression.[208] Recently, Kim (2015) suggested a potential role for HER3 in perineural invasion in HNSCC.[209] Expression of HER3 in HNSCC cell lines was reported and activation of HER3 resulted in increased migration and invasion of the tumour cells. Using a co-culture model, chemotactic invasion towards the DRG in a HER3 signalling dependent fashion was observed. In a novel neurite-tumour interaction assay the author went on to demonstrate inhibition of perineural migration by downregulation of HER3 expression. This recent study puts forward the NRG1:HER3 axis as another novel candidate for investigation in perineural spread cSCCHN.

Furthermore, comparable to dual EGFR/HER2 targeting, several studies have now shown that dual inhibition of HER3 and EGFR is efficacious in multiple tumour models.[200] Moreover, inhibition of HER3 phosphorylation has been correlated with anti-proliferative activity of tyrosine kinase inhibitors in colorectal, pancreatic and NSCLC cell lines, suggesting that optimal EGFR signalling inhibition requires simultaneous inhibition of HER3 signalling.[210]

We were unfortunately unsuccessful in our initial attempts to optimise a HER3 immunostaining protocol for FFPE tissue to allow assessment of HER3 expression in perineural spread cSCCHN. The DAKO (DAK-H3-IC) monoclonal antibody used was highly specific on Western blot and cellular immunofluorescence studies. Despite being recognised as the most specific antibody for tissue staining in a recent review article, the application to immunohistochemistry and immunofluorescence in FFPE tissue remains challenging.[179] Using this antibody on the automated Ventana research platform we were unable to attain positive staining in any of the predicted positive tissue controls utilised within our study timeframe. This remains a promising area for further optimisation and future research.

Similarly, despite positive findings on immunoblot and cell immunofluorescence with highly specific CST antibodies targeting the EphA3 and EphB4 receptors, we were unable to achieve specific reproducible immunostaining on positive control FFPE tissues. We anticipate ongoing collaboration with our colleagues in the Boyd laboratory (QIMR Berghofer) to refine antigen retrieval methods and other conditions for FFPE tissue. Alternative approaches could be to target the ephrin ligand as a surrogate marker or trial immunostaining in fresh frozen tissue specimens to avoid the antigenic disruption inherent in the fixation process. Again, this remains an area for ongoing optimisation and research in our laboratory.

The multiplex fluorescent imaging we achieved with pathology standard antibodies to cytokeratin and myelin, is representative of an ideal technique for examining this anatomically unique disease process. Although such techniques have limited application in the clinical setting due to time and cost constraints, secondary immunofluorescence allows high resolution examination of different components of the nerve-tumour microenvironment in the research setting. We hope to apply this method to novel proteins of interest including ErbB and Eph receptors. As discussed earlier, it is probably the balance of RTK expression and activity that dictates the malignant phenotype, and the demonstrated ability to examine multiple receptors and their temporo-spatial relationships provides an avenue for further pursuit.

8.5 The biomarker expression profile of perineural spread of cSCCHN suggests independent or inter-dependent underlying mechanisms

We aimed to determine the expression profile of common cancer biomarkers and correlate with relevant clinicopathological factors. To our knowledge, no previous study has examined the expression or dysregulation of the cell cycle proteins p16 or p53 in perineural spread of carcinoma. Equally, Ki-67 as a marker of cellular proliferation and aggressive disease has not previously been examined. Previous data from our institution published by Warren et al (2016) has consistently shown that cSCCHN with PNS is more likely to be moderately or poorly differentiated.[142] This was confirmed in our series with 95% specimens exhibiting moderate or poor differentiation. Also consistent with the natural history of this disease, a significant proportion of patients in our cohort had an unknown primary or an index lesion could not be assessed or recorded at the time of presentation with perineural disease. This is common in perineural spread and one of the inherent challenges for research in this field. A negative correlation between level of EGFR expression and degree of SCC differentiation has previously been reported in primary cutaneous lesions and in oral cavity SCC and other malignancies.[211] However, due to small numbers we were not able to explore this relationship in perineural spread cSCCHN in our series.

Ki-67 proliferation index is a well characterised marker of cellular proliferation and aggressive disease course. Proliferation index has previously been used to assess perineural invasion in the *in vitro* model developed by Ayala et al (2001).[45] However, to our knowledge, no author has previously examined proliferation status of perineural spread at the tissue level. The monoclonal antibody for Ki-67 antigen is highly specific. However, interpretation of Ki-67 staining is challenging and prone to inter-observer variability. We combated this by using two staining methods, a manual cell count and automated analysis using an online deconvolution algorithm. There was a reasonable degree of correlation between these two methods for specimens for diffuse tumour. The minimal numbers of tumour cells and abundance of other stromal and inflammatory elements in other specimens, consistent with the disease anatomy, limited the application of the automated method necessitating the use of standalone manual cell counts in these cases.

The optimal Ki-67 cut-off for prognostic assessment is unknown. Values ranging between 15-30% as a threshold for clinically significant proliferation have been suggested previously,

while other authors have suggested using the median value of Ki-67 labelling index as a cut-off within a population or series.[173] In our series, median and mean values approximated 30% so this was applied as the threshold for highly proliferative tumours. In our cohort, 50% of cSCCHN with PNS had proliferation index ≥30% and were considered highly proliferative, with a range up to 55.4%. Several lesions (10%) had low proliferation < 15%. We conclude that perineural spread exhibits a spectrum of proliferation comparable to other presentations of cSCC and non-cutaneous SCC (verbal communication, Ian Brown, 2016). This is consistent with the variable clinical picture of slow to rapidly progressive disease seen in perineural spread. Using time from onset of neuropathic symptoms to diagnosis of perineural spread as a surrogate clinical marker of aggressiveness, we sought to correlate these two factors. In our cohort, median time to diagnosis was 4 months (range, 1-60 months) and a mean time of approximately 11 months. This is comparable to previous studies, which quote an average delay of 6-18 months from symptom onset to definitive diagnosis of perineural spread, usually on MR neurography.[142] Although we expected a linear correlation between Ki-67 proliferation index and rapidity of presentation, this was not supported by our data to statistical significance. There is a significant margin of error in the retrospective estimate of symptom duration by patients and it may be that other markers of aggressiveness may be more representative for future work. Irrespective, once sufficient follow-up data is available, survival analysis using the Kaplan-Meier method would be applicable with univariate and multivariate analyses likely to be informative. Ki-67 may have role in disease prognostication and allow rationalisation of therapy, as has recently been demonstrated in mucosal HNSCC. It has also been examined as an independent or combination therapeutic target in other settings.

8.5.1 A subset of perineural spread is strongly positive for p16, which represents a potential biomarker

To our knowledge this is the first study to assess p16 status in perineural spread cSCCHN and by surrogate consider the possible role of chronic HPV infection in the pathogenesis of this process. Nearly one third (30%) of our cohort were strongly positive for p16 and met the clinical threshold for p16 positivity used in mucosal HNSCC. Lower thresholds for positivity have been used in other studies of cSCC, which may have overestimated the incidence. Although there is no agreed definition, we used the method published in recent literature assessing primary and nodal metastatic lesions.[172] As to whether it is viral or UVR associated dysregulation in the p16 pathway that has led to significant overexpression in a subset of perineural spread cSCCHN, it is difficult to say. Unlike other studies, we did not perform FISH

or PCR for the presence of high-risk HPV subtypes. Although these could be performed in future, the presence of viral DNA has been shown to be less clinically significant than the surrogate p16 marker, which is a validated prognostic factor independent of HPV status in oropharyngeal SCC.[152] The hypothesis that chronic viral infection and associated inflammation facilitates or contributes perineural invasion of carcinoma requires further investigation with appropriately designed studies. A potential role for neurotropic viruses in the mechanisms of perineural spread and even as a means of targeting therapy to the nerve microenvironment could also be considered in future studies.

8.5.2. The p53 pathway appears to be dysregulated in a subset of perineural spread

We built on earlier work by our collaborators at QIMR Berghofer by completing immunohistochemical staining for p53 across our cohort.[142] Reproducible specific staining was achieved, which displayed one of three patterns described by previous authors in ovarian and colorectal cancers.[147] Importantly, staining was performed using identical methodology to allow pooling of data. Earlier mutational analyses have shown the TP53 gene to be mutated in more than 50% of cSCC with aggressive tumours, including those with incidental PNI.[132] In perineural spread cSCCHN we would expect a high mutational background secondary to UVR as observed in primary and metastatic cSCC. It is unsurprising that in our cohort an abnormal staining pattern for p53 was observed in 65% of specimens, with half the tumours exhibiting diffuse staining pattern consistent with reactive over-expression and 15% having no positive staining consistent with loss of function of this integral tumour suppressor gene. Certainly these findings support the assertion of our collaborators that the p53 pathway is implicated in perineural spread cSCCHN.[142] The question remains whether this is simply a bystander effect or a conserved signature of UVR exposure and the index lesion. Alternatively, further dysregulation at the molecular level may be critically important in the processes of perineural invasion and spread. As with other potential biomarkers examined in our study, future survival analyses will be informative regarding their clinical utility as prognostic factors. In our study, we were also unable to establish a statistically significant correlation between EGFR status or localisation and any of the biomarkers examined, unfortunately limited largely by small numbers. In the research setting we would support ongoing acquisition of biopsies and staining for Ki-67, p16 and p53 in anticipation of further analyses.

8.6 Final discussion

Knowledge of the molecular profile and drivers for a cancer sub-type is imperative to targeting therapy. Increasing research focus is centred on multivalent antibody therapy or multi-targeted approaches. For example, one research group recently demonstrated efficient and selective light-controlled tumour cell killing *in vitro* for cells positive for both EGFR and Ki-67 via a dual targeting approach.[97] Multivalent antibody therapy to the ErbB family remains the frontier in cancer therapy, particularly in the fight to overcome resistance. Further characterisation of other RTKs, including HER3 and the Eph receptor family, is needed in the context of perineural spread cSCCHN. In particular, based on our cell data and given the availability of highly specific monoclonal antibodies, suitable candidates for further research would include EphA2, EphB2 and EphB4. The advantage of immunohistochemistry-based biomarkers is that they offer significant potential for rapid translation to clinical practice compared to biomarkers requiring more complicated, time-consuming and expensive methods. Recently, a small multi-marker panel using simple immunohistochemistry methods to evaluate 5-hydroxymethylcytosine (5hmC), Ki-67 and p16 has shown promise as an adjunct for prognostication in melanoma.[212] Evidently, significant optimisation is required to achieve reliable reproducible staining in fixed tissue but we hope a similar panel may be applicable in perineural spread to better risk stratify patients and allow treatment rationalisation. Some cases of perineural spread progress slowly towards the brainstem and may not affect the patient in their lifetime if they are elderly and/or have significant comorbidities. Other cases progress rapidly, with significant morbidity, justifying aggressive intervention. There is a high risk of recurrence, particularly given the anatomical constraints of oncologic resection, and close clinical and radiological follow-up is required. Identification of novel biomarkers would aid prognostication from biopsy or resection specimens, may inform risk of progression or recurrence and thus allow appropriate rationalisation of therapy and informed follow-up. In this era of personalised medicine and technological advances, individualisation of therapy based on the molecular profile of a patients perineural disease is not unforeseeable.

The demonstrated dysregulation of tumour suppressor genes in perineural spread is a notable finding. As discussed earlier, cSCC can be considered as RTK driven via EGFR signalling or driven by dysregulation of the p53 pathway. In our study, EGFR overexpression was almost universal suggesting that perineural spread cSCCHN may be derived from the former group of cutaneous primaries and is thus genetically similar to mucosal HNSCC. Genetic and epigenetic changes in epidermal and dermal cells secondary to solar UVR is certainly the principal

mechanism in any form of cSCC and tumour cells typically harbour driver mutations that reflect this. However it is evidently these changes in the context of concomitant alterations in the microenvironment that facilitates progression of precursor lesions to invasive SCC, and SCC to more malignant forms of the disease, including tumours with perineural invasion and/or spread.[131] Further consideration of RTK signalling in the context of the nerve-tumour microenvironment is required either using established *in vitro* models or other novel approaches. Loss of immune surveillance and the presence of HPV are two other risk factors, best demonstrated in the development of cSCC in the immunosuppressed population. Although immunosuppression is not seen to be a risk factor for perineural spread, the inflammatory infiltrate associated with PNS of cSCCHN and changes in T-cell subsets previously reported by our collaborators support a possibly interplay between chronic HPV infection, chronic inflammation, significant UVR exposure and either the p53 pathway or dysregulation EGFR trafficking in both cSCCHN and perineural spread of the same. This led us to consider p53 and p16 expression at an early stage in our investigation into perineural disease. Together with Ki-67 proliferation index this provides an indication that there are probably diverse underlying mechanisms driving perineural spread of carcinoma.

Our findings support a significant role for dysregulation of EGFR trafficking. As such we have revealed potential biomarker and also a clinically relevant therapeutic target. Larger numbers are certainly needed but given our tertiary centre sees 25 patients amenable to surgical resection per year, tissue acquisition remains an ongoing challenge. Moving into the established subcutaneous mouse model at an early stage is justified to ensure any benefits can be translated to the current generation of patients suffering from this morbid disease. We similarly anticipate early recruitment of patients with recalcitrant end-stage perineural disease who have either failed or are unsuitable for conventional therapy into a recently approved clinical trial which uses a dynamin inhibitor in combination with cetuximab to target EGFR at the cell surface.[213-215] Trapping the EGFR at the plasma membrane through dynamin inhibition in the perineural spread cohort has conceivable advantage beyond monotherapy given the significant tumour heterogeneity observed in our study.

8.7 Future directions

Further research is required to elucidate the underlying mechanisms of perineural spread of carcinoma. We have potentially uncovered an important biomarker and made a significant step forward in detection of EGFR overexpression. However, it is undoubtedly the interplay of

several mechanisms that culminate in this unique disease process. To build directly on our current findings we anticipate utilising existing *in vitro* and *in vivo* models as described above. Our collaborators at the QIMR Berghofer have utilised a DRG co-culture model and a subcutaneous murine model of perineural spread. Subject to ethics approval, we would also aim to commence a mouse study with a therapeutic anti-EGFR antibody with appropriate control arms. Success in the murine model may allow us to enrol select patients who have failed conventional therapy to a recently approved phase I clinical trial targeting the EGFR with cetuximab in combination with prochlorperazine (CESTEM trial).[215] Reversing the heterogeneity of the cohort by co-administering a dynamin inhibitor could be expected to provide additional benefit, as shown in a proof of mechanism study recently by our laboratory.[213-215]

9.0 Conclusion

Our findings clearly have direct clinical implications. A role for EGFR in perineural spread is supported while HER2 does not appear to be involved. Subcellular localization of the receptor may have implications in targeting therapy and overcoming resistance to current therapies. The EGFR may represent an opportunity to more accurately predict perineural spread from the index lesion, prognosticate patients, rationalise therapy and inform follow-up. Knowledge of the co-existing biomarker profile and future survival analyses may shed further light. Existing targeted therapies to the epidermal growth factor receptor could be re-purposed for use in perineural spread and clinical trials for novel/combination therapies could be extended to patients with recurrent and/or unresectable perineural spread of carcinoma. Ultimately, it is hoped we can improve patient morbidity and mortality not only in cutaneous squamous cell carcinoma of the head and neck, but in other neurotropic malignancy.

10.0 References

1. Ramirez CC, Federman DG, Kirsner RS. Skin cancer as an occupational disease: the effect of ultraviolet and other forms of radiation. Int J Dermatol. 2005 Feb;44(2):95–100.

2. Perera E, Gnaneswaran N, Staines C, Win AK, Sinclair R. Incidence and prevalence of non-melanoma skin cancer in Australia: A systematic review. Australas J Dermatol. 2015 Nov;56(4):258–67.

3. Buettner PG, Raasch BA. Incidence rates of skin cancer in Townsville, Australia. Int J Cancer. 1998 Nov 23;78(5):587–93.

4. Cancer in Australia 2014: actual incidence data from 1982 to 2011 and mortality data from 1982 to 2012 with projections to 2014. Asia Pac J Clin Oncol. 2015 Sep;11(3):208–20.

5. Skin cancer in Australia. Canberra: AIHW; 2016. Report No.: Cat. no. CAN 96.

6. Jambusaria-Pahlajani A, Miller CJ, Quon H, Smith N, Klein RQ, Schmults CD. Surgical monotherapy versus surgery plus adjuvant radiotherapy in high-risk cutaneous squamous cell carcinoma: a systematic review of outcomes. Dermatol Surg. 2009 Apr;35(4):574–85.

7. Clayman GL, Lee JJ, Holsinger FC, Zhou X, Duvic M, El-Naggar AK, et al. Mortality risk from squamous cell skin cancer. J Clin Oncol. 2005 Feb 1;23(4):759–65.

8. Thompson AK, Kelley BF, Prokop LJ, Murad MH, Baum CL. Risk Factors for Cutaneous Squamous Cell Carcinoma Recurrence, Metastasis, and Disease-Specific Death: A Systematic Review and Meta-analysis. JAMA Dermatol. 2016 Jan 15;152(4):419–28.

9. Staples MP, Elwood M, Burton RC, Williams JL, Marks R, Giles GG. Non-melanoma skin cancer in Australia: the 2002 national survey and trends since 1985. Med J Aust. 2006 Jan 2;184(1):6–10.

10. Fransen M, Karahalios A, Sharma N, English DR, Giles GG, Sinclair RD. Non-melanoma skin cancer in Australia. Med J Aust. 2012 Nov 21;197(10):565–8.

11. Frunza A, Slavescu D, Lascar I. Perineural invasion in head and neck cancers - a review. J Med Life. Carol Davila - University Press; 2014 Jun 15;7(2):121–3.

12. Bapat AA, Hostetter G, Hoff Von DD, Han H. Perineural invasion and associated pain in pancreatic cancer. Nat Rev Cancer. Nature Publishing Group; 2011 Oct;11(10):695–707.

13. Marchesi F, Piemonti L, Mantovani A, Allavena P. Molecular mechanisms of perineural invasion, a forgotten pathway of dissemination and metastasis. Cytokine Growth Factor Rev. 2010 Feb;21(1):77–82.

14. Panizza B, Warren T. Perineural invasion of head and neck skin cancer: diagnostic and therapeutic implications. Curr Oncol Rep. 2013 Apr;15(2):128–33.

15. Batsakis JG. Nerves and neurotropic carcinomas. Ann Otol Rhinol Laryngol. 1985 Jul;94(4 Pt 1):426–7.
16. Larson DL, Rodin AE, Roberts DK, O'Steen WK, Rapperport AS, Lewis SR. Perineural lymphatics: myth or fact. Am J Surg. 1966 Oct;112(4):488–92.
17. Young B, Lowe J, Stevens A, Heath J. Nervous tissues. Wheater's Functional Histology. Elsevier; 2006. 29 p.
18. Akert K, Sandri C, Weibel ER, Peper K, Moor H. The fine structure of the perineural endothelium. Cell Tissue Res. 1976 Jan 27;165(3):281–95.
19. Stolinski C. Structure and composition of the outer connective tissue sheaths of peripheral nerve. J Anat. Wiley-Blackwell; 1995 Feb;186 (Pt 1)(Pt 1):123–30.
20. Panizza B, Warren TA, Solares CA, Boyle GM, Lambie D, Brown I. Histopathological features of clinical perineural invasion of cutaneous squamous cell carcinoma of the head and neck and the potential implications for treatment. Head Neck. 2014 Nov;36(11):1611–8.
21. Brown IS. Pathology of Perineural Spread. J Neurol Surg B Skull Base. 2016 Feb 26;77(2):124–30.
22. Warren TA, Whiteman DC, Porceddu SV, Panizza BJ. Insight into the epidemiology of cutaneous squamous cell carcinoma with perineural spread. Head Neck. 2016 Apr 4;38(9):1416–20.
23. Moonis G, Cunnane MB, Emerick K, Curtin H. Patterns of perineural tumor spread in head and neck cancer. Magn Reson Imaging Clin N Am. 2012 Jun 15;20(3):435–46.
24. Panizza B, Warren TA, Lambie D, Brown I. The fallacy of skip lesions as an example of misinterpretations being propagated in the scientific literature. Oral Oncol. 2012 Oct;48(10):e33–4–authorreplye37.
25. Gandhi MR, Panizza B, Kennedy D. Detecting and defining the anatomic extent of large nerve perineural spread of malignancy: comparing “targeted” MRI with the histologic findings following surgery. Sturgis EM, editor. Head Neck. Wiley Subscription Services, Inc., A Wiley Company; 2011 Apr;33(4):469–75.
26. Warren T, Panizza B. Managing perineural and skull base involvement. In: Riffat F, Palme C, Veness M, editors. Non-melanoma skin cancer of the head and neck. New Delhi, India; 2015. pp. 117–30.
27. Buchanan L, De'Ambrosis B, DeAmbrosis K, Warren T, Huilgol S, Soyer HP, et al. Defining incidental perineural invasion: the need for a national registry. Australas J Dermatol. 2014 May;55(2):107–10.

28. Lewis Kelso R, Colome-Grimmer MI, Uchida T, Wang HQ, Wagner RF. p75(NGFR) immunostaining for the detection of perineural invasion by cutaneous squamous cell carcinoma. Dermatol Surg. 2006 Feb;32(2):177–83.
29. Berlingeri-Ramos AC, Detweiler CJ, Wagner RF, Kelly BC. Dual S-100-AE1/3 Immunohistochemistry to Detect Perineural Invasion in Nonmelanoma Skin Cancers. J Skin Cancer. Hindawi Publishing Corporation; 2015;2015(7):620235–6.
30. Farasat S, Yu SS, Neel VA, Nehal KS, Lardaro T, Mihm MC, et al. A new American Joint Committee on Cancer staging system for cutaneous squamous cell carcinoma: creation and rationale for inclusion of tumor (T) characteristics. J Am Acad Dermatol. 2011 Jun;64(6):1051–9.
31. Frydenlund N, Leone DA, Mitchell B, Abbas O, Dhingra J, Mahalingam M. Perineural invasion in cutaneous squamous cell carcinoma: role of immunohistochemistry, anatomical site, and the high-affinity nerve growth factor receptor TrkA. Hum Pathol. 2015 Aug;46(8):1209–16.
32. Feasel AM, Brown TJ, Bogle MA, Tschen JA, Nelson BR. Perineural invasion of cutaneous malignancies. Dermatol Surg. 2001 Jun;27(6):531–42.
33. Gupta A, Veness M, De'Ambrosis B, Selva D, Huilgol SC. Management of squamous cell and basal cell carcinomas of the head and neck with perineural invasion. Australas J Dermatol. 2015 Mar 11;:n/a–n/a.
34. Warren TA, Nagle CM, Bowman J, Panizza BJ. The Natural History and Treatment Outcomes of Perineural Spread of Malignancy within the Head and Neck. J Neurol Surg B Skull Base. 2016 Mar 10;77(2):107–12.
35. Lin C, Tripcony L, Keller J, Poulsen M, Dickie G. Cutaneous carcinoma of the head and neck with clinical features of perineural infiltration treated with radiotherapy. Clin Oncol (R Coll Radiol). 2013 Jun;25(6):362–7.
36. Solares CA, Lee K, Parmar P, O'Rourke P, Panizza B. Epidemiology of clinical perineural invasion in cutaneous squamous cell carcinoma of the head and neck. Otolaryngol Head Neck Surg. SAGE Publications; 2012 May;146(5):746–51.
37. Warren TA, Panizza B, Porceddu SV, Gandhi M, Patel P, Wood M, et al. Outcomes after surgery and postoperative radiotherapy for perineural spread of head and neck cutaneous squamous cell carcinoma. Head Neck. 2014 Dec 24;:n/a–n/a.
38. Dantas AN, Morais EF de, Macedo RA de P, Tinôco JM de L, Morais M de LS de A. Clinicopathological characteristics and perineural invasion in adenoid cystic carcinoma: a systematic review. Braz J Otorhinolaryngol. 2015 May;81(3):329–35.

39. Vincenzi B, Zoccoli A, Pantano F, Venditti O, Galluzzo S. Cetuximab: from bench to bedside. Curr Cancer Drug Targets. 2010 Feb;10(1):80–95.
40. Magrini SM, Buglione M, Corvò R, Pirtoli L, Paiar F, Ponticelli P, et al. Cetuximab and Radiotherapy Versus Cisplatin and Radiotherapy for Locally Advanced Head and Neck Cancer: A Randomized Phase II Trial. J Clin Oncol. American Society of Clinical Oncology; 2015 Dec 7;:JCO631671.
41. Cavel O, Shomron O, Shabtay A, Vital J, Trejo-Leider L, Weizman N, et al. Endoneurial macrophages induce perineural invasion of pancreatic cancer cells by secretion of GDNF and activation of RET tyrosine kinase receptor. Cancer Res. American Association for Cancer Research; 2012 Nov 15;72(22):5733–43.
42. Deborde S, Omelchenko T, Lyubchik A, Zhou Y, He S, McNamara WF, et al. Schwann cells induce cancer cell dispersion and invasion. Journal of Clinical Investigation. American Society for Clinical Investigation; 2016 Apr 1;126(4):1538–54.
43. Chawla S, Warren TA, Wockner LF, Lambie DLJ, Brown IS, Martin TPC, et al. Galectin-1 is associated with poor prognosis in patients with cutaneous head and neck cancer with perineural spread. Cancer Immunol Immunother. Springer Berlin Heidelberg; 2016 Jan 12;:1–10.
44. Scanlon CS, Banerjee R, Inglehart RC, Liu M, Russo N, Hariharan A, et al. Galanin modulates the neural niche to favour perineural invasion in head and neck cancer. Nat Commun. 2015;6:6885.
45. Ayala GE, Wheeler TM, Shine HD, Schmelz M, Frolov A, Chakraborty S, et al. In vitro dorsal root ganglia and human prostate cell line interaction: redefining perineural invasion in prostate cancer. Prostate. 2001 Nov 1;49(3):213–23.
46. Ayala GE, Dai H, Ittmann M, Li R, Powell M, Frolov A, et al. Growth and survival mechanisms associated with perineural invasion in prostate cancer. Cancer Res. American Association for Cancer Research; 2004 Sep 1;64(17):6082–90.
47. Bakst RL, Wong RJ. Mechanisms of Perineural Invasion. J Neurol Surg B Skull Base. 2016 Mar 10;77(2):96–106.
48. Abiatari I, DeOliveira T, Kerkadze V, Schwager C, Esposito I, Giese NA, et al. Consensus transcriptome signature of perineural invasion in pancreatic carcinoma. Mol Cancer Ther. American Association for Cancer Research; 2009 Jun;8(6):1494–504.
49. Stopczynski RE, Normolle DP, Hartman DJ, Ying H, DeBerry JJ, Bielefeldt K, et al. Neuroplastic changes occur early in the development of pancreatic ductal adenocarcinoma. Cancer Res. 2014 Mar 15;74(6):1718–27.

50. Hibi T, Mori T, Fukuma M, Yamazaki K, Hashiguchi A, Yamada T, et al. Synuclein-gamma is closely involved in perineural invasion and distant metastasis in mouse models and is a novel prognostic factor in pancreatic cancer. Clin Cancer Res. 2009 Apr 15;15(8):2864–71.
51. Gardiner D. Perineural spread of cutaneous malignancy in a live mouse and ganglion-tumour co-culture model. Panizza B, Boyle GM, editors. [Brisbane]: The University of Queensland; 1 p.
52. Koide N, Yamada T, Shibata R, Mori T, Fukuma M, Yamazaki K, et al. Establishment of perineural invasion models and analysis of gene expression revealed an invariant chain (CD74) as a possible molecule involved in perineural invasion in pancreatic cancer. Clin Cancer Res. 2006 Apr 15;12(8):2419–26.
53. Gil Z, Cavel O, Kelly K, Brader P, Rein A, Gao SP, et al. Paracrine regulation of pancreatic cancer cell invasion by peripheral nerves. J Natl Cancer Inst. 2010 Jan 20;102(2):107–18.
54. Bakst RL, Lee N, He S, Chernichenko N, Chen C-H, Linkov G, et al. Radiation impairs perineural invasion by modulating the nerve microenvironment. Camphausen K, editor. PLoS ONE. Public Library of Science; 2012;7(6):e39925.
55. Molloy NH, Read DE, Gorman AM. Nerve growth factor in cancer cell death and survival. Cancers (Basel). Molecular Diversity Preservation International; 2011;3(1):510–30.
56. Geldof AA, Van Haarst EP, Newling DWW. Neurotrophic factors in prostate and prostatic cancer. Prostate Cancer Prostatic Dis. 1998 Sep;1(5):236–41.
57. Kolokythas A, Cox DP, Dekker N, Schmidt BL. Nerve growth factor and tyrosine kinase A receptor in oral squamous cell carcinoma: is there an association with perineural invasion? J Oral Maxillofac Surg. 2010 Jun;68(6):1290–5.
58. Kobayashi K, Ando M, Saito Y, Kondo K, Omura G, Shinozaki-Ushiku A, et al. Nerve Growth Factor Signals as Possible Pathogenic Biomarkers for Perineural Invasion in Adenoid Cystic Carcinoma. Otolaryngol Head Neck Surg. SAGE Publications; 2015 Aug;153(2):218–24.
59. Dollé L, Yazidi-Belkoura El I, Adriaenssens E, Nurcombe V, Hondermarck H. Nerve growth factor overexpression and autocrine loop in breast cancer cells. Oncogene. 2003 Aug 28;22(36):5592–601.
60. Naderi A, Hughes-Davies L. Nerve growth factor/nuclear factor-kappaB pathway as a therapeutic target in breast cancer. J Cancer Res Clin Oncol. 2009 Feb;135(2):211–6.
61. Adriaenssens E, Vanhecke E, Saule P, Mougel A, Page A, Romon R, et al. Nerve growth factor is a potential therapeutic target in breast cancer. Cancer Res. 2008 Jan 15;68(2):346–51.

62. Verbeke S, Meignan S, Lagadec C, Germain E, Hondermarck H, Adriaenssens E, et al. Overexpression of p75(NTR) increases survival of breast cancer cells through p21(waf1). Cell Signal. 2010 Dec;22(12):1864–73.
63. Anolik RB, Aung PP, Bhawan J. P75 neurotrophin receptor expression in squamous cell carcinoma. Am J Dermatopathol. 2015 Feb;37(2):160–1.
64. Chen-Tsai CP, Colome-Grimmer M, Wagner RF. Correlations among neural cell adhesion molecule, nerve growth factor, and its receptors, TrkA, TrkB, TrkC, and p75, in perineural invasion by basal cell and cutaneous squamous cell carcinomas. Dermatol Surg. Blackwell Science Inc; 2004 Jul;30(7):1009–16.
65. Ketterer K, Rao S, Friess H, Weiss J, Büchler MW, Korc M. Reverse transcription-PCR analysis of laser-captured cells points to potential paracrine and autocrine actions of neurotrophins in pancreatic cancer. Clin Cancer Res. 2003 Nov 1;9(14):5127–36.
66. Miknyoczki SJ, Lang D, Huang L, Klein-Szanto AJ, Dionne CA, Ruggeri BA. Neurotrophins and Trk receptors in human pancreatic ductal adenocarcinoma: expression patterns and effects on in vitro invasive behavior. Int J Cancer. 1999 May 5;81(3):417–27.
67. Gao L, Bo H, Wang Y, Zhang J, Zhu M. Neurotrophic Factor Artemin Promotes Invasiveness and Neurotrophic Function of Pancreatic Adenocarcinoma In Vivo and In Vitro. Pancreas. 2015 Jan;44(1):134–43.
68. He S, Chen C-H, Chernichenko N, He S, Bakst RL, Barajas F, et al. GFRα1 released by nerves enhances cancer cell perineural invasion through GDNF-RET signaling. Proc Natl Acad Sci USA. 2014 Apr 28;111(19):E2008–17.
69. Hutcheson JA, Vural E, Korourian S, Hanna E. Neural cell adhesion molecule expression in adenoid cystic carcinoma of the head and neck. Laryngoscope. 2000 Jun 14;110(6):946–8.
70. Shang J, Sheng L, Wang K, Shui Y, Wei Q. Expression of neural cell adhesion molecule in salivary adenoid cystic carcinoma and its correlation with perineural invasion. Oncol Rep. 2007 Dec;18(6):1413–6.
71. Solares CA, Brown I, Boyle GM, Parsons PG, Panizza B. Neural cell adhesion molecule expression: no correlation with perineural invasion in cutaneous squamous cell carcinoma of the head and neck. Head Neck. Wiley Subscription Services, Inc., A Wiley Company; 2009 Jun;31(6):802–6.
72. McLaughlin RB, Montone KT, Wall SJ, Chalian AA, Weinstein GS, Roberts SA, et al. Nerve cell adhesion molecule expression in squamous cell carcinoma of the head and neck: a predictor of propensity toward perineural spread. Laryngoscope. 1999 May;109(5):821–6.

73. Vural E, Hutcheson J, Korourian S, Kechelava S, Hanna E. Correlation of neural cell adhesion molecules with perineural spread of squamous cell carcinoma of the head and neck. Otolaryngol Head Neck Surg. 2000 May;122(5):717–20.
74. He S, He S, Chen C-H, Deborde S, Bakst RL, Chernichenko N, et al. The chemokine (CCL2-CCR2) signaling axis mediates perineural invasion. Mol Cancer Res. 2015 Feb;13(2):380–90.
75. Marchesi F, Piemonti L, Fedele G, Destro A, Roncalli M, Albarello L, et al. The chemokine receptor CX3CR1 is involved in the neural tropism and malignant behavior of pancreatic ductal adenocarcinoma. Cancer Res. 2008 Nov 1;68(21):9060–9.
76. Giaginis C, Tsoukalas N, Bournakis E, Alexandrou P, Kavantzas N, Patsouris E, et al. Ephrin (Eph) receptor A1, A4, A5 and A7 expression in human non-small cell lung carcinoma: associations with clinicopathological parameters, tumor proliferative capacity and patients' survival. BMC Clin Pathol. BioMed Central; 2014;14(1):8.
77. Hafner C, Becker B, Landthaler M, Vogt T. Expression profile of Eph receptors and ephrin ligands in human skin and downregulation of EphA1 in nonmelanoma skin cancer. Mod Pathol. 2006 Oct;19(10):1369–77.
78. Pasquale EB. Eph receptors and ephrins in cancer: bidirectional signalling and beyond. Nat Rev Cancer. Nature Publishing Group; 2010 Mar;10(3):165–80.
79. Bradshaw RA, Dennis EA. Handbook of Cell Signaling, 2/e. Academic Press; 2009. 1 p.
80. Huot J. Ephrin signaling in axon guidance. Prog Neuropsychopharmacol Biol Psychiatry. 2004 Aug;28(5):813–8.
81. Wijeratne DT, Rodger J, Wood FM, Fear MW. The role of Eph receptors and Ephrins in the skin. Int J Dermatol. 2016 Jan;55(1):3–10.
82. Alonso-Colmenar LM. Eph/ephrin signaling in cancer: intricate, puzzling and ... fascinating! Cell Adh Migr. Taylor & Francis; 2012 Mar;6(2):100–1.
83. Shao Z, Zhu F, Song K, Zhang H, Liu K, Shang Z. EphA2/ephrinA1 mRNA expression and protein production in adenoid cystic carcinoma of salivary gland. J Oral Maxillofac Surg. 2013 May;71(5):869–78.
84. Walker-Daniels J, Hess AR, Hendrix MJC, Kinch MS. Differential regulation of EphA2 in normal and malignant cells. Am J Pathol. 2003 Mar 26;162(4):1037–42.
85. Walker-Daniels J, Coffman K, Azimi M, Rhim JS, Bostwick DG, Snyder P, et al. Overexpression of the EphA2 tyrosine kinase in prostate cancer. Prostate. 1999 Nov 2;41(4):275–80.

86. Zelinski DP, Zantek ND, Stewart JC, Irizarry AR, Kinch MS. EphA2 overexpression causes tumorigenesis of mammary epithelial cells. Cancer Res. 2001 Mar 31;61(5):2301–6.
87. Hu M, Carles-Kinch KL, Zelinski DP, Kinch MS. EphA2 induction of fibronectin creates a permissive microenvironment for malignant cells. Mol Cancer Res. 2004 Oct 23;2(10):533–40.
88. Udayakumar D, Zhang G, Ji Z, Njauw C-N, Mroz P, Tsao H. EphA2 is a critical oncogene in melanoma. Oncogene. 2011 Jun 13;30(50):4921–9.
89. Wykosky J, Debinski W. The EphA2 receptor and ephrinA1 ligand in solid tumors: function and therapeutic targeting. Mol Cancer Res. 2008 Dec;6(12):1795–806.
90. Wykosky J, Gibo DM, Stanton C, Debinski W. EphA2 as a novel molecular marker and target in glioblastoma multiforme. Mol Cancer Res. 2005 Oct 29;3(10):541–51.
91. Kikuchi S, Kaibe N, Morimoto K, Fukui H, Niwa H, Maeyama Y, et al. Overexpression of Ephrin A2 receptors in cancer stromal cells is a prognostic factor for the relapse of gastric cancer. Gastric Cancer. Springer Japan; 2015 Jul;18(3):485–94.
92. Xi H-Q, Wu X-S, Wei B, Chen L. Aberrant expression of EphA3 in gastric carcinoma: correlation with tumor angiogenesis and survival. J Gastroenterol. Springer Japan; 2012 Jul;47(7):785–94.
93. Li M, Yang C, Liu X, Yuan L, Zhang F, Wang M, et al. EphA3 promotes malignant transformation of colorectal epithelial cells by upregulating oncogenic pathways. Cancer Lett. 2016 Oct 6;383(2):195–203.
94. Farshchian M, Nissinen L, Siljamäki E, Riihilä P, Toriseva M, Kivisaari A, et al. EphB2 Promotes Progression of Cutaneous Squamous Cell Carcinoma. J Invest Dermatol. 2015 Jul;135(7):1882–92.
95. Ferluga S, Tomé CML, Herpai DM, D'Agostino R, Debinski W. Simultaneous targeting of Eph receptors in glioblastoma. Oncotarget. 2016 Aug 6;7(37):59860–76.
96. Wang SD, Rath P, Lal B, Richard J-P, Li Y, Goodwin CR, et al. EphB2 receptor controls proliferation/migration dichotomy of glioblastoma by interacting with focal adhesion kinase. Oncogene. 2012 Feb 6;31(50):5132–43.
97. Wang S, Hüttmann G, Scholzen T, Zhang Z, Vogel A, Hasan T, et al. A light-controlled switch after dual targeting of proliferating tumor cells via the membrane receptor EGFR and the nuclear protein Ki-67. Sci Rep. 2016 Jun 1;6:27032.
98. Gao Q, Liu W, Cai J, Li M, Gao Y, Lin W, et al. EphB2 promotes cervical cancer progression by inducing epithelial-mesenchymal transition. Hum Pathol. 2014 Feb;45(2):372–81.

99. Husa A-M, MagiÄ ÅE, Larsson M, Fornander T, Pérez-Tenorio G. EPH/ephrin profile and EPHB2 expression predicts patient survival in breast cancer. Oncotarget. 2016 Feb 8;.
100. Ferguson BD, Tretiakova MS, Lingen MW, Gill PS, Salgia R. Expression of the EPHB4 receptor tyrosine kinase in head and neck and renal malignancies--implications for solid tumors and potential for therapeutic inhibition. Growth Factors. 2014 Dec;32(6):202–6.
101. Ferguson BD, Liu R, Rolle CE, Tan Y-HC, Krasnoperov V, Kanteti R, et al. The EphB4 receptor tyrosine kinase promotes lung cancer growth: a potential novel therapeutic target. PLoS ONE. 2013 Jul 2;8(7):e67668.
102. Guo H, Miao H, Gerber L, Singh J, Denning MF, Gilliam AC, et al. Disruption of EphA2 receptor tyrosine kinase leads to increased susceptibility to carcinogenesis in mouse skin. Cancer Res. 2006 Jul 20;66(14):7050–8.
103. Wang X, Xu H, Cao G, Wu Z, Wang J. Loss of EphA3 Protein Expression Is Associated With Advanced TNM Stage in Clear-Cell Renal Cell Carcinoma. Clin Genitourin Cancer. 2016 Aug 8;.
104. Huusko P, Ponciano-Jackson D, Wolf M, Kiefer JA, Azorsa DO, Tuzmen S, et al. Nonsense-mediated decay microarray analysis identifies mutations of EPHB2 in human prostate cancer. Nat Genet. 2004 Aug 8;36(9):979–83.
105. Alazzouzi H, Davalos V, Kokko A, Domingo E, Woerner SM, Wilson AJ, et al. Mechanisms of inactivation of the receptor tyrosine kinase EPHB2 in colorectal tumors. Cancer Res. 2005 Nov 17;65(22):10170–3.
106. Lugli A, Spichtin H, Maurer R, Mirlacher M, Kiefer J, Huusko P, et al. EphB2 expression across 138 human tumor types in a tissue microarray: high levels of expression in gastrointestinal cancers. Clin Cancer Res. 2005 Sep 17;11(18):6450–8.
107. Davalos V, Dopeso H, Velho S, Ferreira AM, Cirnes L, Díaz-Chico N, et al. High EPHB2 mutation rate in gastric but not endometrial tumors with microsatellite instability. Oncogene. 2006 Jul 3;26(2):308–11.
108. Li X, Choi WW, Yan R, Yu H, Krasnoperov V, Kumar SR, et al. The differential expression of EphB2 and EphB4 receptor kinases in normal bladder and in transitional cell carcinoma of the bladder. PLoS ONE. 2014 Aug 22;9(8):e105326.
109. Miyazaki K, Inokuchi M, Takagi Y, Kato K, Kojima K, Sugihara K. EphA4 is a prognostic factor in gastric cancer. BMC Clin Pathol. BioMed Central; 2013;13(1):19.
110. Farshchian M, Nissinen L, Siljamäki E, Riihilä P, Toriseva M, Kivisaari A, et al. EphB2 Promotes Progression of Cutaneous Squamous Cell Carcinoma. J Invest Dermatol. 2015 Jul;135(7):1882–92.

111. Xi H-Q, Wu X-S, Wei B, Chen L. Eph receptors and ephrins as targets for cancer therapy. J Cell Mol Med. 2012 Dec;16(12):2894–909.
112. Kobayashi H, Kitamura T, Sekiguchi M, Homma MK, Kabuyama Y, Konno S-I, et al. Involvement of EphB1 receptor/EphrinB2 ligand in neuropathic pain. Spine. 2007 Jul 1;32(15):1592–8.
113. Roskoski R. The ErbB/HER family of protein-tyrosine kinases and cancer. Pharmacol Res. 2013 Nov 20;79:34–74.
114. Lemmon MA, Schlessinger J, Ferguson KM. The EGFR family: not so prototypical receptor tyrosine kinases. Cold Spring Harb Perspect Biol. 2014 Apr 1;6(4):a020768.
115. Sharma SV, Bell DW, Settleman J, Haber DA. Epidermal growth factor receptor mutations in lung cancer. Nat Rev Cancer. 2007 Feb 24;7(3):169–81.
116. Roskoski R. ErbB/HER protein-tyrosine kinases: Structures and small molecule inhibitors. Pharmacol Res. 2014 Jun 11;87:42–59.
117. Sorkin A, Goh LK. Endocytosis and intracellular trafficking of ErbBs. Exp Cell Res. 2009 Mar 12;315(4):683–96.
118. Amessou M, Ebrahim AS, Dilly A, Joseph M, Tabolina M, Chukkapalli S, et al. Spatio-temporal regulation of EGFR signaling by the Eps15 homology domain-containing protein 3 (EHD3). Oncotarget. 2016 Nov 5;7(48):79203–16.
119. Arteaga CL, Chinratanalab W, Carter MB. Inhibitors of HER2/neu (erbB-2) signal transduction. Semin Oncol. 2002 Jan 5;28(6 Suppl 18):30–5.
120. Tseng Y-H, Tseng Y-C, Lin Y-H, Lee Y-C, Perng R-P, Whang-Peng J, et al. Epidermal Growth Factor Receptor (EGFR)-Tyrosine Kinase Inhibitor Treatment and Salvage Chemotherapy in EGFR-Mutated Elderly Pulmonary Adenocarcinoma Patients. Oncologist. 2015 Jun 8;20(7):758–66.
121. Fanotto V, Ongaro E, Rihawi K, Avallone A, Silvestris N, Fornaro L, et al. HER-2 inhibition in gastric and colorectal cancers: tangible achievements, novel acquisitions and future perspectives. Oncotarget. 2016 Aug 20;7(42):69060–74.
122. Yarden Y. Biology of HER2 and its importance in breast cancer. Oncology. 2001 Nov 6;61 Suppl 2:1–13.
123. Mahipal A, Grothey A. Role of Biologics in First-Line Treatment of Colorectal Cancer. J Oncol Pract. 2016 Dec 13;12(12):1219–28.
124. Redman JM, Hill EM, AlDeghaither D, Weiner LM. Mechanisms of action of therapeutic antibodies for cancer. Mol Immunol. 2015 Oct;67(2 Pt A):28–45.

125. Okines A, Cunningham D, Chau I. Targeting the human EGFR family in esophagogastric cancer. Nat Rev Clin Oncol. 2011 Apr 5;8(8):492–503.
126. Scott AM, Wolchok JD, Old LJ. Antibody therapy of cancer. Nat Rev Cancer. 2012 Mar 22;12(4):278–87.
127. Srivastava RM, Lee SC, Filho PAA, Lord CA, Jie H-B, Davidson HC, et al. Cetuximab-activated natural killer and dendritic cells collaborate to trigger tumor antigen-specific T-cell immunity in head and neck cancer patients. Clin Cancer Res. 2013 Feb 26;19(7):1858–72.
128. Brandsma AM, Broeke Ten T, Nederend M, Meulenbroek LAPM, van Tetering G, Meyer S, et al. Simultaneous Targeting of FcγRs and FcαRI Enhances Tumor Cell Killing. Cancer Immunol Res. 2015 Sep 25;3(12):1316–24.
129. Mitsui H, Suárez-Fariñas M, Gulati N, Shah KR, Cannizzaro MV, Coats I, et al. Gene expression profiling of the leading edge of cutaneous squamous cell carcinoma: IL-24-driven MMP-7. J Invest Dermatol. 2013 Nov 22;134(5):1418–27.
130. Darr OA, Colacino JA, Tang AL, McHugh JB, Bellile EL, Bradford CR, et al. Epigenetic alterations in metastatic cutaneous carcinoma. Head Neck. 2014 Jun 27;37(7):994–1001.
131. Nissinen L, Farshchian M, Riihilä P, Kähäri V-M. New perspectives on role of tumor microenvironment in progression of cutaneous squamous cell carcinoma. Cell Tissue Res. 2016 Jul 14;365(3):691–702.
132. Pickering CR, Zhou JH, Lee JJ, Drummond JA, Peng SA, Saade RE, et al. Mutational landscape of aggressive cutaneous squamous cell carcinoma. Clin Cancer Res. American Association for Cancer Research; 2014 Dec 15;20(24):6582–92.
133. Gaffney DC, Soyer HP, Simpson F. The epidermal growth factor receptor in squamous cell carcinoma: An emerging drug target. Australas J Dermatol. 2014 Feb;55(1):24–34.
134. Leffell DJ. The scientific basis of skin cancer. J Am Acad Dermatol. 1999 Dec 22;42(1 Pt 2):18–22.
135. Joseph SR, Endo-Munoz L, Gaffney DC, Saunders NA, Simpson F. Dysregulation of epidermal growth factor receptor in actinic keratosis and squamous cell carcinoma. Curr Probl Dermatol. Basel: S. KARGER AG; 2015;46:20–7.
136. Ke H, Harris R, Coloff JL, Jin JY, Leshin B, de Marval PM, et al. The c-Jun NH2-terminal kinase 2 plays a dominant role in human epidermal neoplasia. Cancer Res. 2010 Mar 30;70(8):3080–8.
137. Dooley TP, Reddy SP, Wilborn TW, Davis RL. Biomarkers of human cutaneous squamous cell carcinoma from tissues and cell lines identified by DNA microarrays and qRT-PCR. Biochem Biophys Res Commun. 2003 Jul 11;306(4):1026–36.

138. Li YY, Hanna GJ, Laga AC, Haddad RI, Lorch JH, Hammerman PS. Genomic analysis of metastatic cutaneous squamous cell carcinoma. Clin Cancer Res. American Association for Cancer Research; 2015 Mar 15;21(6):1447–56.
139. Al-Rohil RN, Tarasen AJ, Carlson JA, Wang K, Johnson A, Yelensky R, et al. Evaluation of 122 advanced-stage cutaneous squamous cell carcinomas by comprehensive genomic profiling opens the door for new routes to targeted therapies. Cancer. 2016 Jan 15;122(2):249–57.
140. Al-Rohil RN, Tarasen AJ, Carlson JA, Wang K, Johnson A, Yelensky R, et al. Evaluation of 122 advanced-stage cutaneous squamous cell carcinomas by comprehensive genomic profiling opens the door for new routes to targeted therapies. Cancer. 2016 Jan 15;122(2):249–57.
141. Mays AC, Chou J. Gene Variability between Perineural-Positive and Perineural-Negative Squamous Cell Skin Cancers. International Journal of Genomic Medicine. 2015;03(02).
142. Warren TA, Broit N, Simmons JL, Pierce CJ, Chawla S, Lambie DLJ, et al. Expression profiling of cutaneous squamous cell carcinoma with perineural invasion implicates the p53 pathway in the process. Sci Rep. 2016 Sep 26;6:34081.
143. Brady CA, Attardi LD. p53 at a glance. J Cell Sci. 2010 Oct 14;123(Pt 15):2527–32.
144. Stracquadanio G, Wang X, Wallace MD, Grawenda AM, Zhang P, Hewitt J, et al. The importance of p53 pathway genetics in inherited and somatic cancer genomes. Nat Rev Cancer. 2016 Mar 25;16(4):251–65.
145. Pickering CR, Zhou JH, Lee JJ, Drummond JA, Peng SA, Saade RE, et al. Mutational landscape of aggressive cutaneous squamous cell carcinoma. Clin Cancer Res. American Association for Cancer Research; 2014 Dec 15;20(24):6582–92.
146. Idikio HA. Immunohistochemistry in diagnostic surgical pathology: contributions of protein life-cycle, use of evidence-based methods and data normalization on interpretation of immunohistochemical stains. Int J Clin Exp Pathol. 2009 Nov 25;3(2):169–76.
147. Nyiraneza C, Jouret-Mourin A, Kartheuser A, Camby P, Plomteux O, Detry R, et al. Distinctive patterns of p53 protein expression and microsatellite instability in human colorectal cancer. Hum Pathol. 2011 Jun 12;42(12):1897–910.
148. Yemelyanova A, Vang R, Kshirsagar M, Lu D, Marks MA, Shih IM, et al. Immunohistochemical staining patterns of p53 can serve as a surrogate marker for TP53 mutations in ovarian carcinoma: an immunohistochemical and nucleotide sequencing analysis. Mod Pathol. 2011 May 6;24(9):1248–53.

149. Romagosa C, Simonetti S, López-Vicente L, Mazo A, Lleonart ME, Castellvi J, et al. p16(Ink4a) overexpression in cancer: a tumor suppressor gene associated with senescence and high-grade tumors. Oncogene. 2011 Feb 7;30(18):2087–97.
150. Gonzalez S, Serrano M. A new mechanism of inactivation of the INK4/ARF locus. Cell Cycle. 2006 Jul 1;5(13):1382–4.
151. Mulvany NJ, Allen DG, Wilson SM. Diagnostic utility of p16INK4a: a reappraisal of its use in cervical biopsies. Anticancer Res. 2008 May 1;40(4):335–44.
152. Mollenhauer M, Assmann G, Zengel P, Guntinas-Lichius O, Ihrler S. [HPV-associated oropharyngeal carcinoma. Status quo and relationship with cancer of unknown primary]. Pathologe. 2014 Mar 13;35(2):127.
153. Reuschenbach M, Wagner S, Würdemann N, Sharma SJ, Prigge E-S, Sauer M, et al. [Human papillomavirus and squamous cell cancer of the head and neck region : Prognostic, therapeutic and prophylactic implications]. HNO. 2016 Feb 10;.
154. Hong AM, Dobbins TA, Lee CS, Jones D, Harnett GB, Armstrong BK, et al. Human papillomavirus predicts outcome in oropharyngeal cancer in patients treated primarily with surgery or radiation therapy. Br J Cancer. 2010 Oct 19;103(10):1510–7.
155. Forslund O, Ly H, Reid C, Higgins G. A broad spectrum of human papillomavirus types is present in the skin of Australian patients with non-melanoma skin cancers and solar keratosis. Br J Dermatol. 2003 Jul;149(1):64–73.
156. Hodges A, Smoller BR. Immunohistochemical comparison of p16 expression in actinic keratoses and squamous cell carcinomas of the skin. Mod Pathol. Nature Publishing Group; 2002 Nov;15(11):1121–5.
157. Rohrbach MR, Britt CJ, Schwalbe M, Wieland AM, Hartig GK. p16 Immunohistochemistry Is a Useful Diagnostic Adjunct in Cases of Metastatic Cervical Carcinoma of Unknown Origin. J Oral Maxillofac Surg. 2016 Aug 30;.
158. McDowell LJ, Young RJ, Johnston ML, Tan T-J, Kleid S, Liu CS, et al. p16-positive lymph node metastases from cutaneous head and neck squamous cell carcinoma: No association with high-risk human papillomavirus or prognosis and implications for the workup of the unknown primary. Cancer. 2016 Apr 15;122(8):1201–8.
159. Beadle BM, William WN, McLemore MS, Sturgis EM, Williams MD. p16 expression in cutaneous squamous carcinomas with neck metastases: a potential pitfall in identifying unknown primaries of the head and neck. Head Neck. 2013 Nov;35(11):1527–33.

160. Compton AM, Moore-Medlin T, Herman-Ferdinandez L, Clark C, Caldito GC, Wang XI, et al. Human papillomavirus in metastatic lymph nodes from unknown primary head and neck squamous cell carcinoma. Otolaryngol Head Neck Surg. 2011 Apr 16;145(1):51–7.
161. Wolf GT, Chepeha DB, Bellile E, Nguyen A, Thomas D, McHugh J. Tumor infiltrating lymphocytes (TIL) and prognosis in oral cavity squamous carcinoma: a preliminary study. Oral Oncol. 2014 Oct 3;51(1):90–5.
162. Dalianis T. Human papillomavirus and oropharyngeal cancer, the epidemics, and significance of additional clinical biomarkers for prediction of response to therapy (Review). Int J Oncol. Spandidos Publications; 2014 Mar 21;44(6):1799–805.
163. Bullwinkel J, Baron-Lühr B, Lüdemann A, Wohlenberg C, Gerdes J, Scholzen T. Ki-67 protein is associated with ribosomal RNA transcription in quiescent and proliferating cells. J Cell Physiol. 2005 Oct 6;206(3):624–35.
164. González-González R, Molina-Frechero N, Carreón-Burciaga RG, López-Verdín S, Robles-Bonilla C, Pereira-Prado V, et al. Comparison between Manual and Automated Methods for Ki-67 Immunoexpression Quantification in Ameloblastomas. Anal Cell Pathol (Amst). 2016 Oct 24;2016:7486989.
165. Yerushalmi R, Woods R, Ravdin PM, Hayes MM, Gelmon KA. Ki67 in breast cancer: prognostic and predictive potential. Lancet Oncol. 2010 Feb 16;11(2):174–83.
166. Jung S-Y, Han W, Lee JW, Ko E, Kim E, Yu J-H, et al. Ki-67 expression gives additional prognostic information on St. Gallen 2007 and Adjuvant! Online risk categories in early breast cancer. Ann Surg Oncol. 2009 Feb 14;16(5):1112–21.
167. Li S, Zhan H, Peng S. [Expression of epidermal growth factor receptor Ki67 and p16 in human middle ear cholesteatoma]. Lin Chung Er Bi Yan Hou Tou Jing Wai Ke Za Zhi. 2008 Nov;22(21):987–91.
168. Richards-Taylor S, Ewings SM, Jaynes E, Tilley C, Ellis SG, Armstrong T, et al. The assessment of Ki-67 as a prognostic marker in neuroendocrine tumours: a systematic review and meta-analysis. J Clin Pathol. 2015 Dec 17;69(7):612–8.
169. Marinescu A, Stepan AE, Mărgăritescu C, Marinescu AM, Zăvoi RE, Simionescu CE, et al. P53, p16 and Ki67 immunoexpression in cutaneous squamous cell carcinoma and its precursor lesions. Rom J Morphol Embryol. 2016;57(2 Suppl):691–6.
170. Bedir R, Güçer H, Şehitoğlu İ, Yurdakul C, Bağcı P, Üstüner P. The Role of p16, p21, p27, p53 and Ki-67 Expression in the Differential Diagnosis of Cutaneous Squamous Cell Carcinomas and Keratoacanthomas: An Immunohistochemical Study. Balkan Med J. 2016 Mar;33(2):121–7.

171. Hirsch FR, Varella-Garcia M, Bunn PA, Di Maria MV, Veve R, Bremmes RM, et al. Epidermal growth factor receptor in non-small-cell lung carcinomas: correlation between gene copy number and protein expression and impact on prognosis. J Clin Oncol. 2003 Oct 15;21(20):3798–807.
172. McDowell LJ, Young RJ, Johnston ML, Tan T-J, Kleid S, Liu CS, et al. p16-positive lymph node metastases from cutaneous head and neck squamous cell carcinoma: No association with high-risk human papillomavirus or prognosis and implications for the workup of the unknown primary. Cancer. 2016 Feb 16;:n/a–n/a.
173. Tuominen VJ, Ruotoistenmäki S, Viitanen A, Jumppanen M, Isola J. ImmunoRatio: a publicly available web application for quantitative image analysis of estrogen receptor (ER), progesterone receptor (PR), and Ki-67. Breast Cancer Res. 2010 Jul 27;12(4):R56.
174. Fulawka L, Halon A. Proliferation Index Evaluation in Breast Cancer Using ImageJ and ImmunoRatio Applications. Anticancer Res. 2016 Jul 29;36(8):3965–72.
175. Uhlén M, Fagerberg L, Hallström BM, Lindskog C, Oksvold P, Mardinoglu A, et al. Proteomics. Tissue-based map of the human proteome. Science. 2015 Jan 24;347(6220):1260419.
176. Giard DJ, Aaronson SA, Todaro GJ, Arnstein P, Kersey JH, Dosik H, et al. In vitro cultivation of human tumors: establishment of cell lines derived from a series of solid tumors. J Natl Cancer Inst. 1973 Nov 1;51(5):1417–23.
177. Moore GE, Merrick SB, Woods LK, Arabasz NM. A human squamous cell carcinoma cell line. Cancer Res. 1975 Oct;35(10):2684–8.
178. Dicker AJ, Serewko MM, Dahler AL, Khanna KK, Kaur P, Li A, et al. Functional characterization of cultured cells derived from an intraepidermal carcinoma of the skin (IEC-1). Exp Cell Res. 2000 Jul 18;258(2):352–60.
179. Luhtala S, Staff S, Barok M, Tanner M, Isola J. Comparison of Antibodies for Immunohistochemistry-based Detection of HER3 in Breast Cancer. Appl Immunohistochem Mol Morphol. 2016 Jul 6;:1.
180. White BEP, Getsios S. Eph receptor and ephrin function in breast, gut, and skin epithelia. Cell Adh Migr. 2014 Dec 9;8(4):327–38.
181. Lin S, Gordon K, Kaplan N, Getsios S. Ligand targeting of EphA2 enhances keratinocyte adhesion and differentiation via desmoglein 1. Mol Biol Cell. 2010 Sep 22;21(22):3902–14.
182. Walsh R, Blumenberg M. Eph-2B, acting as an extracellular ligand, induces differentiation markers in epidermal keratinocytes. J Cell Physiol. 2011 Aug 3;227(6):2330–40.

183. Liu Y, Zhang X, Yu C-Y, Qiu Y-Z, Huang D-H, Zhou X-J, et al. [EphA2 promotes angiogenesis and metastasis of head and neck squamous cell carcinoma in vivo]. Zhonghua Er Bi Yan Hou Tou Jing Wai Ke Za Zhi. 2012 Jan;47(1):53–7.
184. Liu Y, Zhang X, Qiu Y, Huang D, Zhang S, Xie L, et al. Clinical significance of EphA2 expression in squamous-cell carcinoma of the head and neck. J Cancer Res Clin Oncol. 2011 May;137(5):761–9.
185. Shen W, Xi H, Zhang K, Cui J, Li J, Wang N, et al. Prognostic role of EphA2 in various human carcinomas: a meta-analysis of 23 related studies. Growth Factors. Taylor & Francis; 2014 Dec;32(6):247–53.
186. Larsen AB, Stockhausen M-T, Poulsen HS. Cell adhesion and EGFR activation regulate EphA2 expression in cancer. Cell Signal. 2009 Dec 2;22(4):636–44.
187. De Robertis M, Loiacono L, Fusilli C, Poeta ML, Mazza T, Sanchez M, et al. Dysregulation of EGFR Pathway in EphA2 Cell Subpopulation Significantly Associates with Poor Prognosis in Colorectal Cancer. Clin Cancer Res. 2016 Jul 11;23(1):159–70.
188. Kotoula V, Lambaki S, Televantou D, Kalogera-Fountzila A, Nikolaou A, Markou K, et al. STAT-Related Profiles Are Associated with Patient Response to Targeted Treatments in Locally Advanced SCCHN. Transl Oncol. 2011 Feb 1;4(1):47–58.
189. Maubec E, Duvillard P, Velasco V, Crickx B, Avril M-F. Immunohistochemical analysis of EGFR and HER-2 in patients with metastatic squamous cell carcinoma of the skin. Anticancer Res. International Institute of Anticancer Research; 2005 May 4;25(2B):1205–10.
190. Ch'ng S, Low I, Ng D, Brasch H, Sullivan M, Davis P, et al. Epidermal growth factor receptor: a novel biomarker for aggressive head and neck cutaneous squamous cell carcinoma. Hum Pathol. 2008 Mar;39(3):344–9.
191. Schneider MR, Yarden Y. The EGFR-HER2 module: a stem cell approach to understanding a prime target and driver of solid tumors. Oncogene. 2015 Oct 5;35(23):2949–60.
192. Grandis JR, Melhem MF, Barnes EL, Tweardy DJ. Quantitative immunohistochemical analysis of transforming growth factor-alpha and epidermal growth factor receptor in patients with squamous cell carcinoma of the head and neck. Cancer. 1996 Sep 15;78(6):1284–92.
193. Cañueto J, Cardeñoso E, García JL, Santos-Briz Á, Castellanos-Martín A, Fernández-López E, et al. EGFR expression is associated with poor outcome in cutaneous squamous cell carcinoma. Br J Dermatol. 2016 Aug 11;.

194. Shimizu T, Izumi H, Oga A, Furumoto H, Murakami T, Ofuji R, et al. Epidermal growth factor receptor overexpression and genetic aberrations in metastatic squamous-cell carcinoma of the skin. Dermatology (Basel). 2001;202(3):203–6.
195. Krähn G, Leiter U, Kaskel P, Udart M, Utikal J, Bezold G, et al. Coexpression patterns of EGFR, HER2, HER3 and HER4 in non-melanoma skin cancer. Eur J Cancer. 2001 Jan;37(2):251–9.
196. Mosesson Y, Mills GB, Yarden Y. Derailed endocytosis: an emerging feature of cancer. Nat Rev Cancer. 2008 Oct 25;8(11):835–50.
197. Sacco AG, Cohen EE. Current Treatment Options for Recurrent or Metastatic Head and Neck Squamous Cell Carcinoma. J Clin Oncol. American Society of Clinical Oncology; 2015 Sep 8;33(29):3305–13.
198. Wollina U. Update of cetuximab for non-melanoma skin cancer. Expert Opin Biol Ther. 2014 Jan 6;14(2):271–6.
199. Fournier P, Schirrmacher V. Bispecific antibodies and trispecific immunocytokines for targeting the immune system against cancer: preparing for the future. BioDrugs. 2013 Jan 19;27(1):35–53.
200. Castoldi R, Schanzer J, Panke C, Jucknischke U, Neubert NJ, Croasdale R, et al. TetraMabs: simultaneous targeting of four oncogenic receptor tyrosine kinases for tumor growth inhibition in heterogeneous tumor cell populations. Protein Eng Des Sel. 2016 Aug 29;29(10):467–75.
201. Gray ME, Lee S, McDowell AL, Erskine M, Loh QTM, Grice O, et al. Dual targeting of EGFR and ERBB2 pathways produces a synergistic effect on cancer cell proliferation and migration in vitro. Vet Comp Oncol. 2016 May 27;.
202. Arteaga CL, Sliwkowski MX, Osborne CK, Perez EA, Puglisi F, Gianni L. Treatment of HER2-positive breast cancer: current status and future perspectives. Nat Rev Clin Oncol. 2011 Nov 29;9(1):16–32.
203. Iida M, Bahrar H, Brand TM, Pearson HE, Coan JP, Orbuch RA, et al. Targeting the HER Family with Pan-HER Effectively Overcomes Resistance to Cetuximab. Mol Cancer Ther. 2016 Jul 15;15(9):2175–86.
204. Wolff AC, Hammond MEH, Schwartz JN, Hagerty KL, Allred DC, Cote RJ, et al. American Society of Clinical Oncology/College of American Pathologists guideline recommendations for human epidermal growth factor receptor 2 testing in breast cancer. Arch Pathol Lab Med. 2007 Jan 1;131(1):18–43.

205. Powell WC, Hicks DG, Prescott N, Tarr SM, Laniauskas S, Williams T, et al. A new rabbit monoclonal antibody (4B5) for the immunohistochemical (IHC) determination of the HER2 status in breast cancer: comparison with CB11, fluorescence in situ hybridization (FISH), and interlaboratory reproducibility. Appl Immunohistochem Mol Morphol. 2007 Jun 1;15(1):94–102.
206. Birkeland AC, Yanik M, Tillman BN, Scott MV, Foltin SK, Mann JE, et al. Identification of Targetable ERBB2 Aberrations in Head and Neck Squamous Cell Carcinoma. JAMA Otolaryngol Head Neck Surg. 2016 Apr 15;142(6):559–67.
207. Fuchs I, Vorsteher N, Bühler H, Evers K, Sehouli J, Schaller G, et al. The prognostic significance of human epidermal growth factor receptor correlations in squamous cell cervical carcinoma. Anticancer Res. International Institute of Anticancer Research; 2007 May 1;27(2):959–63.
208. Krähn G, Leiter U, Kaskel P, Udart M, Utikal J, Bezold G, et al. Coexpression patterns of EGFR, HER2, HER3 and HER4 in non-melanoma skin cancer. Eur J Cancer. 2001 Feb 13;37(2):251–9.
209. Kim S-W. Mechanism of perineural invasion in head and neck cancer. Oral Oncol. Pittsburgh; 2015 May;51(5):30–1.
210. Jiang N, Saba NF, Chen ZG. Advances in Targeting HER3 as an Anticancer Therapy. Chemother Res Pract. 2012 Nov 7;2012:817304.
211. Ulanovski D, Stern Y, Roizman P, Shpitzer T, Popovtzer A, Feinmesser R. Expression of EGFR and Cerb-B2 as prognostic factors in cancer of the tongue. Oral Oncol. 2004 Mar 10;40(5):532–7.
212. Romaine ST, Wells-Jordan P, de Haro T, Dave-Thakrar A, North J, Pringle JH, et al. A small multimarker panel using simple immunohistochemistry methods is an adjunct to stage for cutaneous melanoma prognosis. Melanoma Res. 2016 Oct 26;26(6):580–7.
213. Simpson F, Saunders N. Methods for classifying tumors and uses therefor. Brisbane; PCT/AU2013/001247, 2012.
214. Simpson F, Saunders N. Use of endocytosis inhibitors and antibodies for cancer therapy. Brisbane; PCT/AU2013/001246, 2012.
215. Simpson F, Saunders N. Methods for classifying tumors and uses therefor. Brisbane; provisional application AU2015900484, 2015.

11.0 Appendix A

11.1 Appendix A Representative confocal imaging of cell immunofluorescence

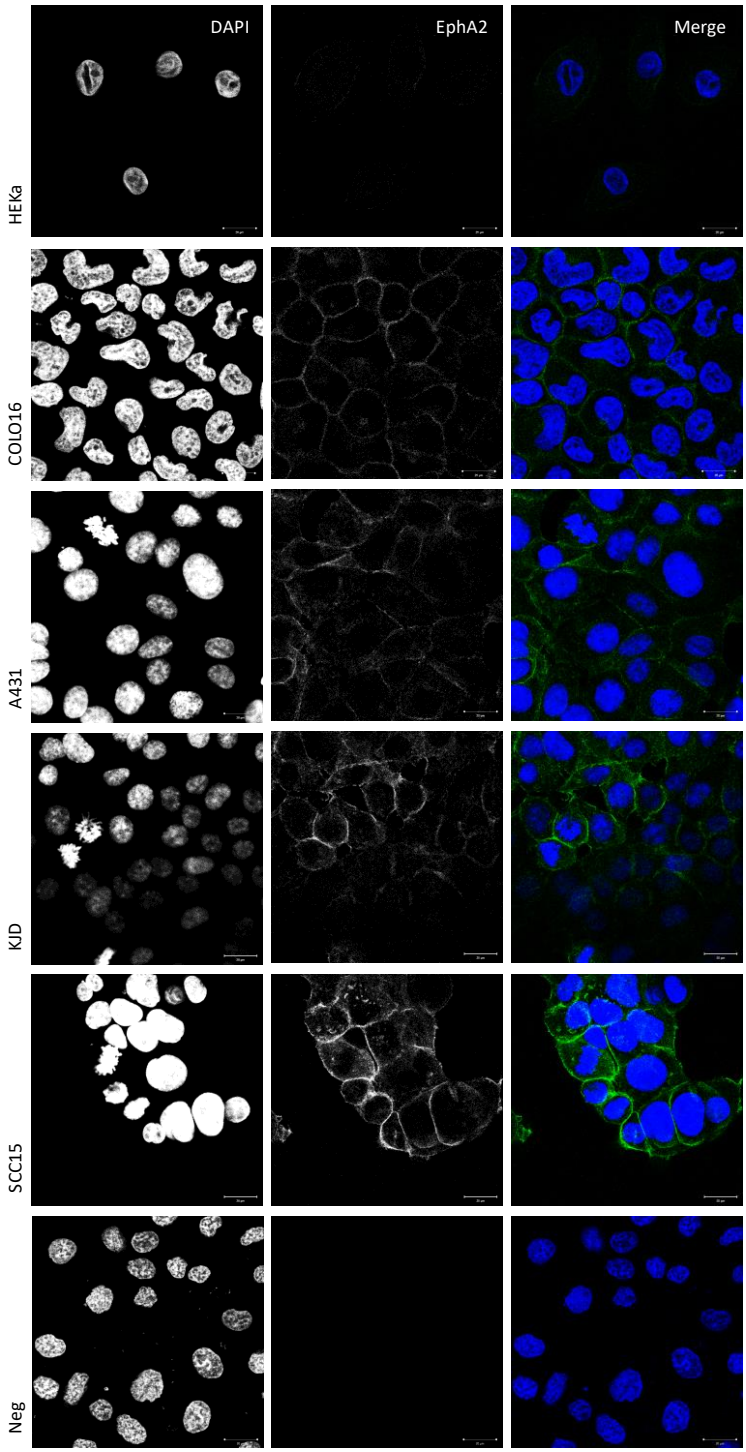

Figure A1 Confocal immunofluorescence images of human cell lines stained with antibody to EphA2 receptor. Images are displayed from left to right as isolated blue channel (DAPI stained nuclei), isolated green channel (anti-EphA2) and merge channel. Secondary anti-rabbit Alexa-488 was used. Negative control (Neg) was A431 cells labelled with secondary antibody only (lower panel). Scale bar = 20μm.

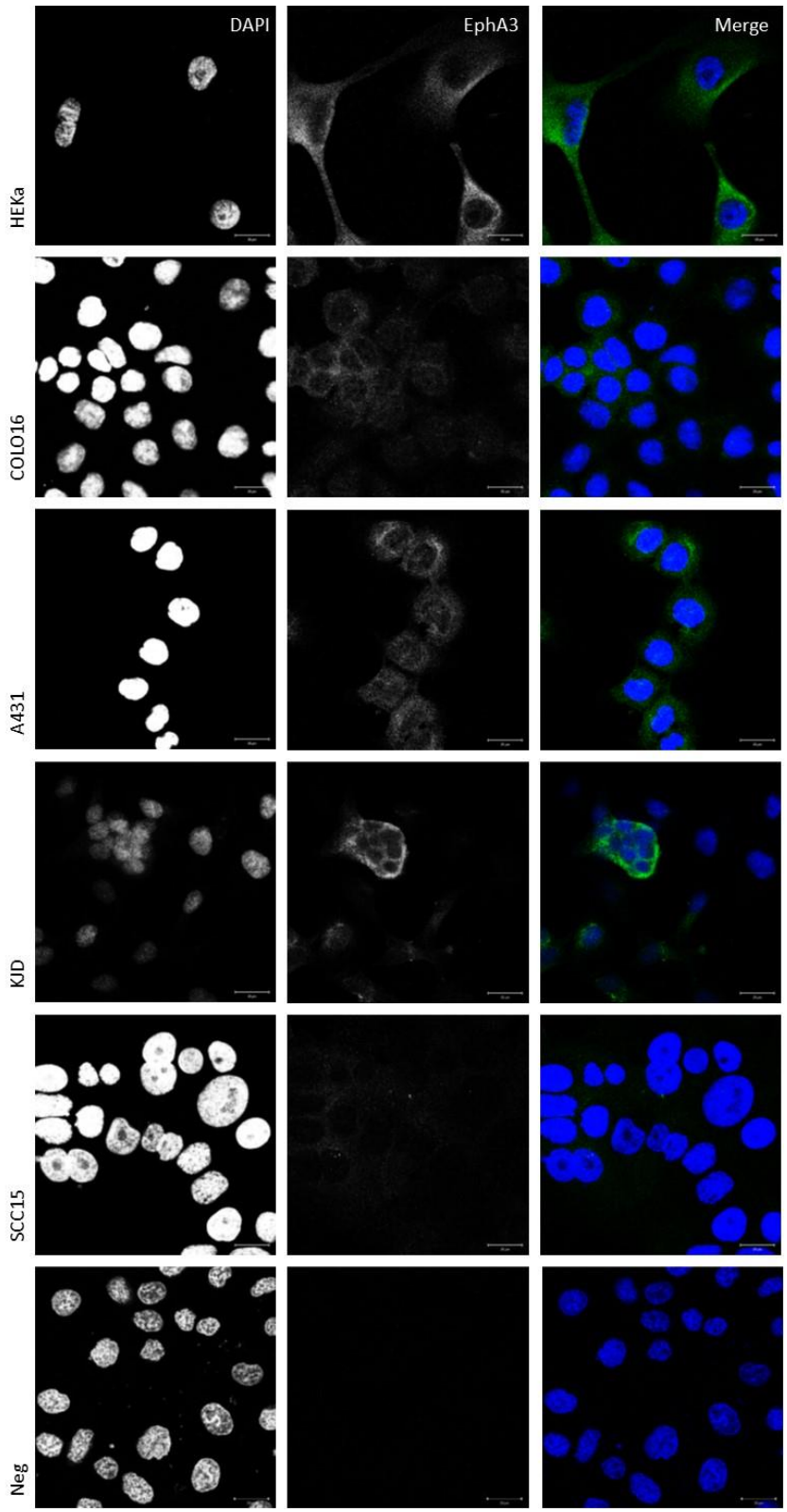

Figure A2 Confocal immunofluorescence images of human cell lines stained with antibody to EphA3 receptor. Images are displayed from left to right as isolated blue channel (DAPI stained nuclei), isolated green channel (anti-EphA3) and merge channel. Secondary anti-rabbit Alexa-488 was used. Negative control (Neg) was A431 cells labelled with secondary antibody only (lower panel). Scale bar = 20μm

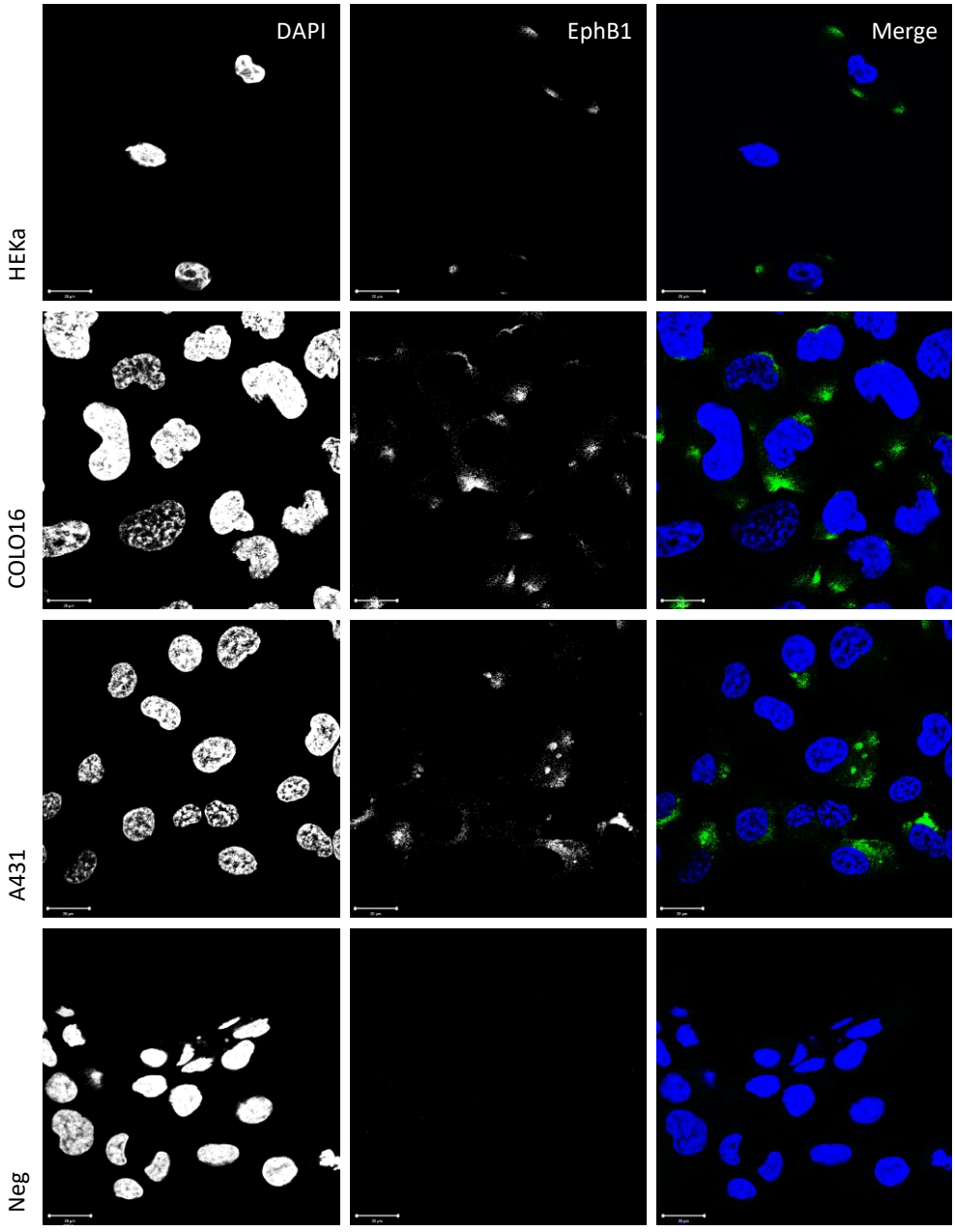

Figure A3 Confocal immunofluorescence images of human cell lines stained with antibody to EphB1 receptor. Images are displayed from left to right as isolated blue channel (DAPI stained nuclei), isolated green channel (anti-EphB2) and merge channel. Secondary anti-mouse Alexa-488 was used. Negative control (Neg) was A431 cells labelled with secondary antibody only (lower panel). Scale bar = 20μm.

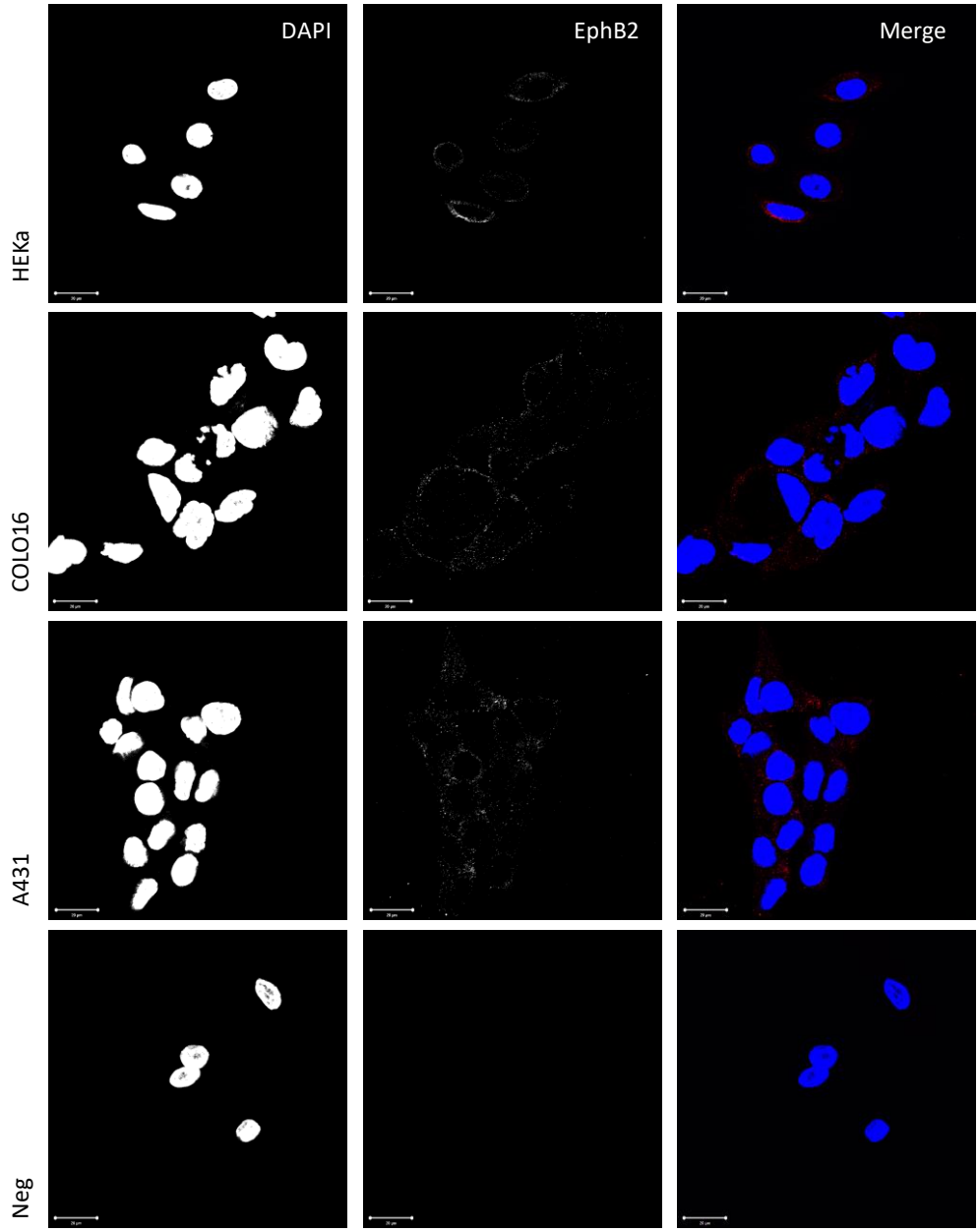

Figure A4 Confocal immunofluorescence images of human cell lines stained with antibody to EphB2 receptor. Images are displayed from left to right as isolated blue channel (DAPI stained nuclei), isolated red (anti-EphB2) channel and merge channel. Secondary anti-goat Alexa-555 was used. Negative control (Neg) was HEKa cells labelled with secondary antibody only (lower panel). Scale bar = 20μm.

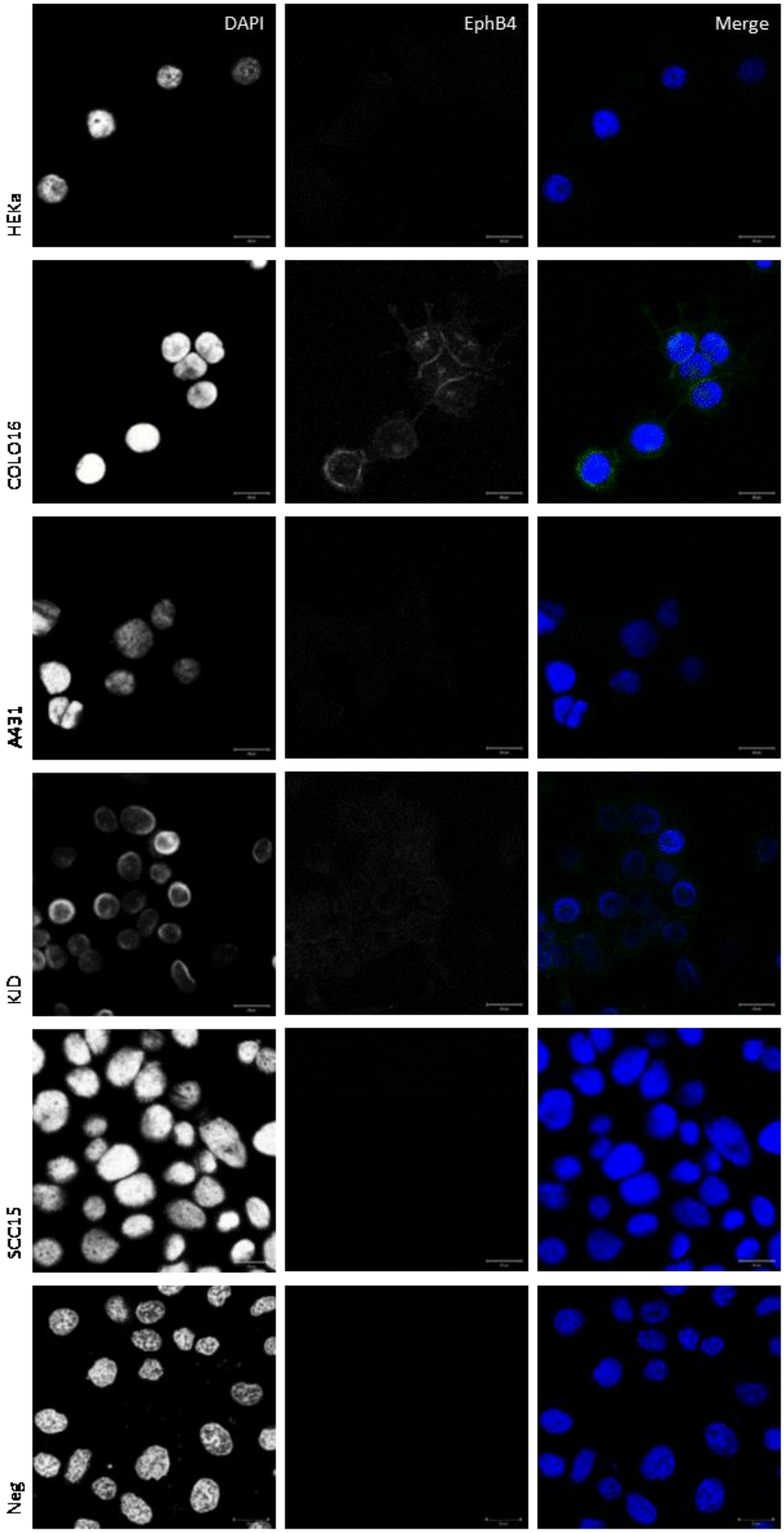

Figure A5 Confocal immunofluorescence images of human cell lines stained with antibody to EphB4 receptor. Images are displayed from left to right as isolated blue channel (DAPI stained nuclei), isolated green (anti-EphB4) channel and merge channel. Secondary anti-rabbit Alexa-488 was used. Negative control (Neg) was A431 cells labelled with secondary antibody only (lower panel). Scale bar = 20μm.